

IMPROVEMENT OF THE ELECTRIC FIELD DISTRIBUTION IN THE
MEDIUM VOLTAGE GAS INSULATED INDUCTIVE VOLTAGE
TRANSFORMERS

A THESIS SUBMITTED TO
THE GRADUATE SCHOOL OF NATURAL AND APPLIED SCIENCES
OF
MIDDLE EAST TECHNICAL UNIVERSITY

BY

MELİH VAR

IN PARTIAL FULFILLMENT OF THE REQUIREMENTS
FOR
THE DEGREE OF MASTER OF SCIENCE
IN
ELECTRICAL AND ELECTRONICS ENGINEERING

AUGUST 2017

Approval of the thesis:

**IMPROVEMENT OF THE ELECTRIC FIELD DISTRIBUTION IN THE
MEDIUM VOLTAGE GAS INSULATED INDUCTIVE VOLTAGE
TRANSFORMERS**

submitted by **MELİH VAR** in partial fulfillment of the requirements for the degree
of **Master of Science in Electrical and Electronics Engineering Department,**
Middle East Technical University by,

Prof. Dr. M. Gülbin Dural Ünver
Dean, Graduate School of **Natural and Applied Sciences**

Prof. Dr. Tolga Çiloğlu
Head of Department, **Electrical and Electronics Engineering**

Assist. Prof. Dr. Ozan Keysan
Supervisor, **Electrical and Electronics Eng. Dept., METU**

Examining Committee Members

Prof. Dr. Muammer Ermiş
Electrical and Electronics Eng. Dept., METU

Assist. Prof. Dr. Ozan Keysan
Electrical and Electronics Eng. Dept., METU

Assist. Prof. Dr. Murat Göl
Electrical and Electronics Eng. Dept., METU

Prof. Dr. İres İskender
Electrical and Electronics Eng. Dept., Gazi Univ.

Prof. Dr. Işık Çadircı
Electrical and Electronics Eng. Dept., Hacettepe Univ.

Date: 23.08.2017

I hereby declare that all information in this document has been obtained and presented in accordance with academic rules and ethical conduct. I also declare that, as required by these rules and conduct, I have fully cited and referenced all material and results that are not original to this work.

Name, Last Name : MELİH VAR

Signature :

ABSTRACT

IMPROVEMENT OF THE ELECTRIC FIELD DISTRIBUTION IN THE MEDIUM VOLTAGE GAS INSULATED INDUCTIVE VOLTAGE TRANSFORMERS

Var, Melih

M.Sc., Department of Electrical and Electronics Engineering

Supervisor: Assist. Prof. Dr. Ozan Keysan

August 2017, 109 pages

Voltage transformers are commonly used in medium voltage systems for both protection and measurement purposes. These transformers are designed to satisfy the mandatory IEC requirements at the lowest possible cost. The average life expectancy of such transformer is about 20 years, reliability and robustness are of the utmost importance. The main cause of failure during rated operation is the deterioration of the solid insulation by partial discharges. Partial discharges, unless there is a manufacturing error, develops in the highest electric field zones in the transformer which means the expected life and reliability are limited by that zone. The purpose of this thesis is to improve the winding design of a problematic transformer such that the electric field distribution within the transformer will be as homogeneous as possible. The finite elements models of the winding layers and epoxy resin envelopment will be constructed and the fields will be inspected by 2D and 3D simulations. By utilizing the data gained from the simulations and considering the real life limitations prototypes will be constructed and tested with respect to according standards. The designs will be iteratively corrected to find the spot where the electric field is safely within the withstood limits of the respective insulating materials Moreover the feedbacks from the manufacturing process and the real life tests will be used to evaluate the tradeoffs between the different

designs. The final coil design will be smaller in size due to the more uniform distribution of the electric field thus lowering the production cost. The reliability will increase and the routine test success rates will be improved. Additionally, it will be compatible with the IEC 61869-3 standard.

Keywords; inductive voltage transformer, electric field distribution, winding layer design.

ÖZ

ORTA GERİLİM GAZ İZOLASYONLU ENDÜKTİF GERİLİM TRAFOLARININ ELEKTRİK ALAN DAĞILIMLARININ İYİLEŞTİRİLMESİ

Var, Melih

Yüksek Lisans, Elektrik ve Elektronik Mühendisliği Bölümü

Danışman : Yrd. Doç. Dr. Ozan Keysan

Ağustos 2017, 109 sayfa

Gerilim trafoları orta gerilim sistemlerinde ölçü ve koruma amaçları için kullanılmaktadır. Bu tip trafoların tasarımında üretim maliyeti en asgari şekilde tutmak amaçlanırken aynı zamanda da IEC standartlarına uygunluk göz önünde bulundurulur. Beklenen çalışma ömrü 20 yıl civarında olup bu süre zarfındaki güvenilirlik önemlidir. Nominal çalışma şartları altında trafolarda arızanın esas nedeni katı yalıtımın kısmi deşarjlara bağlı olarak süreç içerisinde aşınmasıdır. Kısmi deşarj, eğer bir üretim hatası yok ise, trafonun içerisindeki en yüksek alan şiddetine sahip bölgede meydana gelir, bu da demektir ki trafonun ömrü ve güvenilirliği bu bölge tarafından sınırlanır. Bu tezin amacı trafonun sargılarının yerleşimini ayarlayarak elektrik alan dağılımını olabildiğince eşit olmasını sağlamaktır. Bunun için sargıların ve sargıların üstünde bulunan katı yalıtımın sonlu eleman modelleri oluşturularak 2D ve 3D elektrik alan dağılımı analizleri yapılacaktır. Simülasyonlardan elde edilen bilgiler kullanılarak ve gerçek üretim şartları da göz önünde bulundurularak prototip üretimleri yapıp test edilecektir. Daha sonrasında ise simülasyon datası ile test sonuçları karşılaştırılıp farklı dizaynlar arasındaki avantajlar ve dezavantajlar ortaya konulacaktır. Sonuç olarak

ıkacak olan tasarım alanın dzgn dađılımı sebebiyle daha ufak ve ucuz olacaktır. Gvenilirlikte artış rutin testlerde ise hata yzdesinde azalma olacaktır. Son tasarım ayrıca IEC 61896-3 standardına uygun olacaktır.

Anahtar Kelimeler: endktif gerilim trafosu, elektrik alan dađılımı, bobin katman dizaynı.

To my family

ACKNOWLEDGMENTS

Firstly, I would like to express my sincere gratitude to Assist. Prof. Dr. Ozan Keysan for his strong guidance and endless encouragement. The door to his office was always open whenever I ran into a trouble spot or had a question about my research or writing. I feel really lucky to be one of his first graduate students.

I wish to express my sincere thanks to Hüseyin Arabul and EMEK ELEKTRİK ENDÜSTRİSİ A.Ş. for their valuable support throughout my graduate studies. Accredited laboratory and component resources have benefited my work greatly.

I would like to thank my colleagues Alpay Partal, Yalçın Kılıç and İsmail Yerlikaya for their enduring support. Their guidance has always been invaluable to me during the process. They shared all of their knowledge and experience during my studies.

I would also like to thank Sencer Aydın and Bulut Ertürk for their friendship and invaluable support during all my studies.

Finally, I must express my very profound gratitude to my family. Their patience, trust and encouragement have always had a critical importance in my life. Without having their support, I would not be able to complete this work.

TABLE OF CONTENTS

| | |
|----------------------------|-----|
| ABSTRACT | v |
| ÖZ | vii |
| ACKNOWLEDGMENTS | x |
| TABLE OF CONTENTS..... | xi |
| LIST OF TABLES | xiv |
| LIST OF FIGURES | xvi |
| LIST OF ABBREVIATIONS..... | xix |

CHAPTERS

| | |
|--|-----------|
| 1. INTRODUCTION..... | 1 |
| 1.1. GAS INSULATED INDUCTIVE VOLTAGE TRANSFORMER..... | 2 |
| 1.2. PROBLEM DEFINITION | 4 |
| 1.3. GT30A DESIGN PARAMETERS | 5 |
| 1.3.1 <i>GT30a Test Data</i> | 8 |
| 1.4. METHODOLOGY | 10 |
| 1.4.1 <i>Application of Finite Element Analysis to the GT30a</i> | 11 |
| 2. EVALUATION & SOLUTION OF THE PARTIAL DISCHARGE PROBLEM..... | 13 |
| 2.1. PARTIAL DISCHARGES..... | 14 |
| 2.1.1 <i>Partial Discharge Detection Test</i> | 17 |
| 2.2. INSULATING MATERIALS USED IN MV VOLTAGE TRANSFORMERS..... | 18 |
| 2.2.1 <i>Properties of the Epoxy Resin</i> | 21 |
| 2.2.2 <i>Properties of the Insulating Paper</i> | 23 |
| 2.2.3 <i>Properties of the Insulating Gases</i> | 24 |
| 2.3. MANUFACTURING PROCESS | 26 |
| 2.4. FACTORS EFFECTING THE ELECTRICAL FIELD DISTRIBUTION | 28 |
| 2.4.1 <i>Usage of the Electric Field Screen</i> | 29 |
| 2.4.2 <i>Effect of the Dielectric Constant in the Field Distribution</i> | 32 |

| | | |
|-----------|---|-----------|
| 2.4.3 | <i>Sealing of the Coil Ends</i> | 35 |
| 2.4.4 | <i>Modification of the Original Design</i> | 37 |
| 2.5. | CHAPTER SUMMARY | 38 |
| 3. | LAYER DESIGN & MODELING | 41 |
| 3.1. | BASIC LAYER STRUCTURE..... | 42 |
| 3.2. | MINIMIZATION OF THE ELECTRICAL FIELD..... | 46 |
| 3.3. | REDUCTION OF THE COMPUTATION TIME | 47 |
| 3.3.1 | <i>Determination of the Minimum Possible Model Area</i> | 49 |
| 3.4. | LAYER TEMPLATE DETERMINATION | 53 |
| 3.4.1 | <i>Stepped Layer Templates</i> | 53 |
| 3.5. | LAYER TEMPLATE CALCULATION FOR GT30A..... | 57 |
| 3.5.1 | <i>Layer Components of the GT30a</i> | 57 |
| 3.5.2 | <i>Critical Electric Field Intensity</i> | 58 |
| 3.5.3 | <i>Simulation of the Layer Templates</i> | 58 |
| 3.6. | MANUFACTURING TIME & NUMBER OF STEPS | 62 |
| 3.7. | IRREGULAR LAYER DESIGN..... | 63 |
| 3.8. | CHAPTER SUMMARY | 66 |
| 4. | LAYER LENGTH DETERMINATION FOR THE HIGH VOLTAGE COIL | 67 |
| 4.1. | 3D MODELING OF THE LAYERS | 68 |
| 4.1.1 | <i>Meshing Strategy</i> | 69 |
| 4.2. | 3D TO 2D MAPPING..... | 71 |
| 4.3. | 2D MODELING..... | 74 |
| 4.3.1 | <i>2D Model of the Original Design</i> | 74 |
| 4.3.2 | <i>2D Model of the Modified Design</i> | 77 |
| 4.3.3 | <i>Construction of the Final Design</i> | 79 |
| 4.3.4 | <i>Selection of the Layer Templates</i> | 82 |
| 4.4. | CHAPTER SUMMARY | 82 |
| 5. | EXPERIMENTAL RESULTS | 85 |

| | | |
|-----------|--|------------|
| 5.1. | TESTS APPLIED TO THE FINAL DESIGN | 86 |
| 5.1.1 | <i>Standard Lightning Impulse Test</i> | 86 |
| 5.1.2 | <i>Temperature-rise Test</i> | 88 |
| 5.1.3 | <i>Test for Accuracy</i> | 89 |
| 5.1.4 | <i>Power Frequency Withstand and PD Test</i> | 90 |
| 5.1.5 | <i>Power Frequency Withstand and PD test with the Leaked Gas</i> | 92 |
| 5.2. | COMPARISON OF THE INITIAL, MODIFIED AND THE FINAL DESIGN | 93 |
| 5.2.1 | <i>Material and Production Time Comparison</i> | 94 |
| 5.2.2 | <i>Performance Comparison</i> | 94 |
| 5.3. | DESIGN TRADE OFFS | 95 |
| 5.4. | CHAPTER SUMMARY | 96 |
| 6. | CONCLUSIONS & FUTURE WORK..... | 99 |
| 6.1. | CONCLUSIONS | 99 |
| 6.2. | FUTURE WORK..... | 101 |
| | REFERENCES..... | 103 |
| | APPENDIX | 107 |
| | GT30a Core Drawing | 107 |
| | Gt30a Original Design Winding Diagram | 108 |
| | Gt30a Final Design Winding Diagram | 109 |

LIST OF TABLES

TABLES

| | |
|---|----|
| TABLE 1-1 DESIGN PROPERTIES OF THE GT30A | 6 |
| TABLE 1-2 LIST OF THE TESTS ACCORDING TO IEC 61869-3[8]..... | 7 |
| TABLE 1-3 DESIGN DATA OF THE GT30A | 8 |
| TABLE 1-4 ROUTINE TEST RESULTS OF THE GT30A BETWEEN 2012 AND 2016..... | 8 |
| TABLE 1-6 PARTIAL DISCHARGE TEST VOLTAGES AND PERMISSIBLE LEVELS FROM IEC 61869-1[10]..... | 10 |
| TABLE 2-1 BASIC PHYSICAL PROPERTIES OF MAJOR INSULATING MATERIALS [23] | 20 |
| TABLE 2-2 EPOXY RESIN MIXTURE RECEIPT | 22 |
| TABLE 2-3 ELECTRICAL PROPERTIES OF THE EPOXY RESIN MIXTURE..... | 22 |
| TABLE 2-4 ELECTRICAL PROPERTIES OF THE INSULATING PAPER USED IN GT30A | 24 |
| TABLE 2-5 SIMULATION RESULTS FOR DIFFERENT SCREEN SIZE AND POSITIONS FOR FIGURE 2-10..... | 31 |
| TABLE 2-6 DIELECTRIC CONSTANTS AND STRENGTH OF INSULATING MATERIALS USED IN GT30A | 33 |
| TABLE 2-7 PROPERTIES OF AW 106 | 37 |
| TABLE 2-8 ROUTINE TEST RESULTS COMPARISON OF THE MODIFIED AND ORIGINAL GT30A | 38 |
| TABLE 3-1 LAYER SIMULATION PARAMETERS | 43 |
| TABLE 3-2 SIMULATION PARAMETERS OF THE LAYER USED IN THE GA..... | 46 |
| TABLE 3-3 SIMULATION PARAMETERS FOR THE MINIMUM LENGTH DETERMINATION | 50 |
| TABLE 3-4 GT30A LAYER DETERMINATION SIMULATION PARAMETERS | 59 |
| TABLE 3-5 POSSIBLE LAYER TEMPLATES FOR THE GT30A..... | 61 |
| TABLE 3-6 COMPARISON OF THE COIL MANUFACTURING | 63 |
| TABLE 3-7 INSPECTION OF THE 1-3-4-4-2 STEP POINTS..... | 65 |
| TABLE 4-1 3D VS 2D ANALYSIS RESULT COMPARISON | 73 |
| TABLE 4-2 2D SIMULATION PARAMETERS | 74 |
| TABLE 4-3 COMPARISON OF THE ORIGINAL AND FINAL DESIGNS LAYER PARAMETERS | 83 |

| | |
|--|----|
| TABLE 5-1 ACCURACY TEST RESULT OF THE FINAL AND THE ORIGINAL DESIGN..... | 89 |
| TABLE 5-2 POWER FREQUENCY AND PARTIAL DISCHARGE TEST RESULTS WITH 5 BAR INSULATING GAS | 91 |
| TABLE 5-3 POWER FREQUENCY AND PARTIAL DISCHARGE TEST RESULTS WITH LEAKED INSULATING GAS | 93 |
| TABLE 5-4 MATERIAL AND PRODUCTION TIME COMPARISON OF THE COILS | 94 |
| TABLE 5-5 ELECTRICAL FIELD PERFORMANCE COMPARISON OF THE DESIGNS..... | 95 |

LIST OF FIGURES

FIGURES

| | |
|--|----|
| FIGURE 1-1 A GAS INSULATED MV VOLTAGE TRANSFORMER INSTALLED IN A 36kV 630A SWITCHGEAR EQUIPMENT | 3 |
| FIGURE 1-2 THE BASIC STRUCTURE OF MV GAS INDUCTIVE VOLTAGE TRANSFORMER | 4 |
| FIGURE 1-3 PUNCTURED PRIMARY COIL OF THE GT30A | 9 |
| FIGURE 1-4 CONVERGENCE IN RESULTS[11] | 11 |
| FIGURE 1-5 HV WINDING OF THE MV INDUCTIVE VOLTAGE TRANSFORMER SIDEVIEW | 12 |
| FIGURE 1-6 CROSS SECTION OF A MV INDUCTIVE VOLTAGE TRANSFORMER | 12 |
| FIGURE 2-1 A BRANCH TYPE ELECTRICAL TREE GROWING THROUGH TRANSPARENT RESIN INSULATION FROM A FINE POINT ELECTRODE[20] | 16 |
| FIGURE 2-2 PD MAGNITUDE AS A FUNCTION OF SPHERICAL CAVITY SIZE FOR 15 kV, EPR CABLE GEOMETRY ASSUMING THAT THE CAVITY DISCHARGES AT THE PEAK OF A 2.5 PU EXCITATION (30 kV).[17] | 17 |
| FIGURE 2-3 PARTIAL DISCHARGE TEST EQUIPMENT (BIDDLE 666035-01) | 18 |
| FIGURE 2-4 BREAKDOWN VOLTAGES (V_{MIX}) AS A FUNCTION OF PERCENT SF ₆ IN SF ₆ - N ₂ MIXTURES[30] | 26 |
| FIGURE 2-5 WINDING OF THE PRIMARY COIL | 27 |
| FIGURE 2-6 TRANSFORMER COILS UNDER HEAT TREATMENT | 27 |
| FIGURE 2-7 WINDING ASSEMBLY IN TO THE MOULD | 28 |
| FIGURE 2-8 TOP VIEW OF HV SCREEN (COVERED WITH CARBON PAPER) AND GROUND SCREEN OF A GAS INSULATED MV VOLTAGE TRANSFORMER | 29 |
| FIGURE 2-9 SCREEN POSITIONS IN A HV WINDING OF A MV VOLTAGE TRANSFORMER | 30 |
| FIGURE 2-10 SIDE VIEW OF THE COIL AND THE SCREEN ON MAXWELL X-Y PLANE | 31 |
| FIGURE 2-11 ELECTRIC FIELD DISTRIBUTION IN A MEDIUM WITH SINGLE TYPE DIELECTRIC | 32 |
| FIGURE 2-12 ELECTRIC FIELD DISTRIBUTION IN A MEDIUM WITH TWO DIFFERENT DIELECTRIC | 33 |
| FIGURE 2-13 SLICE OF THE TRANSFORMER WITH STEPPED PAPER | 34 |

| | |
|---|----|
| FIGURE 2-14 SLICE OF THE TRANSFORMER WITH CONSTANT PAPER LENGTH..... | 34 |
| FIGURE 2-15 SIDE OF THE COIL AFTER THE WINDING PROCESS | 35 |
| FIGURE 2-16 COIL WITHOUT EPOXY RESIN PENETRATION..... | 35 |
| FIGURE 2-17 COIL WITH EPOXY RESIN FILLED IN BETWEEN INSULATION PAPERS | 36 |
| FIGURE 2-18 COIL WITH CAVITY CAUSED BY THE EPOXY RESIN ON THE CONDUCTOR SURFACE..... | 36 |
| FIGURE 2-19 AW106 APPLIED COIL SURFACE | 37 |
| FIGURE 3-1 WINDING SECTION OF A VOLTAGE TRANSFORMER..... | 42 |
| FIGURE 3-2 STRAIGHT LAYER DESIGN | 43 |
| FIGURE 3-3 ELECTRIC FIELD DISTRIBUTION IN STRAIGHT LAYER DESIGN | 44 |
| FIGURE 3-4 TWO STEP LAYER DESIGN | 45 |
| FIGURE 3-5 ELECTRIC FIELD DISTRIBUTION IN TWO STEP LAYER DESIGN | 45 |
| FIGURE 3-6 RESULT OF THE INITIAL GA OPTIMIZATION | 47 |
| FIGURE 3-7 MODIFICATION OF THE GA SOLUTION WHERE THE 30 TURNS ARE REMOVED | 48 |
| FIGURE 3-8 MV VOLTAGE TRANSFORMER LAYER EXAMPLE | 49 |
| FIGURE 3-9 REPRESENTED PART OF THE WHOLE LAYER | 50 |
| FIGURE 3-10 FE ANALYSIS MESHING DENSITY OF THE REPRESENTED LAYER | 51 |
| FIGURE 3-11 MAXIMUM FIELD VS. ANALYZED LENGTH (A)0.1MM INSULATION THICKNESS UP TO $k=15.2$ (B) 0.3MM INSULATION THICKNESS UP TO $k=11.6$ (C) 0.6MM INSULATION THICKNESS UP TO $k=5.8$ | 52 |
| FIGURE 3-12 NORMAL STEP TYPES (A) STRAIGHT (B) 2 STEP (C) 3 STEP..... | 55 |
| FIGURE 3-13 SHIFTED STEPS TYPES(A) 2-1 (B) 2-2-1 (C) 2-2-2-1..... | 56 |
| FIGURE 3-14. SIMULATED PART OF THE LAYERS FOR GT30A TEMPLATE DETERMINATION..... | 59 |
| FIGURE 3-15 MESH DENSITY OF THE LAYER TEMPLATE SIMULATION | 60 |
| FIGURE 3-16 INSULATION THICKNESS VS. LAYER LENGTH FOR THE LAYERS..... | 62 |
| FIGURE 3-17 1-3-4-4-2 LAYER TEMPLATE | 64 |
| FIGURE 4-1 CONVERSION OF THE WIRES TO THE FOILS FOR THE SIMULATION..... | 68 |
| FIGURE 4-2 3D ANALYSIS OF A SINGLE COPPER FOIL WITH AUTOMATIC MESHING | 69 |

| | |
|--|----|
| FIGURE 4-3 MESH DENSITY PLOT WITH THE DENSITY FOCUSED ON THE EDGE OF THE COPPER FOIL | 70 |
| FIGURE 4-4 ELECTRICAL FIELD GRADIENT OF THE AREA WITH FOCUSED MESH | 71 |
| FIGURE 4-5 SIDE VIEW OF THE 3D ANALYSIS OF THE COPPER FOIL | 72 |
| FIGURE 4-6 CROSS SECTION OF THE HIGHEST ELECTRICAL FIELD AREA OF THE 3D ANALYSIS REPRESENTED IN X-Y PLANE | 72 |
| FIGURE 4-7 2D ELECTRICAL FIELD ANALYSIS OF THE ORIGINAL GT30A..... | 75 |
| FIGURE 4-8 ELECTRICAL FIELD DISTRIBUTION AT THE END POINT OF THE 106MM LAYER OF THE ORIGINAL GT30A | 76 |
| FIGURE 4-9 ELECTRICAL FIELD DISTRIBUTION AT THE END POINT OF THE 86MM LAYER OF THE ORIGINAL GT30A | 76 |
| FIGURE 4-10 ELECTRICAL FIELD DISTRIBUTION AT THE END POINT OF THE 66MM LAYER OF THE ORIGINAL GT30A | 77 |
| FIGURE 4-11 ELECTRICAL FIELD DISTRIBUTION OF THE MODIFIED DESIGN | 78 |
| FIGURE 4-12 ELECTRICAL FIELD DISTRIBUTION OF THE FINAL DESIGN | 81 |
| FIGURE 4-13 ORIGINAL COIL (LEFT) AND FINAL COIL(RIGHT)..... | 84 |
| FIGURE 5-1 STANDARD LIGHTNING IMPULSE TEST SETUP | 87 |
| FIGURE 5-2 STANDARD LIGHTNING IMPULSE TEST POSITIVE WAVEFORM..... | 88 |
| FIGURE 5-3 TEMPERATURE RISE TEST RESULTS | 89 |
| FIGURE 5-4 PARTIAL DISCHARGE TEST SETUP..... | 91 |

LIST OF ABBREVIATIONS

| | |
|----------------|---|
| AC | Alternating Current |
| APG | Automatic Pressure Gelation |
| ASTM | American Section of the International Association for Testing Materials |
| CT | Current Transformer |
| DC | Direct Current |
| EPR | Ethylene Propylene Rubber |
| FEM | Finite Elements Method |
| GA | Genetic Algorithm |
| HV | High Voltage |
| IEC | International Electrotechnical Commission |
| LV | Low Voltage |
| MV | Medium Voltage |
| pbw | Percent by Weight |
| PD | Partial Discharge |
| pu | Per Unit |
| RMS | Root Mean Square |
| T _g | Glass Transition Temperature |
| VT | Voltage Transformer |

CHAPTER 1

INTRODUCTION

Transformers are devices for transforming alternative voltages and currents[1]. The history of the transformer starts with the device that Michael Faraday constructed in 1831, with a closed iron core and two independent coils [2]. The technology behind the transformers are well known and transformers are large and expensive equipments of the power transmission and distribution systems.

Instrument transformer is a type of transformer that reduces either line voltage or line current to a measurable level thus effectively providing isolation for the measuring devices. Voltage transformers are instrument transformers that provide voltage signals to the measurement devices or protecting relays [3]. There are three types of voltage transformers;

- Inductive voltage transformer : A basic single phase low power induction machine
- Capacitive voltage transformer : Inductive voltage transformer with a capacitive divider in the primary terminal voltage.
- Optical voltage transformer : The voltages are measured by making use of the Pockels effect instead of step down with electrical induction. Smaller than the conventional measurement systems[4].

The electrical power systems are growing in capacity and voltage thus the sizes of the conventional instrument transformers are increasing [5]. With the increased power ratings of the systems even small measurement errors corresponds to large amount of miscalculated energy. Therefore, instrument transformers should increase their precision. A method to increase the accuracy of a conventional voltage transformer is to use an electronic device that actively compensates for the error [6].

In the medium voltage range (1-35 kV according to IEC 60038 [7]) the installment of the electronic correction device would be costly and the optical transformer are not in the widespread use yet. Therefore only way to decrease the size and increase the accuracy in the MV range voltage transformers at the moment is to modify the conventional designs. This thesis will focus on improving a conventional gas insulated medium voltage inductive voltage transformer.

1.1. Gas Insulated Inductive Voltage Transformer

Gas insulated inductive voltage transformer is a single phase instrument transformer that utilizes gas insulation as the main insulating medium and solid insulation as the mechanical support. These transformers are widely used in the indoor environment of the switchgear equipment to provide voltage signals either for measurement or protecting purposes in the MV range (Figure 1-1).



Figure 1-1 A gas insulated MV voltage transformer installed in a 36kV 630A switchgear equipment

Structure of a typical medium voltage gas insulated voltage transformer consists of:

- Silicon Steel Core
- Primary (high voltage) and secondary (low voltage) windings constructed with magnet wires and isolated with insulating paper
- Epoxy resin envelope

The insulating gas is injected into the coils after the manufacturing of the resin envelope is completed. The respective parts are shown in Figure 1-2.

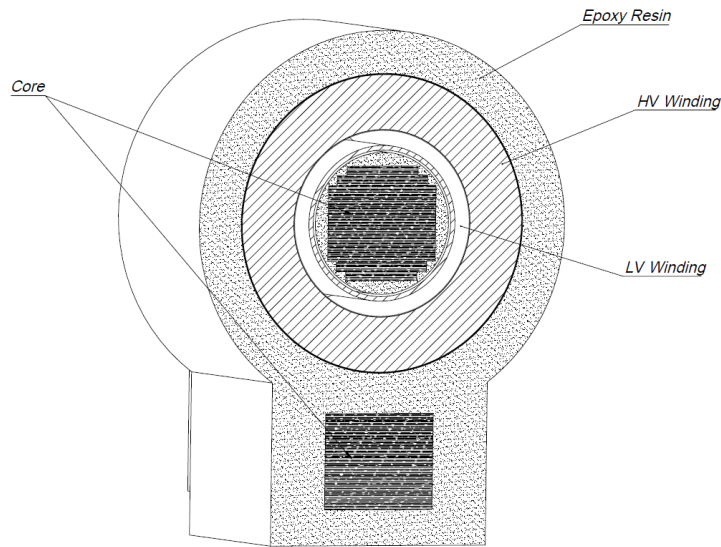


Figure 1-2 The basic structure of MV gas inductive voltage transformer

1.2. Problem Definition

The aim of this thesis to utilize the finite element analysis method to model and improve the electric field distribution of an existing gas insulated MV voltage transformer which is suffering from partial discharges and puncture issues. The transformer studied in this thesis is an 34.5 kV voltage transformer numbered as GT30a.

The focus will be on the electrical design. The magnetic design of the GT30a will not be changed. Electrical gradient throughout the high voltage coil will be modified with geometry changes to distribute the field as uniformly as possible. Unfortunately, the modifications in the electrical design of the high voltage coil will affect the magnetic design thus the accuracy of the GT30a. The final design will be subjected to the accuracy class test and it should be able to comply with the standards. Without doing the magnetic modeling only way to make sure so is to limit the leakage inductance and the copper loss of the coil to the maximum of the current design.

Objectives of the thesis:

- Fixation the partial discharge and the puncture problem
- Reduction of discarded transformers due to manufacturing failures below 2 percent.
- Development of the finite element modeling method of the coil which should be fast & applicable to similar sized transformers.
- Reduction of the coil size thus reduction in the leakage flux & copper resistance and increase in the accuracy class.
- Operational robustness. The transformer should be functional even when the insulating gas pressure is decreased to 1 bar.

With these objectives completed the resultant design and the design method could be further adapted to manufacture either low material cost transformer with the reduction in the core window size and the epoxy resin mold or could be adapted to produce environmentally friendly transformers with low SF₆ content.

1.3. GT30a Design Parameters

GT30a is mainly produced for the Turkish market and the local regulations promotes the IEC standards. As a result, manufacturing and testing of the GT30a is done according to IEC 61869-1 and IEC 61869-3 standards. To be able to carry out the simulations the parameters and the test conditions of the transformer must be known. Each manufactured GT30a must satisfy the parameters given in Table 1-1.

Table 1-1 Design properties of the GT30a

| Properties | Value |
|---|----------------------|
| Designated Model | GT30a |
| Rated System Voltage <small>(line - neutral rms)</small> | $34.5 / \sqrt{3}$ kV |
| Secondary Output Voltage <small>(line - neutral rms)</small> | $100 / \sqrt{3}$ V |
| Rated Frequency | 50 Hz |
| Highest Voltage for Equipment <small>(rms)</small> | 36 kV |
| Rated Power Frequency withstand Voltage <small>(rms)</small> | 70 kV |
| Rated Lightning Impulse Voltage <small>(1.2/50 peak)</small> | 170 kV |
| Rated Burden | 10 VA |
| Rated Voltage Factor | 1.9 for 30 sec |
| Insulation Class | A |
| Rated Accuracy Class | 3P |

To satisfy the IEC standards the transformer must be able to pass the type tests for one time and the routine tests for each transformer manufactured. The list of the tests are given in the Table 1-2. Final design will be subjected to all of the routine tests and the impulse voltage test from the type tests. Other type tests are not essential since the changes will be done will not affect if not improve the outcome of those.

Table 1-2 List of the tests according to IEC 61869-3[8]

| Tests | Clause / Sub-clause |
|--|----------------------------|
| Type tests | 7.2 |
| Temperature-rise test | 7.2.2 |
| Impulse voltage test on primary terminals | 7.2.3 |
| Wet test for out door type transformers | 7.2.4 |
| Electromagnetic Compatibility tests | 7.2.5 |
| Test for accuracy | 7.2.6 |
| Verification of the degree of protection by enclosures | 7.2.7 |
| Enclosures tightness test at ambient temperature | 7.2.8 |
| Pressure test for the enclosure | 7.2.9 |
| Short-circuit with stand capability | 7.2.301 |
| Routine tests | 7.3 |
| Power-frequency voltage withstand tests on primary terminals | 7.3.1 |
| Partial discharge measurement | 7.3.2 |
| Power-frequency voltage withstand tests between sections | 7.3.3 |
| Power-frequency voltage withstand tests on secondary terminals | 7.3.4 |
| Test for accuracy | 7.3.5 |
| Verification of markings | 7.3.6 |
| Enclosures tightness test at ambient temperature | 7.3.7 |
| Pressure test for the enclosure | 7.3.8 |
| Special tests | 7.4 |
| Chopped impulse voltage withstand tests on primary terminals | 7.4.1 |
| Multiple chopped impulse test on primary terminals | 7.4.2 |
| Measurement of capacitance and dielectric dissipation factor | 7.4.3 |
| Transmitted overvoltage test | 7.4.4 |
| Mechanical tests | 7.4.5 |
| Internal arc fault test | 7.4.6 |
| Enclosures tightness test at low and high temperatures | 7.4.7 |
| Gas dew point test | 7.4.8 |
| Corrosion test | 7.4.9 |
| Fire hazard test | 7.4.10 |
| Sample tests | 7.5 |

As mentioned in the section 1.2 the design changes will only be done in the electrical point of view. Some of the data required for the electrical field analysis are obtained from the magnetic design. Other limiting data required is related to the available epoxy resin mold dimensioning. Both are given in Table 1-3.

Table 1-3 Design data of the GT30a

| Data | Value |
|---|--------------|
| Primary wire diameter | Ø0.12 mm |
| Primary number of turns | 50,461 |
| Secondary wire diameter | Ø1.5 mm |
| Secondary number of turns | 147 |
| Secondary winding outer diameter | 77 mm |
| Secondary winding inner diameter | 61.5 mm |
| Core window | 89 x 181mm |
| Core diameter* | 54 mm |
| Maximum allowed primary winding diameter* | 165 mm |
| *Current design is at the limit diameter | |

1.3.1 GT30a Test Data

The main reason that the GT30a is selected as the subject of this thesis is its performance in the routine tests over the 5 years. Another reason is it is the most consumed type of the MV indoor inductive voltage transformer in the local market. In the Table 1-4 the routine tests results of GT30a and the related sub clause of the test from the Table 1-2 are given.

Table 1-4 Routine test results of the GT30a between 2012 and 2016

| Year | Produced | Puncture (7.3.1) | Partial Discharge (7.3.2) | Class (7.3.5) | Other | Total Failure | Percent |
|--------------|-----------------|-----------------------------|--|--------------------------|--------------|--------------------------|----------------|
| 2012 | 328 | 3 | 35 | 0 | 4 | 42 | 12,80% |
| 2013 | 585 | 12 | 29 | 0 | 0 | 41 | 7,01% |
| 2014 | 818 | 6 | 112 | 0 | 14 | 132 | 16,14% |
| 2015 | 1520 | 12 | 271 | 4 | 24 | 311 | 20,46% |
| 2016 | 955 | 61 | 62 | 2 | 9 | 134 | 14,03% |
| Total | 4206 | 94 | 509 | 6 | 51 | 660 | 15,69% |

As can be seen from the Table 1-4 the most dominant failing cause of the GT30a in the routine tests is the partial discharges. The second most common error is the

failure in the one minute power frequency test due to the puncture. Puncture is the complete breakdown of the solid medium that happens when the partial discharges are strong enough to bridge the conductors with the electrical treeing [9]. This occurs in the power frequency routine test in less than one minute of voltage application. A puncture would leave a carbon path which can be identified easily when the failed coil is inspected (Figure 1-3).

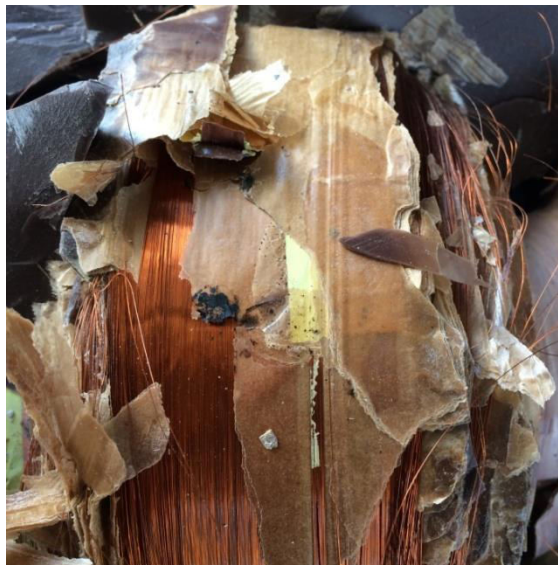


Figure 1-3 Punctured primary coil of the GT30a

High voltage winding is assumed to be the source of both partial discharges and puncture failures since the low voltage winding of the GT30a is only at 100 volts potential where the magnet wire itself prevent the discharge without any additional insulating gas or paper.

Partial discharge test voltages and allowed maximum discharge magnitudes according to IEC 61869-1 are given in the Table 1-5. GT30a is a 36 kV transformer with non effectively earthed neutral system and therefore the partial discharge level should be below 10 pC at 43.2 kV and 5 pC at 24.9 kV. The discharge measurement is done in accordance with IEC 60060 and the noise level of the measurement system should be below the maximum allowed pC level for the given voltage.

Table 1-6 Partial discharge test voltages and permissible levels from IEC 61869-1[10]

| Type of earthing of the neutral system | Instrument Transformer Type | PD test voltage (r.m.s.) kV | Maximum permissible PD level (pC) | |
|---|-----------------------------|-----------------------------------|-----------------------------------|----------|
| | | | Type of insulation | |
| | | | Immersed in Liquid or gas | Solid |
| Earthed neutral system (earth fault factor ≤ 1.4) | CT and earthed VT | U_m $1.2U_m/\sqrt{3}$ | 10 5 | 50 20 |
| | Unearthed VT | $1.2 U_m$ | 5 | 20 |
| Isolated or noneffectively earthed neutral system (earth fault factor ≥ 1.4) | CT and earthed VT | $1.2 U_m$ $1.2 U_m / \sqrt{3}$ | 10 5 | 50 20 |
| | Unearthed VT | $1.2 U_m$ | 5 | 20 |
| NOTE 1 : If the neutral system is not defined, the values given for isolated or non-effectively earthed neutral system. | | | | |
| NOTE 2 : The maximum permissible PD level is also valid for frequencies different from rated frequency. | | | | |
| NOTE 3 : CT for current transformer and VT for voltage transformer. | | | | |

1.4. Methodology

Fulfillment of the objectives defined in section 1.2 will be carried out in a systematic manner. First the partial discharges and its relation with the insulating materials used in the gas insulated MV inductive voltage transformers will be discussed in the chapter 2. Possible solutions to fix the problem without entirely modeling the coil will be presented and the limits for the insulation materials will be determined.

In chapter 3 and chapter 4 modeling and possible modeling simplifications of the high voltage winding will be introduced. The electrical field gradient simulation of the high voltage winding of the GT30a will be carried out with ANSYS Maxwell software.

Lastly in chapter 5 a new design that have been created with the help of the knowledge accumulated in the chapters 2, 3 and 4 will be manufactured. The final

design will be subjected to tests and its performance will be compared to the initial design.

1.4.1 Application of Finite Element Analysis to the GT30a

For basic geometries, the electric field can be calculated analytically by utilizing the Gauss Law and superposition principle. As the geometry gets complex it would not be feasible to do the calculations by hand. With enough computational power, numerical methods can be used. Finite elements analysis is a well established numerical method used widely in civil engineering, mechanical engineering, electrical engineering etc. [11].

ANSYS Maxwell 16.0.3 uses the finite elements method to solve the electrical field gradient. The accuracy of the solution at a given point depends on the mesh density at that position thus the number of elements (Figure 1-4). As the number of elements increase the error margin of the numerical solution decreases[12].

However high number of elements will increase the computational time. Therefore the mesh density will be focused only on the areas where high electrical gradient is expected.

Another way to reduce the computational time is to exploit the symmetry, if available, to convert the design from 3D to 2D. In chapter 3 the layers of the coil will be modeled as 2D around the Z axis (Figure 1-5).

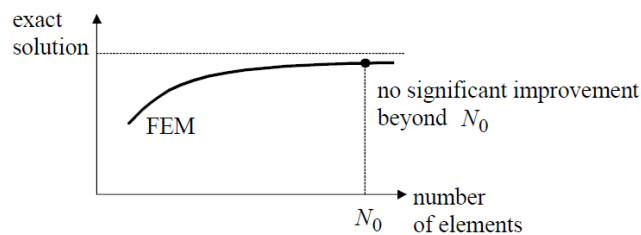


Figure 1-4 Convergence in results[11]

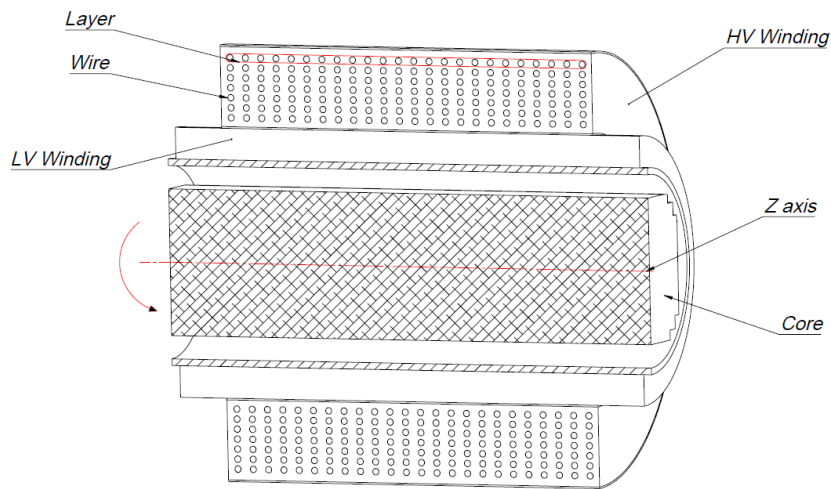


Figure 1-5 Hv winding of the mv inductive voltage transformer sideview

In chapter 4 the core will be modeled thus there will not be any symmetry axis. To simplify the model, 3D analysis will be carried out at a set of points and it will be compared with the 2D extruded model result and a rough mapping will be done with the cross section where the electric field is the maximum (Figure 1-6).

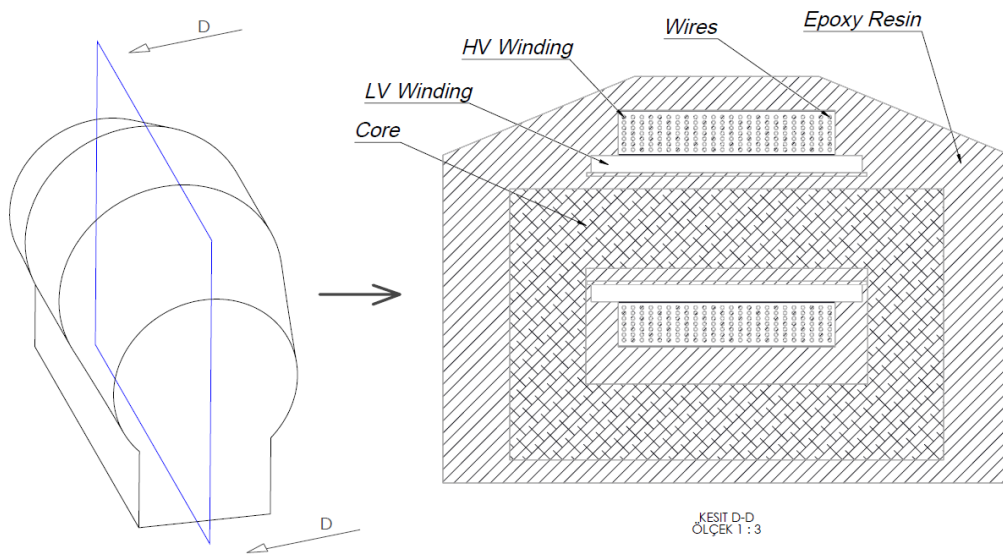


Figure 1-6 Cross section of a MV inductive voltage transformer

CHAPTER 2

EVALUATION & SOLUTION OF THE PARTIAL DISCHARGE PROBLEM

The aim of this section is first of all to provide a better understanding of the partial discharge (PD) phenomena. To be able to fix the PD problem which is the reason that GT30a has high failure rates the PD mechanism must thoroughly investigated.

In the literature failures of the solid insulations forced the investigation of the PD mechanism. The work on the partial discharges are started in 1960s and matured in 1970s and their calculation, test methods and responses under different circumstances are still argued[13].

Partial discharges are directly related to the breakdown strength of the insulating materials. The behaviors and limitations of the insulating materials used in MV voltage transformers must be determined to both evaluate the current design and to create a new design. To accomplish this goal the literature on the related insulating materials will be inspected.

Electrical parameters such as breakdown voltage or partial discharge inception level of the materials are not dependent on the applied voltage but rather the electrical field gradient. Field gradient distribution for the same voltage level is related to the design geometry and the properties of the utilized insulating materials.

The failure rate and trend of the transformer discussed in the chapter 1 does not indicates a serious design mistake but rather a field value being close to the limit of

the material. A randomly occurring mistake in the production process is also probable.

Possible small adjustments to the geometry which would reduce the electric field gradient at the critical points will be discussed and at they will be applied to the GT30a to fix the design without making major changes. The test data before and after the adjustments will be compared at the end of the chapter.

2.1. Partial Discharges

It is clear from the Table 1-4 that the main problem in the GT30a is the partial discharge levels being over the value allowed for voltage transformers in IEC 61869-1. A better knowledge of partial discharges is required to address this particular problem.

According to IEC 60270 partial discharge defined as a localized electrical discharge that only partially bridges the insulation between conductors and which may or may not occur adjacent to a conductor [14]. Electrical breakdowns, that causes partial discharges, happens when the electrical field stress exceeds the breakdown stress of the insulation material.

When the regional breakdown occurs the electric field rapidly changes and creates a current flow. This current should be large enough to be detected by the measurement equipment and must be repetitive enough to be distinguished from random noise. Only after that it will be diagnosed as the partial discharge. [15]

As in the case of GT30a, a design may pass the voltage withstand tests such as one minute power frequency test, standard lightning impulse test and still can have undesired partial discharges. The reason of this is partial discharges usually do not cause immediate breakdown of the insulating medium but slowly deteriorates it. If a device with partial discharge installed in the field it can fail at a random instance since partial discharges accelerates the aging process. The relationship between the partial discharge magnitude and the insulation life is normally linear. It is also a fact

that a device with higher discharge magnitude will not always fail before with a device with lower value.[16]

Partial discharges are caused by[17]:

- Breakdown in a cavity inside the dielectric material
- Breakdown in a tree inside the dielectric material (Figure 2-1)
- Breakdown in interfaces between different dielectric materials
- Breakdown in a foreign substance inside the dielectric material
- Breakdown around a floating conductor inside the dielectric material

Partial discharges, once incepted, bridge the gap the between electrodes by creating electrical tree in the insulating medium thus short circuit the electrodes[18].

Corona discharge is also a form of partial discharge where the medium is fully composed of dielectric gas. Similar to the PD when the field stress in a gas exceeds the breakdown strength, the gas around the conductor ionizes and acts like a conductor but fails to bridge between the electrodes[19]. Corona discharges occurring at gas insulated coil of the voltage transformer are dangerous since the energy released might damage the insulating paper and create a conductive surface. Test standard do not distinguish between corona or partial discharge, meaning that maximum electric field of the voltage transformers gas insulation should be below the corona inception voltage under the test conditions.

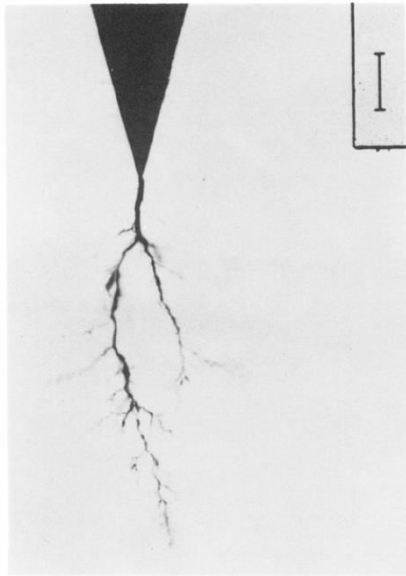


Figure 2-1 A branch type electrical tree growing through transparent resin insulation from a fine point electrode[20]

Partial discharges are not only dependant to the dielectric strength of the material but also the sizes of the cavities in them. As can be seen from Figure 2-2. where an EPR cable with different void diameters tested, partial discharge magnitudes are proportional to the cavity volume in the solid insulation. Vitality of the cavities in the solid insulation are also dependant on the position of the cavity. Small voids caused by the production errors can be tolerated if they are not situated at the high stress points of the transformer. Proper manufacturing of the solid insulation of the MV voltage transformers is required to prevent the formation of the cavities.

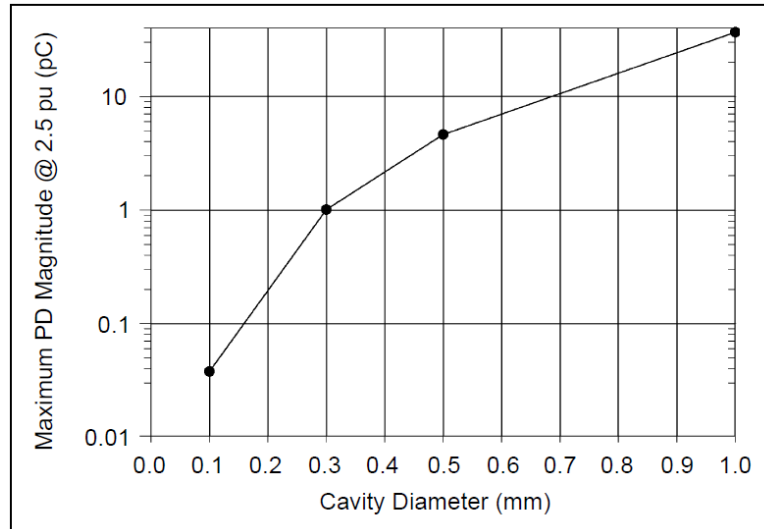


Figure 2-2 PD magnitude as a function of spherical cavity size for 15 kV, EPR cable geometry assuming that the cavity discharges at the peak of a 2.5 pu excitation (30 kV).[17]

2.1.1 Partial Discharge Detection Test

A transformer in the field can be exposed to short term surge voltages and is expected to operate safely after the surge is over. An overvoltage could form an electrical tree and trigger partial discharge. This discharge may continue even after the voltage drops back to the rated value. To simulate such condition, a partial discharge test is carried out after the power frequency test, which is the application of 1.5-3 pu of the rated line voltage. A partial discharge is allowed to occur at the peak voltage of the power frequency test but it should extinguish when the voltage is reduced to partial discharge test level. If the partial discharge test is not applied directly after power frequency test is repeated according to IEC 61869-1 clause 7.3.2.2

Expected lifetime of the solid insulation of the transformers reduces with the presence of the partial discharges. Even with the best equipment available it is hard to detect any signal below the 2 pC level due to electrical noises. To ensure some safety regarding the lifetime of the transformer the partial discharge test voltage itself is above the rated voltage.

The partial discharge equipment (Figure 2-3) used in the test of the GT30a have the maximum test voltage of 100 kV AC and noise level of 3 pC where maximum 5 pC of noise allowed according to IEC 60270.



Figure 2-3 Partial discharge test equipment (Biddle 666035-01)

To ensure the successful results from the partial discharge test each time, the insulating mediums in the gas insulated mv voltage transformer should not exceed their respective breakdown strength limits during the test. A suitable safety margin should also be adopted to reduce failures due to the non idealities such as void cavities caused by the manufacturing errors in the solid insulating mediums.

2.2. Insulating Materials Used in MV Voltage Transformers

In high voltage insulation applications there are various insulation materials in all gas, liquid and solid forms. The main parameter of the insulation material is dielectric strength which varies with the applied voltage being AC, DC or impulse. The other determining parameters of the material choice are the application conditions such as working temperature, type of the casing, humidity etc. and the cost.

The literature on the major insulating materials are settled over the past decades where major changes have been made. Introduction of the SF₆ gas led to development of gas insulated switchgears, advancement of the polymer technology changed the materials used in the power cables and transmission line insulators and resin technology allowed the construction of dry type power transformers.[21]

Urbanization trend shows that due to the increased wages in the major cities both city population and population density increase[22]. This leads to a dense energy consumption and increase the cost of the construction space. Therefore the power equipment, especially at the distribution level, should also be able to provide dense energy in smaller space to be cost efficient.

Fitting the systems with the same power rating to a smaller possible area is the goal of the high voltage equipment design. Optimizing the geometry of the devices would help to achieve this goal which will be practiced at chapter 3. Even with the geometry optimization, the final size of the high voltage devices still would be limited by the strength of the insulating materials. The properties of some of the most common material that are currently utilized are given in Table 2-1.

Table 2-1 Basic physical properties of major insulating materials [23]

| Material | Specific gravity (g/ml) | Relative dielectric constant | Dielectric loss tangent ($\times 10^{-4}$) | Volume resistivity ($\Omega\cdot\text{cm}$) |
|------------------------------|-------------------------|------------------------------|--|---|
| SF ₆ | 6.1×10^{-3} | 1.0 | --- | --- |
| Insulating oil (mineral oil) | 0.88 | 2.2 | 10 | 7.6×10^{15} |
| Kraft paper (oil immersed) | 0.7-0.8 | 3.5 | 38-39 | $2.3-2.4 \times 10^{15}$ |
| Pressboard (oil immersed) | 0.95-1.30 | 4.4 | 50 | 10^{16} |
| Epoxy resin (alumina-filled) | 2.3-2.5 | 5.9-6.2 | 20-50 | 10^{16} |
| Epoxy resin (silica filled) | 1.7-1.8 | 3.8-4.6 | 30-200 | 10^{16} |
| Feldspar porcelain | 2.3-2.5 | 5.0-6.5 | 170-250 | $10^{13} - 10^{14}$ |
| XLPE | 0.93 | 2.2-2.6 | 2-10 | $>10^{16}$ |
| Mica | 2.7-3.1 | 6-8 | 50 | $10^{14} - 10^{15}$ |

Gas insulated voltage transformers are constructed with three different insulation materials which are epoxy resin (solid), SF₆ (gas), insulating paper (solid). Epoxy resin is used to construct the outer envelope of the transformer while the paper provides mechanical support and insulation in between layers of magnet wire. Lastly a pressurized SF₆ fills in the gaps in the coil and increases the overall electrical strength of the coil.

Since there is more than one type of insulation included, the distribution of the electrical field will be effected by the difference of the relative dielectric constants and the design should be done with accordance.

2.2.1 Properties of the Epoxy Resin

Epoxy resin is a mixture consisting of filler (silica, alumina or similar materials), hardener, resin, accelerator and depending on the application flexibilizer. Epoxy resins are widely used in the both low voltage and high voltage applications. In this application the epoxy resin casing of the transformer both provides electrical insulation and mechanical support.

As a solid insulation, epoxy resin has unpredictable breakdown behavior under AC voltage [23]. The breakdowns are caused mostly by the partial discharge. Starting point and the magnitude of the discharge effects the breakdown characteristics. The breakdown time and breakdown voltage both varies in a large range because of the randomness of the partial discharge location [23]. The interpretation of this is the field strength should not be critically close to specified breakdown value of the resin.

Epoxy resin casting has three production steps

- 1) Preparation of the resin mixture
- 2) Casting & curing
- 3) Post-curing

Curing is the process where the chemical bonds of the resin mixture changes at a certain temperature and it takes its solid insulating form. The details of these steps are dependent on the type of the resin used, volume of the product and the casting type.

The mechanical and the electrical properties of the epoxy resin mixture varies with the mixture receipt and resin preparing process. The percent by weight of the materials in the receipt that is used in the manufacturing of the GT30a is given at Table 2-2.

Table 2-2 Epoxy resin mixture receipt

| Mixture | Used | Recommend |
|-----------------|---------|-------------|
| Resin | 100 pbw | 100 pbw |
| Hardener | 85 pbw | 85 pbw |
| Flexibilizer | 20 pbw | 0-20 pbw |
| Accelerator | 0.8 pbw | 0.5-1.5 pbw |
| Filler (Silica) | 385 pbw | 345-385 pbw |

When creating the receipt, electrical breakdown strength should be prioritized over the mechanical properties for the GT30a. The limitations in this application are more electrical than mechanical since there is no force applied on the resin under normal operating conditions.

Flexibilizer should be added at the maximum allowed amount because it reduces the internal mechanical stresses in the epoxy resin. The transformer is susceptible to the thermal shock when it is first released from the mould. Flexibilizer reduces the chance of a micro crack formation. However adding flexibilizer decreases the glass transition temperature (T_g) of the epoxy resin. This is ignored due to the low power nature of the MV voltage transformers.

The electrical properties of the mixture given at the Table 2-2 is as following :

Table 2-3 Electrical properties of the epoxy resin mixture

| Electrical Properties | Test Standard | Value | Unit |
|--------------------------------|---------------|------------------|----------------|
| Breakdown Strength | IEC 243-1 | 24 | kV/mm |
| HV Arc Resistance | ASTM D 485 | 185-190 | s |
| Tracking Resistance solution A | IEC112 | >600-0.0 | CTI |
| Tracking Resistance solution B | IEC112 | >600M-0.0 | CTI |
| Loss Factor (50°C) | IEC250 | 42796 | % |
| Dielectric Constant (50°C) | IEC250 | 4 | E _r |
| Volume Resistivity (50°C) | IEC93 | 10 ¹⁵ | Ω*cm |

Behavior of the resin mixture is dependent on the preparation process. To achieve the properties given at Table 2-3 for every production batch, the process must be

controlled. The temperature, humidity of the facility must be stable. There should be no air current in present to prevent the thermal shock. To avoid the errors caused by the human factor, the resin should be prepared in a fully automatic enclosed system.

After resin mixture is prepared it is casted into the mould. Epoxy resin can be casted either under vacuum or pressure. Epoxy resin casting methods are as following:

- Conventional Casting : The resin is filled to the mould under vacuum. Has long casting and post curing time. Moulds are cheap but multiple moulds are required for the serial production.
- APG : The resin is filled to the mould under pressure. Has short casting and curing time. Final quality is dependent on the ability of the mould to extract the air in the filling process. Moulds are expensive and they get damaged over the time fast due to the pressure.
- Conventional Casting with SF₆ : The resin is filled to the mould under SF₆. Has similar characteristics with the conventional casting. The cavities inside the resin is filled with SF₆ instead of air therefore strength of the cavities increases.

In GT30a the conventional vacuum casting method is utilized. Casting duration is 4 hours and the post cure duration is 12 hours. The electrical strength of the resin will be taken as 24 kV/mm for the analysis. The dielectric constant given in the datasheet of the resin has been verified with a Schering bridge equipment by using 6mm resin plate since it may vary with the mixture and the process.

2.2.2 Properties of the Insulating Paper

Cellulose based insulation papers are mostly used in junction with the mineral oils to provide electrical insulation in the power transformers[24]. There are two reasons behind the usage of the mineral oil as a medium. First the dielectric strength of the paper in oil about 5 times stronger than it is in the air. Secondly the mineral oil also

provides cooling for the coil. For the MV voltage transformers the mineral oil cannot be utilized in junction with paper because it hinders the adhesion between resin and the coil.

The rated load of GT30a is 10 VA. With such low power output the cooling of the transformer is not an issue in the design. Insulating gas is used as an insulating medium instead of mineral oil to compensate the low dielectric strength of the paper. With the insulating gas filled in to the coil and covered the area around the wires, purpose of the paper reduces to providing mechanical support to the wires to hold them in space.

Properties of the insulation paper used in GT30a are given in the Table 2-4 ;

Table 2-4 Electrical properties of the insulating paper used in GT30a

| Properties | Standard | Value | Unit |
|----------------------------|--------------|---------|-------------------|
| Thickness | IEC60641-3-2 | 30± 10% | micron |
| Density | IEC60641-3-2 | 1.0-1.2 | g/cm ³ |
| Electrical Strength in air | IEC60641-3-2 | ≥8 | kV/mm |
| Dielectric Constant (50°C) | IEC60641-3-2 | 2.3 | E _r |
| Moisture Content | IEC60641-3-2 | ≤ 8% | |

The moisture content should be removed by thermal treatment before the epoxy resin casting. The thickness tolerance of the paper will affect the coil design. More precise the paper thickness is the smaller the safety margins could be selected in the coil design.

2.2.3 Properties of the Insulating Gases

Insulating gasses are commonly utilized in the power applications such as gas insulated substations, gas insulated transmission lines, gas insulated transformers, gas insulates circuit breakers etc.[25]. A good insulation gas should have following properties[26]:

- High dielectric strength (relative to air)
- High vapor pressure

- High thermal conductivity
- Chemically inertness

Non-flammable, non toxic and non explosive

SF₆ is a gas that have all of these properties and had been used since 1947 [27]. It is still widely used in the power system equipment manufacturing and it will be the choice of insulation gas in GT30a.

As an insulating gas SF₆ have almost constant breakdown voltage under same conditions although the time to breakdown may vary[23]. This allows construction of a precise design.

The SF₆ is injected into the coil under 5 bar pressure. Although there is a routine leakage test (Table 1-2), MV voltage transformers may leak SF₆ over the years and the gas pressure would drop to the atmospheric pressure.

The corona inception voltage of the SF₆ gas with normal conditions under non-uniform electric field is about 9kV/mm [28].

The corona extinction voltage is more critical than the inception voltage due the nature of the partial discharge test which is argued in 2.1.1. The corona extinction voltage versus the corona inception voltage rates under AC voltage varies between %87-%80 , with the different electrode setups that represents the possible errors in the gas insulated equipments [29].

SF₆ gas is a potent greenhouse gas. In the short term the amount of gas present in the atmosphere is negligible but in the long run it would accumulate in the atmosphere [25]. In the literature it is argued to replace SF₆ gas with possible alternatives . N₂ gas mixtures with small amount of SF₆ is the current solution to reduce amount of the SF₆ released in to the atmosphere.

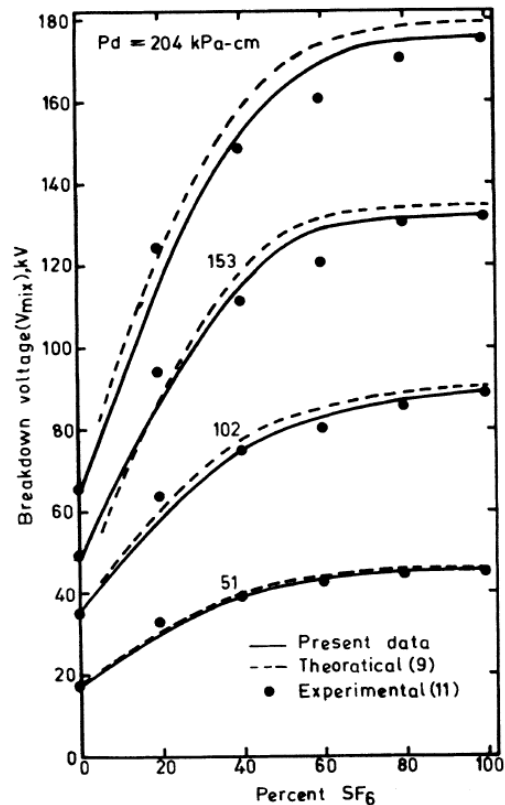


Figure 2-4 Breakdown voltages (V_{mix}) as a function of percent SF₆ in SF₆-N₂ mixtures[30]

The N₂+SF₆ gas mixture could be adapted to the GT30a and the proportion of the mixture could be determined by the volume margin that will be gained from the finite element modeling as the more N₂ in the mixture lower the dielectric strength gets (Figure 2-4).

2.3. Manufacturing Process

The manufacturing process of mv resin & gas insulated voltage transformers have common steps in general. Manufacturing error in one of the steps would cause the partial discharge problem therefore control of the process at each step is required. The production steps of the GT30a are as following;

- 1) Winding of secondary coil on to the mandrel, winding of the insulation between the primary and the secondary coil. Winding of the primary coil (Figure 2-5).

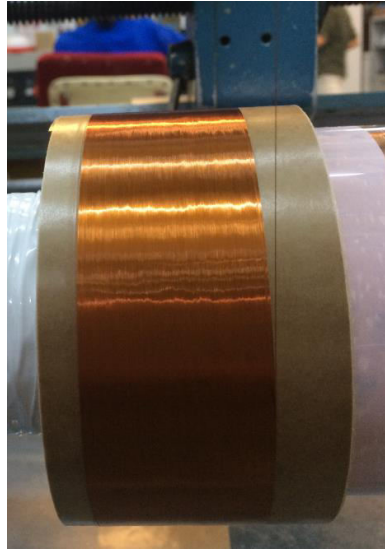


Figure 2-5 Winding of the primary coil

- 2) Attachment of the coil on to the core, coverage of the core with carbon paper & paper insulation.
- 3) Accuracy class control and visual control of the coil to check for winding errors
- 4) Heat treatment of the coil to evaporate the moisture content (Figure 2-6).



Figure 2-6 Transformer coils under heat treatment

5) Assembly of the winding in to the mould (Figure 2-7), pre-heating of the coil & mould to the resin injection temperature

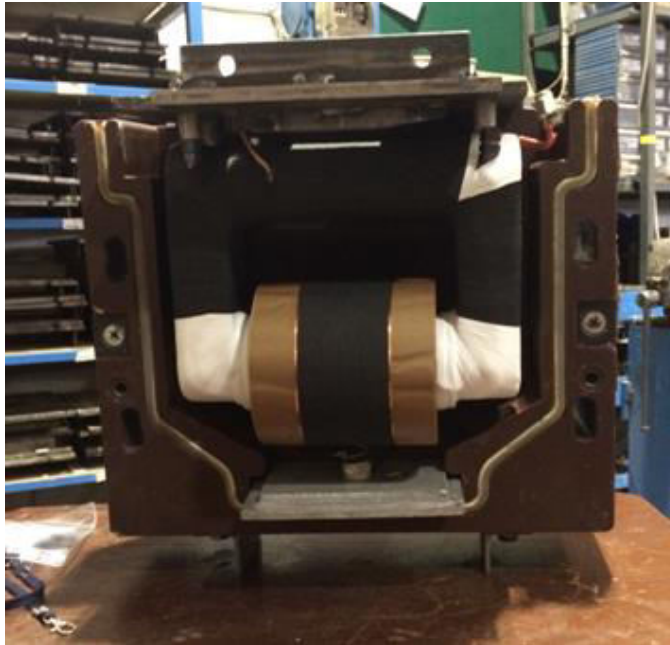


Figure 2-7 Winding assembly in to the mould

- 6) Epoxy resin injection under vacuum
- 7) Curing of the resin
- 8) Detachment of the mould from the coil & post curing of the resin.
- 9) Gas injection & sealing
- 10) Application of the routine tests given in the Table 1-2.

2.4. Factors Effecting the Electrical Field Distribution

Electrical field gradient inside the coil, between the layers of the coil and the core in the GT30a is assumed to be lower than the respective breakdown strength of the epoxy resin, insulating paper and the SF₆ gas used in the construction of the transformer since the design was able to past the type tests and the partial discharges are not occurring in every transformer manufactured. The random

occurrence of the discharges are indicates either a field value being is too close to the critical value or a manufacturing mistake.

Instead of modeling and analyzing the high voltage coil at this stage, possible adjustments to the design are going to be discussed to relieve the electrical stress at the critical points and to make the coil more resistant to the manufacturing errors.

2.4.1 Usage of the Electric Field Screen

At the top and the bottom part of the primary winding two copper screens are used to regulate the electric field similar to their usage in the high voltage cables (Figure 2-9). The bottom screen is at the ground level and the top screen is at the bus-bar voltage. There should be holes on the screen if the gas needs to be able to pass. In GT30a, the bottom screen has holes for this purpose (Figure 2-8).

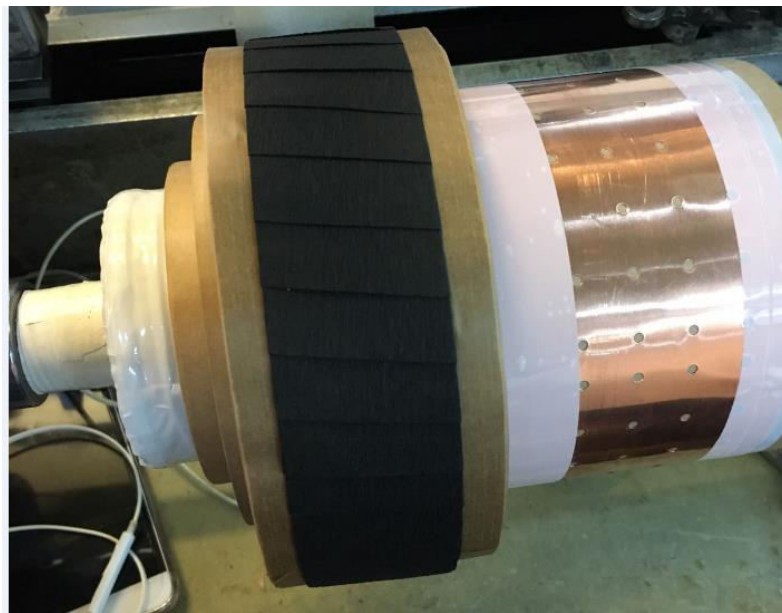


Figure 2-8 Top view of HV screen (covered with carbon paper) and ground screen of a gas insulated MV voltage transformer

Carbon paper is wrapped on top of the high voltage screen in order to increase the adhesion to the epoxy resin. Usage of the carbon paper is optional: if the screen surface that is utilized has good adhesion with the epoxy resin it can be omitted from the design.

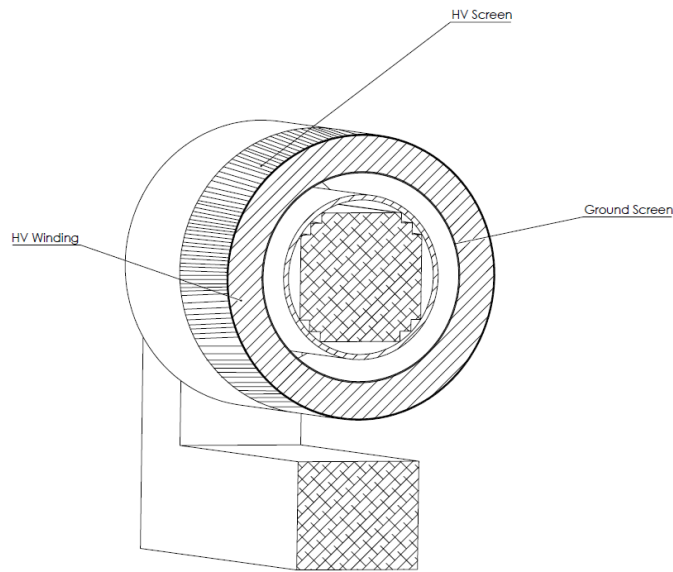


Figure 2-9 Screen positions in a HV winding of a MV voltage transformer

Positioning and the size of the screen affect the field distribution. As the size of the screen increases the maximum electrical field would drop due to the geometry. Making the screen large increases the cost. Large volume of screen also may cause cracks in the resin because of the expansion and contraction of the copper during the transformer curing stage.

To observe the effect of the screen a sample coil will be simulated in the x-y (Figure 2-10) plane by Maxwell. (accuracy of this type of analysis will be discussed in later steps) Wire diameter is selected as 0.12 mm. Winding voltages kept constant for each simulation.

The values that are presented in the Table 2-5 are only for comparison purposes.

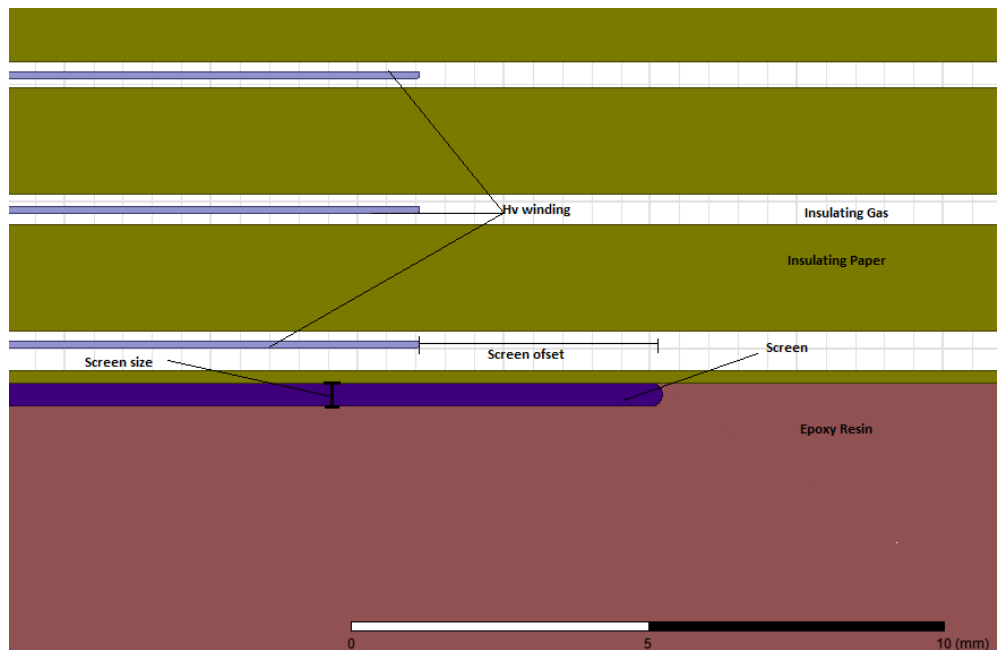


Figure 2-10 Side view of the coil and the screen on Maxwell x-y plane

Table 2-5 Simulation results for different screen size and positions for Figure 2-10

| Screen Size (mm) | Screen Position offset (mm) | Max Efield in the Resin (kV/mm) | Max Efield on the tip of the winding (kV/mm) |
|------------------|-----------------------------|---------------------------------|--|
| 0.1 | 0 | 13,86 | 12,6 |
| 0.1 | 2 | 16,16 | 6,98 |
| 0.1 | 4 | 16,93 | 6,57 |
| 0.2 | 0 | 10.31 | 11.90 |
| 0.2 | 2 | 11.58 | 6,93 |
| 0.2 | 4 | 11,90 | 6,52 |
| 0.4 | 0 | 7,57 | 10.84 |
| 0.4 | 2 | 8,36 | 6,9 |
| 0.4 | 4 | 8,67 | 6,36 |

Remarks;

- The high voltage screen can be positioned few millimeters in front of the last layer of the wires to reduce the stress in the gas while sacrificing the stress in the epoxy resin.
- Overall performance is better with larger screen usage.

2.4.2 Effect of the Dielectric Constant in the Field Distribution

In gas insulated mv voltage transformers there are three different types of insulation material is used as discussed in section 2.2. Each of the materials has different relative dielectric constant and this will affect the electric field distribution.

To evaluate the impact of the E_r on the electrical field distribution two examples with the same cylindrical electrode setup will be simulated. Each electrode has 40 mm diameter. Spacing between the two electrodes is selected as 6mm. Applied voltage is 1 kV. The analysis type is cylindrical around 2D, Z axis. Inspecting the following two example setups will provide hints for the design.

Example 1: Material E_r is selected as 2. The uniformly distributed electric field value is 0,166 kV/mm as can seen from the Figure 2-11.

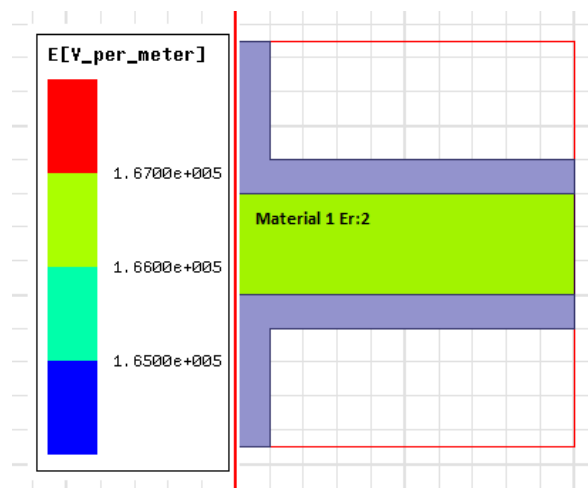


Figure 2-11 Electric field distribution in a medium with single type dielectric

Example 2: Material 1 on the top side has the E_r value 2 and the material 2 bottom has the E_r value 4. Sizes of the dielectrics are the same. In the simulation the electric field value of the material 1 is 0.22 kV/mm and material 2 is 0.11 kV/mm as can be seen from the Figure 2-12.

When both examples are compared it is observed that the maximum electric field increases if there is more than one type of insulating. This increase would be more significant if the difference between the material dielectric constants is large. The

material with low E_r will have more field drop on itself. This is basically a voltage distribution between the capacitances since every dielectric is a capacitor.

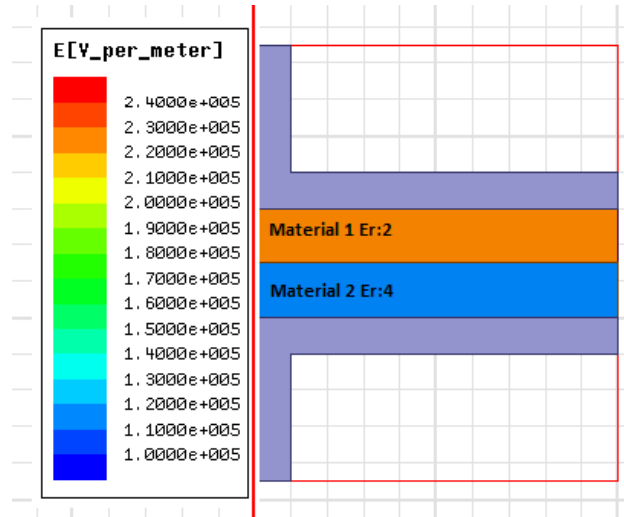


Figure 2-12 Electric field distribution in a medium with two different dielectric

E_r values of the materials used in GT30a and their respective dielectric strength is shown in the Table 2-6.

Table 2-6 Dielectric constants and strength of insulating materials used in GT30a

| Material | Dielectric Constant | Dielectric Strength (kV/mm) |
|-------------------------|---------------------|-----------------------------|
| SF ₆ (1 bar) | 1.002 | 9 |
| Insulation paper | 2.3 | 8 |
| Epoxy resin | 4 | 24 |

Because of its high dielectric constant, the presence of epoxy resin would increase the stress on the insulation paper and the SF₆ gas. Therefore minimal amount of epoxy resin should be used to relieve the stress on the gas and the insulating paper.

Winding of the GT30a is produced with three different types of layers with different length which will be discussed in chapters 3&4. When there is transition from one type of the layer to the another the paper may be cut with respect to the upcoming layer (Figure 2-13) or can be kept at the same length (Figure 2-14).

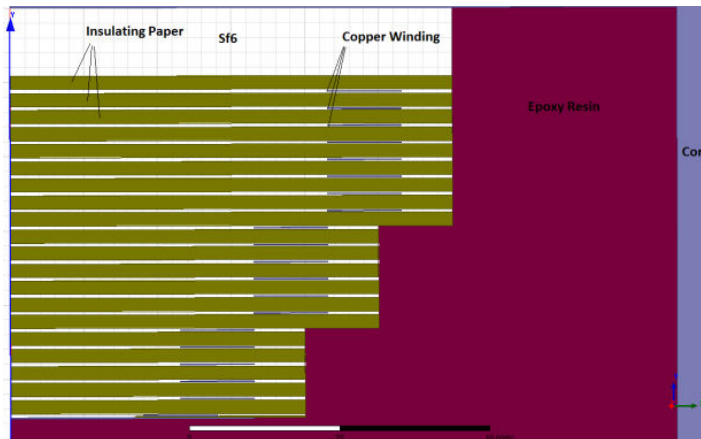


Figure 2-13 Slice of the transformer with stepped paper

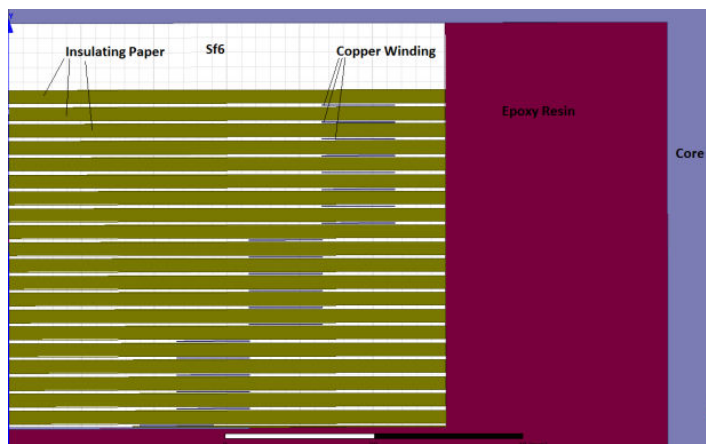


Figure 2-14 Slice of the transformer with constant paper length

The only advantage of the transformer with stepped paper orientation is the slight field stress reduction on the epoxy resin which can be compensated by increasing the screen diameter as discussed in the section 2.4.1. However when the straight paper is used the electrical stress in both in SF₆ and insulating paper decreases. Furthermore, the amount of the resin used in manufacturing also reduces.

Remarks ;

- Material with similar dielectric constants should be selected whenever it is possible or the material with lower dielectric constant should have higher dielectric strength

- Geometry of materials with high dielectric constant should be designed such that its amplification of the electric field on to the materials with lower dielectric constants would be limited

2.4.3 Sealing of the Coil Ends

After the winding process is completed the epoxy resin mixture is injected to the mould containing the coil. Although the resin itself has viscosity around 15000 mPa·s at the injection temperature there is a chance that epoxy resin may penetrate inside the coil from the side (Figure 2-15).



Figure 2-15 Side of the coil after the winding process

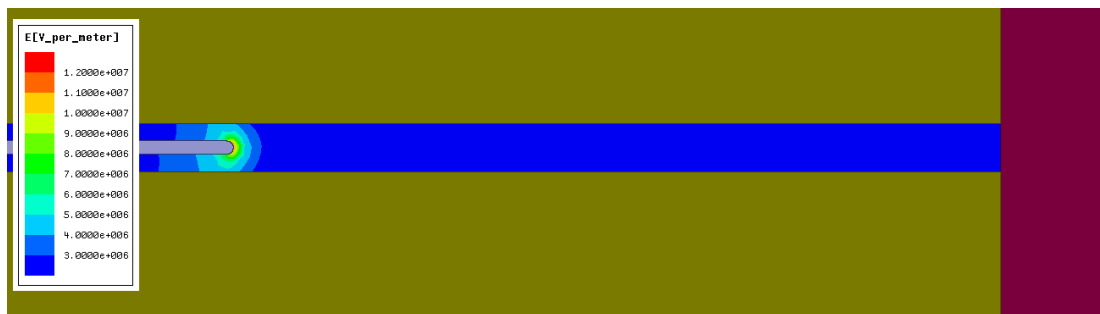


Figure 2-16 Coil without epoxy resin penetration

There are two possible dangerous situations when the epoxy resin is inside the winding :

- The dielectric constant of the resin is higher than the SF₆ and the insulation paper so the filling of the coil with resin would amplify the field stress both of them as discussed in section 2.4.2 (Figure 2-17)

- The resin may trap air and create a large cavity in the surface of the conducting wire and directly trigger the partial discharge and possibly insulation failure as discussed in section 2.1 (Figure 2-18).



Figure 2-17 Coil with epoxy resin filled in between insulation papers

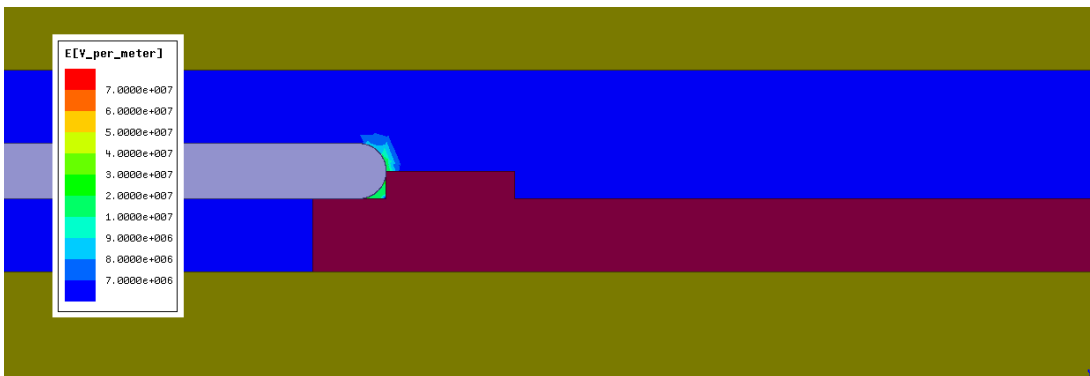


Figure 2-18 Coil with cavity caused by the epoxy resin on the conductor surface

When the results are inspected, it has been found out that the field stress increased about %50 percent when there is presence of the resin in between the insulation papers. When there is a cavity formed the maximum stress is 6 times more than what it should be. Both situations increase the risk of partial discharge at the test voltage.

To prevent the entry of the resin in to the high voltage coil, the coil sides should be covered before the resin injection process (in between the steps 4 and 5 mentioned in section 2.3). The material that the side is covered must have high surface tracking resistance to prevent the surface flashover under operating conditions. The material should also be compatible with the resin used and should not cause any adhesion problems. Lastly, the material should be able to withstand the temperatures at the

curing and the post curing stages of the MV transformer without decomposing. Room temperature cured epoxy resin based AW106 (Table 2-7) manufactured by the Huntsman found to have suitable characteristics.

Table 2-7 Properties of AW 106

| AW 106 | Value | Unit |
|-----------------------------|----------------------|--------------------------|
| Cure Temperature / Duration | 20-150/15-0.1 | °C/hours |
| Dielectric constant | 3.4 | Er |
| Surface resistivity | 1.2×10^{16} | Ω |
| Volume resistivity | 10^{15} | $\Omega \cdot \text{cm}$ |

A thin layer of AW106 should be applied to the side surfaces and cured before the epoxy resin injection (Figure 2-19). This would prevent the intake of the resin to the coil and all the coils would have the expected field distribution as shown in the Figure 2-16. Similar materials can be used for this application. Physical strength of the material used also should be checked if the APG is used instead of the vacuum casting since the pressured resin may tear the material used.



Figure 2-19 AW106 applied coil surface

2.4.4 Modification of the Original Design

So far the factors that may affect the field distribution and therefore the partial discharge inception has been discussed. The following adjustments will be applied to the GT30a without changing the main coil design.

- Original copper screen of the GT30a was 0.1 mm thick and utilized in conjunction with 0.1mm carbon paper. The offset of the screen was zero. The thickness of the copper screen will be increased to 0.2 mm and the offset will be changed to 2 mm.
- There was no precaution for the resin penetration in to the coil in the original design. Coil sides will be covered in the modified design with AW106 as described in section 2.4.3.
- The insulating papers will be kept at full length throughout the coil in the modified design to keep the resin away from the winding.

As the result of these modifications the puncture problem is completely eliminated due to the reduction of the electric field (the amount will be calculated in chapter 4) and prevention of the epoxy resin penetration in to the winding. Occurring frequency of the partial discharges have also been reduced to acceptable levels as can be seen in the Table 2-8. Further improvement in the routine test past rate can be done by idealizing the production process and using lower manufacturing tolerances for this modified design.

Table 2-8 Routine test results comparison of the modified and original GT30a

| Design | Produced | Puncture (7.3.1) | | PD (7.3.2) | | Total failure due to PD and puncture | Percent |
|-----------------|----------|------------------|------------|------------|------------|--------------------------------------|---------|
| | | Count | Percentage | Count | Percentage | | |
| Original | 4206 | 94 | 2.2% | 509 | 12.1% | 603 | 14.3% |
| Modified | 240 | 0 | 0% | 3 | 1.25% | 3 | 1.25% |

2.5. Chapter Summary

In this chapter general knowledge about the partial discharges and the electrical properties of the insulating materials that are used in mv inductive voltage transformer have been obtained. These data will be valuable in the further chapters when evaluating the simulations.

Possible small adjustments that would reduce the stress at the critical points to the transformer have been discussed. These adjustments have been applied to the

transformer without changing the high voltage coil design. As a result the fail rates due to the partial discharges have been reduced to the acceptable levels. Puncture has been occurred in none of the 240 modified transformers produced.

With the partial discharge and the related puncture problem fixed the focus in the following chapters will be diverted to the design of the high voltage coil in order to fulfill the remaining objectives mentioned in section 1.2. Although the major problem in the GT30a is fixed through the modified design, the high voltage coil can be still improved by modeling the electric field distribution. In chapters 3&4 a final design will be created with the help of the FEM and in the last two chapters the modified design, original design and the final design will be compared in terms of performance and cost.

CHAPTER 3

LAYER DESIGN & MODELING

The objective in this chapter is to develop feasible modeling methods for the layers and apply the developed approach on the GT30a. The different layer types will be constructed and the idea behind them will be inspected with the help of finite element analysis method and suitable layer layouts for the gt30a design will be determined.

Repeated wire geometries inside the coils are named as layers. The coil of a single phase voltage transformer is constructed on a rectangular core by winding the wire in the limited area as shown in Figure 3-1. The required number of turns is commonly above 10000 turns in the high voltage coil. Initially layers are designed and then they are repeated until the required number of turns is reached. In a high voltage coil there could be more than one type of layer.

Literature is mainly focused on the power transformer winding design where the transient response, therefore the capacitive modeling & distribution, is the main problem[31]. There are different winding methods such as disc winding, interleaved winding, shielded winding to manufacture the winding to deal with this problem[32]. In power transformers proper cooling is also a requirement in the coil design. Voltage transformers operate at low powers (1-100 VA), therefore the thermodynamic aspect of the layer design will be ignored. Since the structure and the operational problems are different than the power transformers the focus of the MV voltage transformer coil design will be on the partial discharge performance. In

other words the uniformity of the electric field under the steady state condition will be the most important aspect studied in this chapter.

Ease of manufacturing of the coil is also an important parameter in the design since the complex layer design would not only increase the winding duration, but also increases the chance of a failure during the coil production.

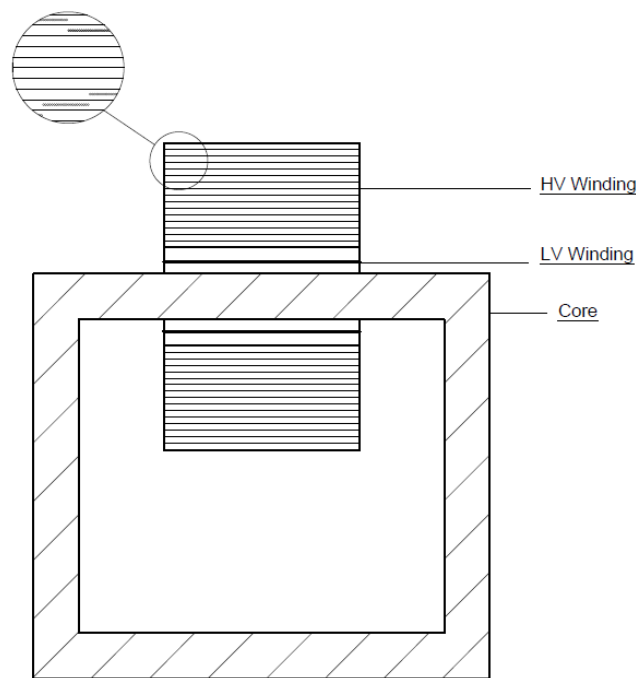


Figure 3-1 Winding section of a voltage transformer

3.1. Basic Layer Structure

Layers are symmetrically designed to provide a smooth distribution of the electrical stress. The main objective of the layer design is to fit the limited area maximum amount of wires while keeping the electrical stress under the predetermined limit value. In order to use the area efficiently, the field stress should be as uniform as possible inside the layer but there are real world limitations such as minimum available insulating paper thickness.

The most simple approach when constructing a layer is to wind the wires in a straight line on to the core while adding the same number of insulating paper with

same thickness in between to ensure symmetry as presented in Figure 3-2. Winding process starts at the one side and continued to the other. When the winding length is reached, insulating papers are wounded on top the wire line and then the turns continue in the opposite direction until again the layer length reached. The process is repeated for each layer until the total number of the turns is obtained.

In order to inspect the electric field distribution inside a layer, finite element analysis are carried out with an example layer that has the data given in Table 3-1. Normally the wires are held in the space with the help of the insulation paper but in this example the presence of the paper is ignored in sake of simplicity.

Table 3-1 Layer simulation parameters

| | | | | | |
|------------------------------|----------------------------------|-------|-----------------------------|-----|---------|
| Total Number of Turns | 200 | turns | Vdrop per turn | 1 | V |
| Wire Diameter | 1 | mm | Layer Inner Diameter | 200 | mm |
| Layer Area | 40x140 | mm | Simulation Error | 0.1 | percent |
| Simulation type | 2D analysis cylindrical around Z | | | | |

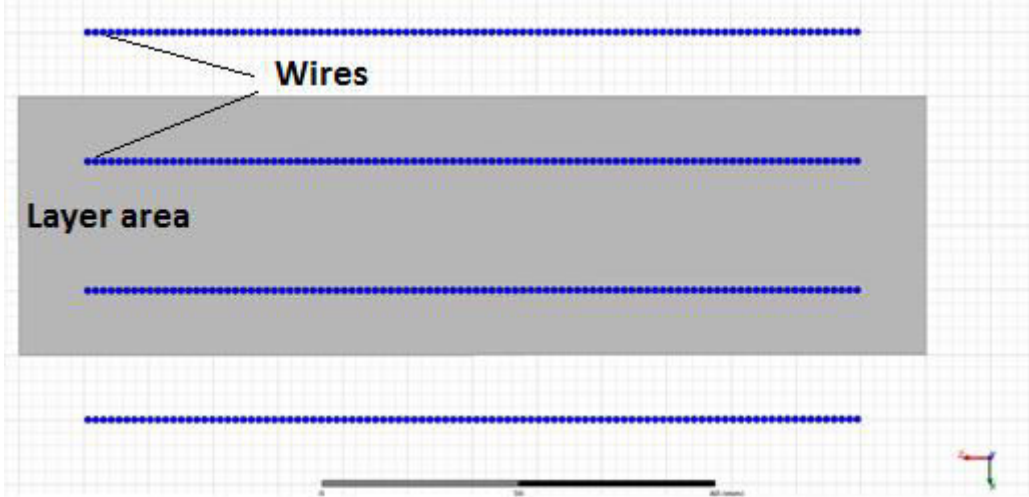


Figure 3-2 Straight layer design

The layer area can be defined as the area of the repeating section with at least one upper and one lower side that covers the whole winding length as shown in Figure 3-2. Voltage increases step-wise as the number of turns increases and the largest

potential difference occurs between the first and the last turn of the winding highlighted with purple circle in the Figure 3-3. Unfortunately it is not possible to put the first and the last turn of the winding in the opposite ends of the layer due to the technique of the winding process. This results in the largest potential difference being situated with the closest proximity turns of upper and the lower part.

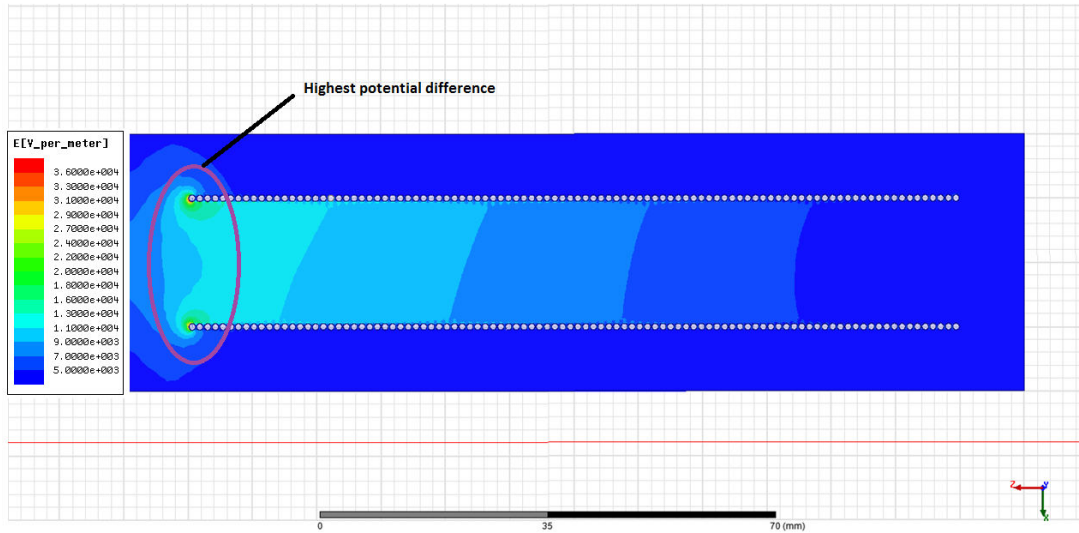


Figure 3-3 Electric field distribution in straight layer design

It is clear from the Figure 3-3 that the electric field is distributed in a highly non-uniform manner across the straight layer. As expected, the highest electrical stress is occurred at the most outer turns of the layer where the potential difference is the highest. The electrical field at the opposite end of the layer is about 10 times smaller which means that the insulation thickness at this part is unnecessary, that makes the layer larger and more expensive than it could be.

In an effort to increase the distance between the high field intensity generating points and reduce the insulation thickness at the low field end, an additional step has been added to the design while keeping the layer area same (Figure 3-4). Then the analysis is repeated under the same conditions as shown in Figure 3-5.



Figure 3-4 Two step layer design

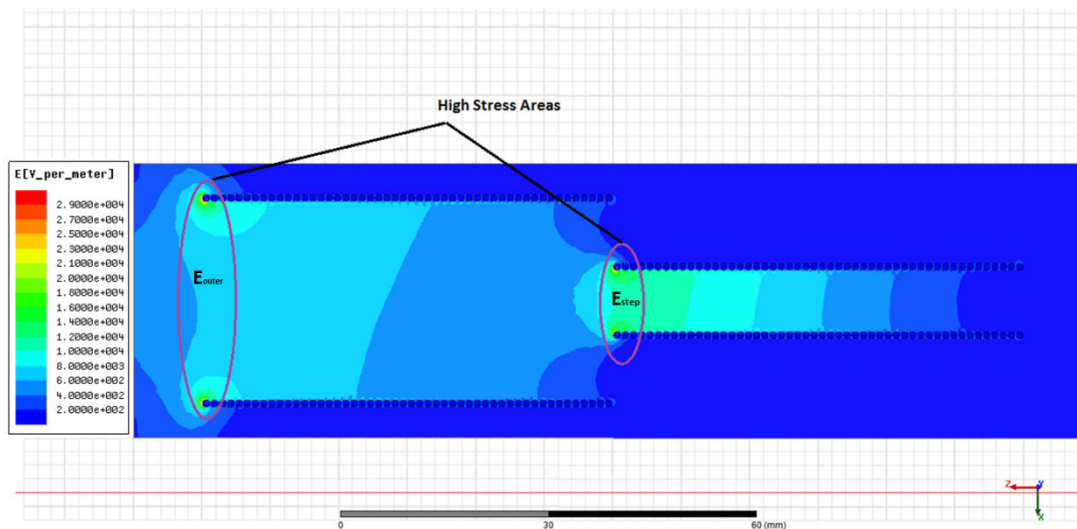


Figure 3-5 Electric field distribution in two step layer design

It can be seen from Figure 3-5 that introducing a step in the middle of the layer instead of continuing the wires in a straight line reduced the maximum electric field intensity from 0.035 kV/mm to 0.028 kV/mm, which is around 20 percent less. The meaning of this is the layer can be fit into a smaller area than the straight design with the same maximum field stress value thus reducing the whole coil. Another important point is that there are now two critical parts instead of a single critical

point in the layer highlighted with purple circle in Figure 3-5 where the electrical field is intensified.

3.2. Minimization of the Electrical Field

It is clear that adding steps helps to reduce the field stress however a better understanding of the relation between the number of steps and the maximum field intensity should be established. If there are no other constraints best design would be the one with lowest electric field intensity. Geometry thus the number of steps for the minimum electric field in a layer can be determined with GA optimization. Position of the turns in the layer area will be used as the input variables.

GA is a robust method of solving complex problems while providing a number of potential solutions, different from the deterministic optimization algorithms the others which point out a single point in space[33]. GA searches a large space of solution and at each cycle creates a new space of solution with using the most successful results. This enables GA to avoid the local minimums in the optimization process. Since the problem at hand involves local minimums GA is decided to be the most suitable choice.

A small simulation example given at the Table 3-2 will be used. The cost function of the optimization is selected as the maximum electric field that occurs in the layer and the objective is to minimize. Thirty generation of solutions simulated with each having one hundred individuals.

Table 3-2 Simulation parameters of the layer used in the GA

| | | | | | |
|------------------------------|----------------------------------|-----------------|-----------------------------|-----|---------|
| Total Number of Turns | 40 | turns | Vdrop per turn | 1 | V |
| Wire Diameter | 1 | mm | Layer Inner Diameter | 200 | mm |
| Layer Area | 30x70 | mm ² | Simulation Error | 0.1 | percent |
| Simulation type | 2D analysis cylindrical around Z | | | | |

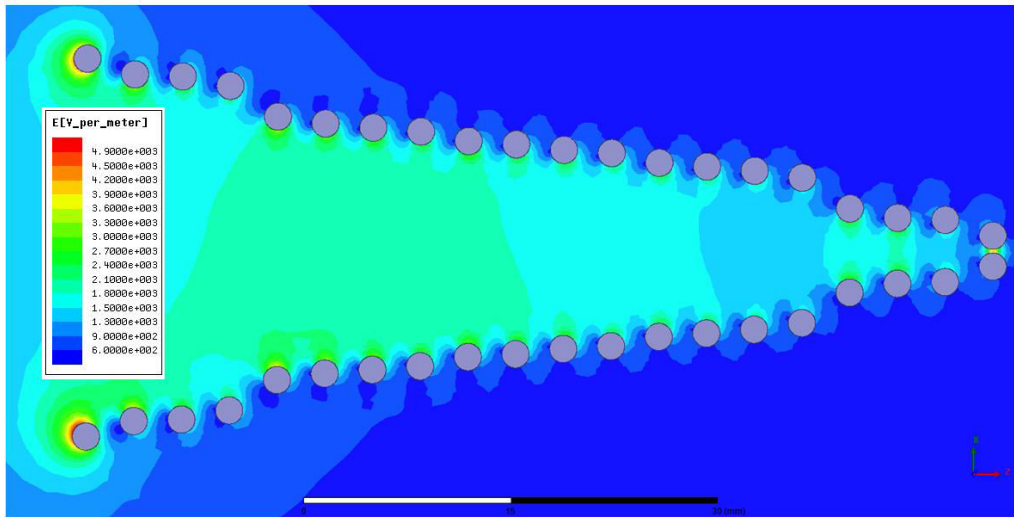


Figure 3-6 Result of the initial GA optimization

When the solution of the optimization given at Figure 3-6 is inspected, it is clear that although some turns have very close positioning, none of the turns are standing at the same line. It can be concluded that in order to achieve the lowest possible maximum field intensity the step number must be equal to the number of turns of the layer. However such design is impractical in MV voltage transformers because of the requirement of nanometer range insulating paper to position the high number of turns which is not available in the market.

This genetic algorithm approach where all the turns have different positioning can be used to design a layer if the number of turns is To increase low in the layer, the required insulation thickness is available and there are no other constraints then the electric field intensity.

3.3. Reduction of the Computation Time

The total time elapsed in a finite elements simulation depends on the number of variables and complexity of the geometry. The duration of the simulation is an important aspect since the modeling method developed in this thesis will be applied to the designs in regular basis.

The geometry of the layers are already simple due to the symmetry around the Z axis but the number of the variables are high because of the number of turns in a MV voltage transformer coil. If an unimportant section of layer a layer can be ignored it would reduce the computation time.

The maximum electric field value has determined by the most outer part of the layer in the analysis that have been done up to now. When the layer modeling is modified by removing some of the inner turns which has less impact on the field intensity while the keeping the position of the outer part turns same as the GA result, following field distribution shown in Figure 3-7 is obtained.

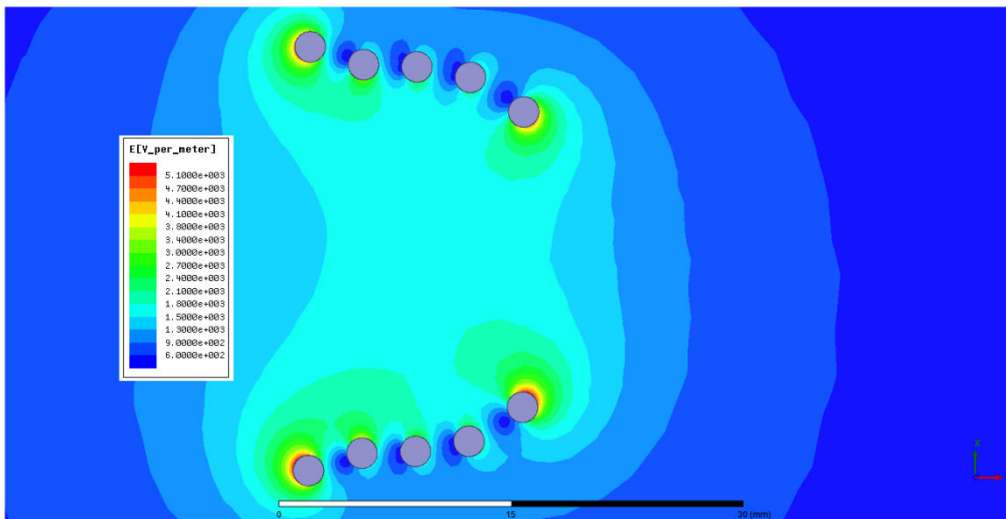


Figure 3-7 Modification of the GA solution where the 30 turns are removed

When the results are compared, the original GA result has a maximum field intensity of 4821 V/m with 40 turns and the modified has 5062 V/m with 10 turns analyzed. The error between the original and the modified model is calculated about %5 percent. Although the simulation result did not change a lot, %75 percent of the layer is removed which reduces the computational time.

If approach of only analyzing the outer part can be applied to the common voltage transformer layer, the speed of the analysis can be increased. Also denser meshing can be applied to increase the accuracy without overwhelming the available computational power.

3.3.1 Determination of the Minimum Possible Model Area

It has been proven that removing a part of the layer reduces the computational time while sacrificing some accuracy. The issue is to determine the percentage of a mv voltage transformer layer can be removed from the simulation model without hurting the analysis results significantly.

A typical voltage transformer coil layer shown in the Figure 3-8 will have over 1000 turns and thus would take a lot of time to exactly model and optimize. Also a very powerful computer is required to do the proper meshing. Therefore it is almost a must that the modeling should be simplified enough to be feasible if it is targeted to be carried out for each design.

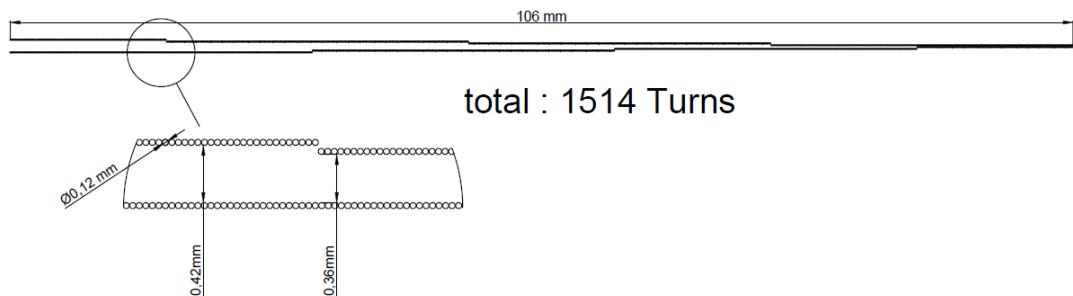


Figure 3-8 MV voltage transformer layer example

The layer designs that are used in MV voltage transformer will consist of long straight sections unlike the design proposed by GA in Figure 3-6, which can be used as an advantage. If the minimal length required to represent the whole layer with minimal error margin can be determined the finite element analysis can be executed in a shorter time frame.

In order to determine this minimum layer length it is assumed to have a layer with properties given in the Table 3-3.

Table 3-3 Simulation parameters for the minimum length determination

| | | | | | |
|-----------------------------------|----------------------------------|-------|---------------------------------|-------------|---------|
| Total Number of Turns | 800 | turns | Insulation Thickness (a) | 0.1/0.3/0.6 | mm |
| Wire Diameter | 0.12 | mm | Layer Inner Diameter | 90 | mm |
| Simulated Layer Length (L) | $k*a$ | mm | Simulation Error | 0.1 | percent |
| Simulation type | 2D analysis cylindrical around Z | | | | |

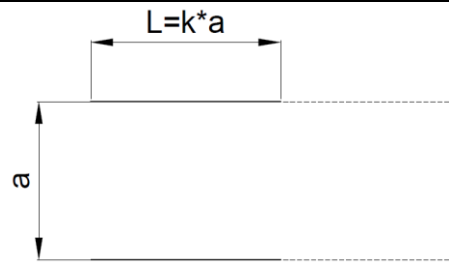


Figure 3-9 Represented part of the whole layer

In this method the whole layer will be represented with a small section as shown in the Figure 3-9 for the various values of the k integer. The behavior of the maximum electrical field will be observed while increasing the value of the k. The point where the effect of the larger k is negligible on the simulation results will be determined. Dense meshing (Fig. 3-10.) is used to decrease the effect of calculation error.

Analyses are carried for three different values of a. The k value is increased until an oscillation due to the simulation error is reached.

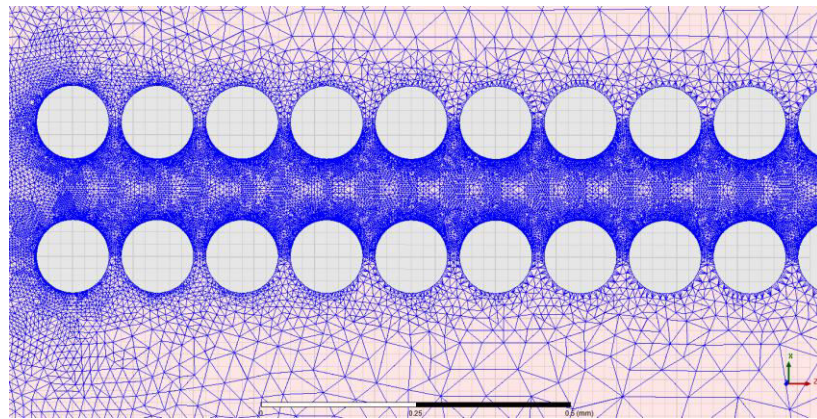
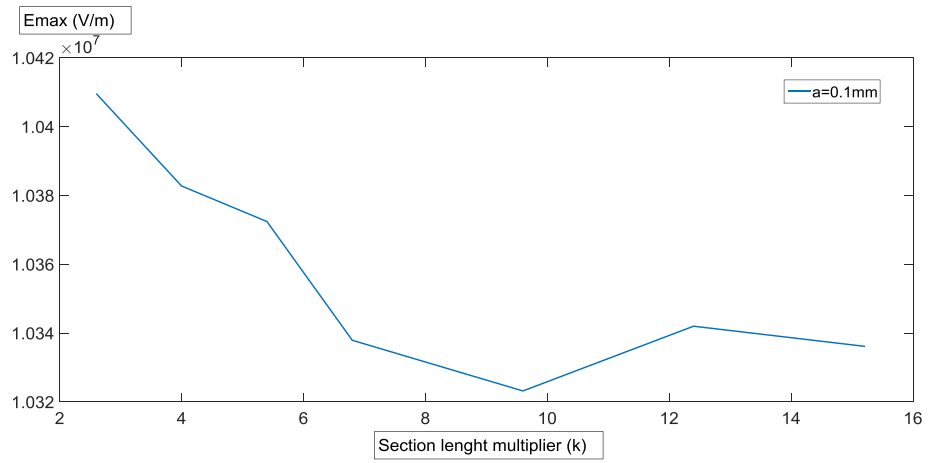
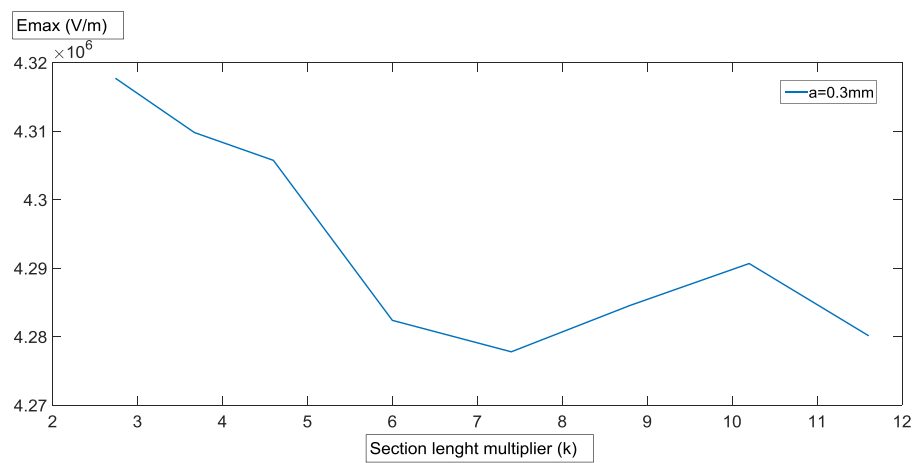


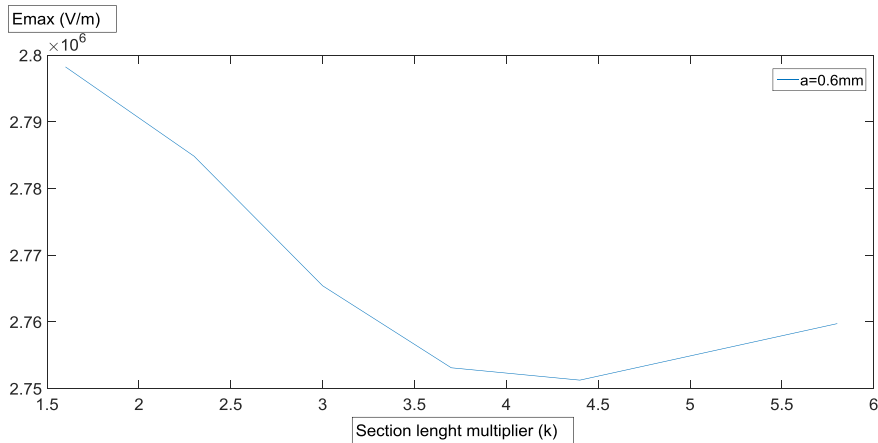
Figure 3-10 FE analysis meshing density of the represented layer



(a)



(b)



(c)

Figure 3-11 Maximum field vs. analyzed length (a)0.1mm insulation thickness up to k=15.2
 (b) 0.3mm insulation thickness up to k=11.6 (c) 0.6mm insulation thickness up to k=5.8

When Figure 3-11 is inspected it can be seen that the results are not deviating much even to small values of the k. The curves start to oscillate around the k=5 point due to the simulation error. In this thesis the k will be chosen minimum as 5 to make sure that the impact of simulating a shorter length is negligible.

If the k value is taken as 5 for the layer presented in the in the Figure 3-8 the length that is required to be simulated can be calculated as $5 \times 0.42 = 2.1$ mm. Comparing it to the whole layer length of 106mm it can be found out that only %2 percent of the turns are required to be represented to have an accurate simulation result. This reduces the drawing time from hours to minutes and 2D simulation time from minutes to seconds. Although simulation model area is shrunk there are two problems;

- Only the most outer region is inspected therefore it must be made sure that the maximum electrical field occurs in this part of the layer and other high stress points are within the limits.
- The layer simulated should not have any step piece that is smaller than 5*k length.

3.4. Layer Template Determination

The electric field can be assumed to be uniformly distributed along the electrodes. As a result the field intensity can be calculated as $E = V/L$ where V is the potential difference and L is the distance between two electrodes. The layers do not have uniformly distributed fields due to the non-linearity caused by their geometry.

The straight wire sections in Figure 3-2 and Figure 3-4 are almost shaped as plate electrodes, in which the distance between plates increases the non-uniformity of the electric field.

In the straight layer design shown in Figure 3-3, there is only one point where the electric field is intensified: the outermost turn of the layer. However, in the two-step layer type there are two points where the electric field is high as shown in Figure 3-5. If the electric field was uniformly distributed then the electric field at the outer section of the layer would be $E_{\text{outer}} = V_{\text{outer}} / L_{\text{outer}}$ and the field intensity where the step has been made would be $E_{\text{step}} = V_{\text{step}} / L_{\text{step}}$. The step in Figure 3-5 is in the middle of the layer which gives $V_{\text{outer}} = 2 * V_{\text{step}}$ and $L_{\text{outer}} = 2 * L_{\text{step}}$, and $E_{\text{outer}} = E_{\text{step}}$. However, when the simulation results are inspected E_{outer} is 34.6 kV/m while E_{step} is 26.5 kV/m. E_{outer} is larger than E_{step} because the electric field is more non-linear at the outer side of the layer since $L_{\text{outer}} > L_{\text{step}}$.

Inspection of a layer with the uniformly assumed electric field (V/L) has the same value for every critical spot requires focus only to one spot where the distance between the wires is longest thus would have the highest electrical field intensity.

3.4.1 Stepped Layer Templates

In this part layer types, where the linear calculation of the electric field ($E = V/L$) is constant at the critical points will be presented. This way the highest actual electrical field value will always occur at the most outer part of the layer and therefore the modeling approach discussed in section 3.3.1 can be used for these templates.

Normal steps that are constructed with even numbers of the insulating paper normal steps shown in Figure 3-12 and shifted steps that are constructed with odd number of the insulating paper shown in Figure 3-13.

In the Figure 3-12 and the Figure 3-13 the variables are defined as:

n = Insulating paper thickness (10 micron, 20 micron, 30 micron. etc)

a = Total insulation thickness of the layer

H = Height required to repeat the layer

E_{outer} = Maximum electric field value of the most outer section

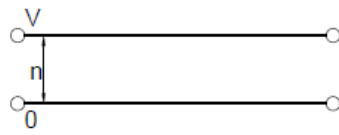
k = Integer

$E_{step(k)}$ = Maximum electric field value of the step k increasing from outside to inside

V = Relative voltage drop

\varnothing = Wire diameter

Straight

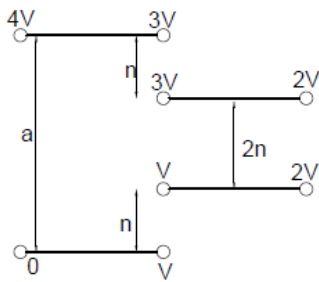


$H = 2kn + 2 \emptyset$
Usable when; $a=kn$

$E_{outer} = V/n$

(a)

2 Step

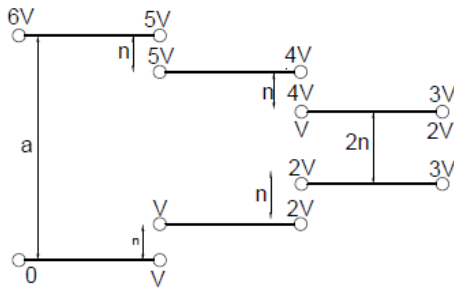


$H = 6kn + 2 \emptyset$
Usable when; $a=4kn$

$E_{outer} = 4V/4n = V/n$
 $E_{step} = (3V-V)/2n=V/n$

(b)

3 Step



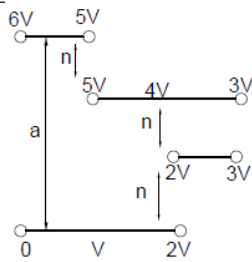
$H = 8kn + 2 \emptyset$
Usable when; $a=6kn$

$E_{outer} = 6V/6n = V/n$
 $E_{step1} = (5V-V)/4n=V/n$
 $E_{step2} = (4V-2V)/2n=V/n$

(c)

Figure 3-12 Normal step types (a) straight (b) 2 step (c) 3 step

2-1

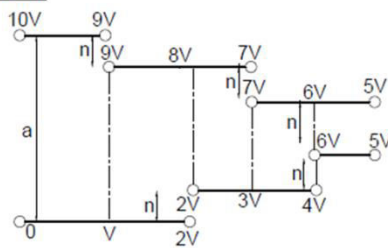


$H = 4kn + 2 \emptyset$
Usable when; $a=3kn$

$E_{outer} = 6V/3n = 2V/n$
 $E_{step1} = (5V-V)/2n = 2V/n$
 $E_{step2} = (4V-2V)/n = 2V/n$

(a)

2-2-1

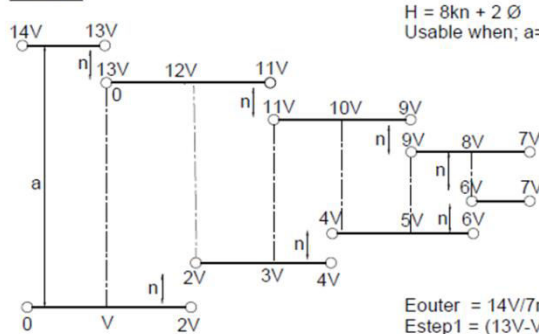


$H = 6kn + 2 \emptyset$
Usable when; $a=5kn$

$E_{outer} = 10V/5n = 2V/n$
 $E_{step1} = (9V-V)/4n = 2V/n$
 $E_{step2} = (8V-2V)/3n = 2V/n$
 $E_{step3} = (7V-3V)/2n = 2V/n$
 $E_{step4} = (6V-V)/n = 2V/n$

(b)

2-2-2-1



$H = 8kn + 2 \emptyset$
Usable when; $a=7kn$

$E_{outer} = 14V/7n = 2V/n$
 $E_{step1} = (13V-V)/6n = 2V/n$
 $E_{step2} = (12V-2V)/5n = 2V/n$
 $E_{step3} = (11V-3V)/4n = 2V/n$
 $E_{step4} = (10V-4V)/3n = 2V/n$
 $E_{step5} = (9V-5V)/2n = 2V/n$
 $E_{step6} = (8V-6V)/n = 2V/n$

(c)

Figure 3-13 Shifted steps types(a) 2-1 (b) 2-2-1 (c) 2-2-2-1

The number of the templates available can be increased infinitely with the usage of the same approach but it should be noted that the maximum step number thus

maximum number of turns can be placed in the same height will be ultimately limited by the section length, insulating paper thickness and manufacturing time.

It is also clear that usability of the templates is dependent on the number of kraft papers in between the most outer layer. When there is large number of paper to work with the variety of templates can be applied for the same section length increases, which enlarges the space where the templates can be selected from. Therefore using thinner insulating paper when constructing the layers is more advantageous compared to the thicker ones.

3.5. Layer Template Calculation for GT30a

The layer templates that have been created in the section 3.4.1 will be adapted to GT30a. Using the method described in the section 3.3.1 a table of possible sets of layers depending on the insulation length will be calculated and tabulated.

With the help of FEM the maximum length without exceeding the critical voltage level will be determined for each possible insulation thickness. In order to carry out the analysis the maximum electric field intensity allowed and the component dimensions needs to be determined.

3.5.1 Layer Components of the GT30a

In the standard production of the GT3a 30 micron kraft paper is used. The width of the core window is 180 mm and it is the limit of the layer length. %10 percent filling of the SF₆ gas in to that gap around the wires is assumed. The multilayer kraft paper layers will be modeled as a single layer.

A 0.12 mm magnet wire is used as the conductor. Insulation thickness of the magnet wire will be ignored in the analysis as the field intensity will not be high enough to break the wire insulation. This assumption also will cause slightly higher (about %5 percent) electric field calculation in the SF₆ medium which will be considered as a safety factor. The distance between the wire centers are taken as 0.14mm which would change depending on the winding machine setting.

3.5.2 Critical Electric Field Intensity

The coil will be subjected the SF₆ gas injection at a pressure of 5 bar. Sealing of this pressure may be damaged during the lifetime of the transformer and in that case the pressure would drop to atmospheric level. Therefore all calculations are performed at 1 bar pressure to fulfill the robustness objective stated in the section 1.2.

The corona inception voltage of the pure SF₆ gas (under normal conditions) is 9 kV/mm. However the corona extinction voltage varies between the 0.87-0.8 of the inception voltage as discussed in the section 2.2.3. This means the corona extinction voltage varies between 7.83-7.2 kV/mm. The field magnitude for the analysis will be selected as 6.5 kV/mm at 25 kV/mm to have some safety margin against the manufacturing and material tolerances.

Another factor in the field intensity selection is the strength of the insulating paper. Throughout the analysis the field intensity of the paper is varied between 2,0-2,5 kV/mm. For the worst case of 2.5 kV/mm, the field intensity at the 1 minute power frequency (70 kV) test can be calculated as $2.8 \times 2.5 = 7$ kV/mm which is smaller than the breakdown strength of the insulating paper. If this value is exceeded, the breakdown strength of the paper, there would be a puncture a risk.

Even when it has been guaranteed that the SF₆ will not be leaked, the critical field strength cannot be selected much higher than the 6,5 kV/mm because the strength of the insulating paper. To go beyond a different type of insulating paper can be used.

3.5.3 Simulation of the Layer Templates

The objective is to match the insulation thickness to the length of the layer which results in the 6.5 kV/mm critical field level by using optimization algorithm. There will be no local minimums so sequential nonlinear programming will be used, which gives the fastest response in this particular problem. The cost function is taken as $(E_{max} - 6500000)^2$. The optimization has only one independent variable which is the voltage of the last turn. From that value other parameters can be calculated. Simulation data are given at the Table 3-4.

Table 3-4 GT30a layer determination simulation parameters

| | | | | | |
|------------------------------|-------|---------|----------------------------------|-------|------------|
| Wire Diameter | 0.12 | mm | Max Layer Length | 180 | mm |
| Paper Thickness | 30 | micron | Inner Diameter | 80 | mm |
| Coil Voltage | 25 | kV | Paper Er | 2,3 | E_0 |
| Total Number of Turns | 50461 | turns | SF₆ Er | 1 | E_0 |
| Efield intensity | 6.5 | kV/mm | Vdrop per Turn | 0.494 | V |
| Simulation Error | %0.1 | percent | Number of Turns Simulated | 25/25 | First/last |

The first and the last 25 turns will be simulated and it will be checked by 5*a rule (Figure 3-14). The thickness of the insulation will be increased 30 micron at a time until the layer length reaches 180 mm. Since the worst case will occur in the innermost layer it will be simulated. Meshing density of the analysis is presented in Figure 3-15.

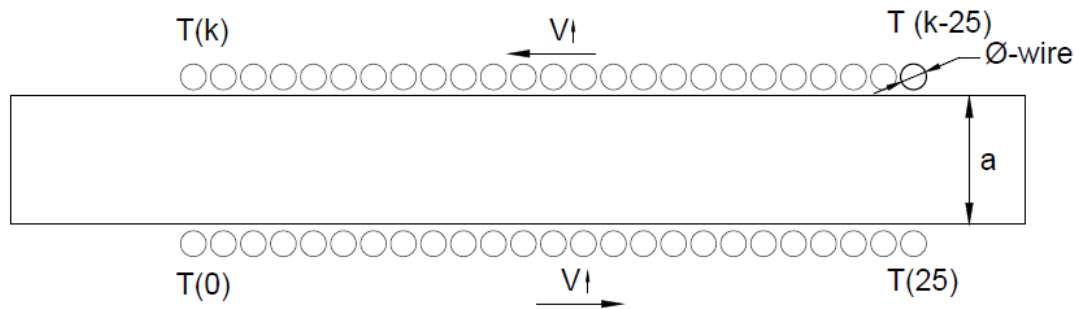


Figure 3-14. Simulated part of the layers for GT30a template determination

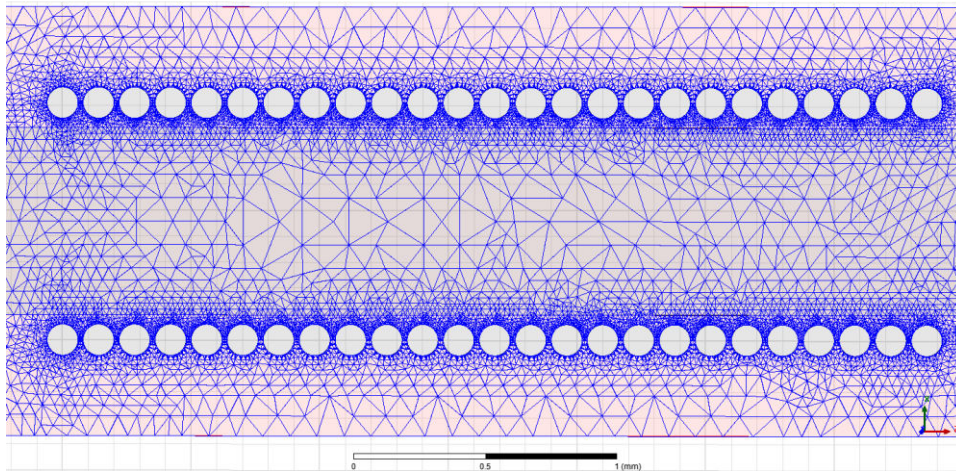


Figure 3-15 Mesh density of the layer template simulation

With the maximum layer length for the each insulation thickness is known, the applicable templates and their calculated properties are tabulated in Table 3-5. By using the number of turns allowed for each end point distances, the area and height for each type of can be calculated by using the formulas of the layer types given in the section 3.4.1. The data presented in the table should be recalculated for other applications where the electrical field intensity, wire diameter, insulating paper thickness and insulating gas may change.

In Table 3-5, the layer types that the original and modified design utilizes are marked with blue while the final design parameters are marked with orange color. Layer lengths of the original and the final design were 106, 86 and 66 mm and all of them use the same layer type which allows up to 121 mm. This proves that the partial discharges in the original designs are not caused because of the field stress in between the layers. It also means that the layer types are selected inefficiently since the 86 mm and 66 mm layers can be fitted in a smaller layer template which would reduce the material cost and the coil volume.

Table 3-5 Possible layer templates for the GT30a

| Insulation Thickness (a)(micron) | Layer Type | Number of Turns (T) | Section length (mm) | H(mm) | Layer Voltage Drop (V) |
|----------------------------------|------------|---------------------|---------------------|-------|------------------------|
| 30 | Straight | 186 | 13,04 | 0,30 | 92 |
| 60 | Straight | 342 | 23,95 | 0,36 | 169 |
| 90 | Straight | 486 | 34,01 | 0,42 | 240 |
| | 2-1 | 486 | 34,01 | 0,36 | 240 |
| 120 | Straight | 619 | 43,36 | 0,48 | 306 |
| | 2 step | 619 | 43,36 | 0,42 | 306 |
| 150 | Straight | 745 | 52,15 | 0,54 | 368 |
| | 2-2-1 | 745 | 52,15 | 0,42 | 368 |
| 180 | Straight | 868 | 60,79 | 0,60 | 429 |
| | 2-1 | 868 | 60,79 | 0,48 | 429 |
| | 3 step | 868 | 60,79 | 0,48 | 429 |
| 210 | Straight | 990 | 69,29 | 0,66 | 489 |
| | 2-2-2-1 | 990 | 69,29 | 0,48 | 489 |
| 240 | Straight | 1101 | 77,09 | 0,72 | 544 |
| | 2 step | 1101 | 77,09 | 0,60 | 544 |
| 270 | Straight | 1213 | 84,88 | 0,78 | 599 |
| | 2-1 | 1213 | 84,88 | 0,60 | 599 |
| | 2-2-2-2-1 | 1213 | 84,88 | 0,54 | 599 |
| 300 | Straight | 1332 | 93,24 | 0,84 | 658 |
| | 2-2-1 | 1332 | 93,24 | 0,60 | 658 |
| 330 | Straight | 1429 | 100,04 | 0,90 | 706 |
| 360 | Straight | 1538 | 107,69 | 0,96 | 760 |
| | 2-1 | 1538 | 107,69 | 0,72 | 760 |
| | 2 step | 1538 | 107,69 | 0,78 | 760 |
| | 3 step | 1538 | 107,69 | 0,72 | 760 |
| 390 | Straight | 1646 | 115,20 | 1,02 | 813 |
| 420 | Straight | 1731 | 121,15 | 1,08 | 855 |
| | 2-2-2-1 | 1731 | 121,15 | 0,72 | 855 |
| 450 | Straight | 1832 | 128,24 | 1,14 | 905 |
| | 2-1 | 1832 | 128,24 | 0,84 | 905 |
| | 2-2-1 | 1832 | 128,24 | 0,78 | 905 |
| 480 | Straight | 1929 | 135,04 | 1,20 | 953 |
| | 2 step | 1929 | 135,04 | 0,96 | 953 |
| 510 | Straight | 2036 | 142,55 | 1,26 | 1006 |
| 540 | Straight | 2123 | 148,64 | 1,32 | 1049 |
| | 2-1 | 2123 | 148,64 | 0,96 | 1049 |
| | 3 step | 2123 | 148,64 | 0,96 | 1049 |
| | 2-2-2-2-1 | 2123 | 148,64 | 0,84 | 1049 |
| 570 | Straight | 2209 | 154,60 | 1,38 | 1091 |
| 600 | Straight | 2296 | 160,69 | 1,44 | 1134 |
| | 2-2-1 | 2296 | 160,69 | 0,96 | 1134 |
| | 2 step | 2296 | 160,69 | 1,14 | 1134 |
| 630 | Straight | 2377 | 166,36 | 1,50 | 1174 |
| | 2-1 | 2377 | 166,36 | 1,08 | 1174 |
| | 2-2-2-1 | 2377 | 166,36 | 0,96 | 1174 |
| 660 | Straight | 2486 | 174,01 | 1,56 | 1228 |
| 690 | Straight | 2565 | 179,53 | 1,62 | 1267 |

The following remarks can be derived from the Table 3-5;

- The length required to be simulated for the longest insulation is $5 \cdot a = 5 \cdot 0.69 = 3,45 \text{ mm}$. For 25 turns the simulated length is $0.14 \cdot 25 = 3,5 \text{ mm}$ which is greater so the table is valid under an acceptable simulation error margin.
- Using a more stepped design is always resulted in smaller height for the same length.
- 3 step design is useless since it has the same height with 2-1 design and has more steps.
- As the insulation thickness increases, the length of the layer does not increase linearly due to the field nonlinearity. Therefore utilizing layers with long lengths might end up consuming more area. The relation of length and height for the layers is presented in the (Figure 3-16).

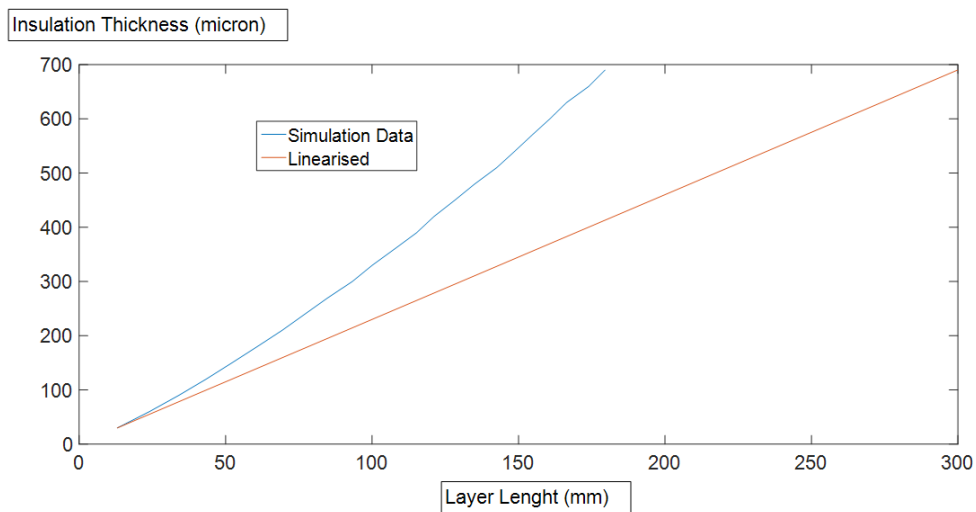


Figure 3-16 Insulation thickness vs. layer length for the layers

3.6. Manufacturing Time & Number of Steps

Regarding the analysis results, it looks better to have as many steps as possible to have a smaller design. However there is a drawback by doing it so; the winding machines rotate fast when winding the turns but slows down after end of each layer

when the machine halts to insert the insulating paper in between. As a result the manufacturing cost increase due to the prolonged production time of the coil.

An exemplary coil winded with 4 different layer templates to prove the point dependent on the machine. Each coil consists of 16000 turns, 140 mm layer length and 0.12 mm wire diameter. The thickness of the insulation paper used is 30 micron. The duration of the winding process is noted in the Table 3-6 for each layer type. The winding durations would change if a different machine is employed.

Table 3-6 Comparison of the coil manufacturing

| Layer type | Winding duration (minutes) |
|------------|----------------------------|
| straight | 42 |
| 2-1 | 52 |
| three step | 63 |
| 2-2-2-2-1 | 72 |

As can be seen from Table 3-6 there is a trade-off between the layer height, thus coil volume and the manufacturing time. When choosing the suitable layers from the table, the design requirements will be considered. If small coils are preferred in the design the increase of the manufacturing time can be overlooked.

3.7. Irregular Layer Design

Up to now in design templates created with a systematic layer construction given in Figure 3-12 and Figure 3-13. Although this method is easy to apply, it actually reduces the space that the layers are selected from.

Assume that it has been decided to use a layer with 125 mm length in GT30a. In that case at least 15*30 mm kraft paper of insulation will be used according to the Table 3-5. For that insulation thickness available regular designs are either straight, 2-1 or 2-2-1. The respective layer heights of those layers are 1,14 mm, 0,84 mm and 0,78 mm.

If the desired volume size even with the 2-2-1 can not be satisfied, layer with 2-2-2-2-2-2-2-1 steps, which is not listed in the table, needs to be used. With 2-2-2-2-2-2-2-1 the layer height will be reduced to 0,72 mm.

A layer that is thinner than 0.72 mm is not possible with 30 micron paper. If 2-2-2-2-2-2-2-1 is chosen to be employed it reduces the coil volume but increases the manufacturing time due to the high number of stops to lay the insulating paper. It would be useful to have a new layer type which has the same total height but less manufacturing time. There is no systematic way to create such design as the normal stepped and shifted designs so the process will be trial and error.

1-3-4-4-2 irregular step design shown in the figure is created for 125mm section length for the application mentioned above by trial and error.

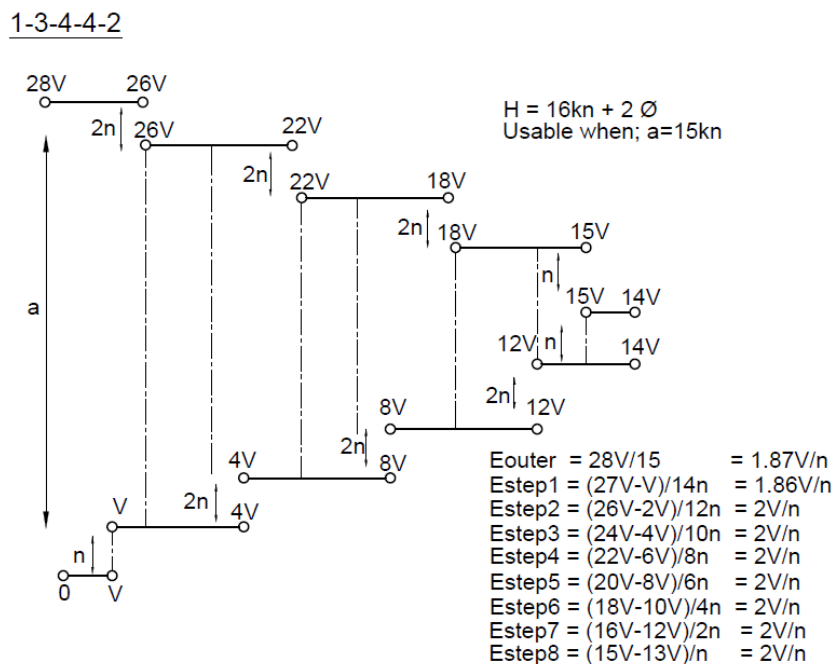


Figure 3-17 1-3-4-4-2 layer template

1-3-4-4-2 does not hold the constant V/L rule so all of the high stress points must be verified to be below the critical stress. In order to do this modeling of the whole layer would consume too much time, instead using the table for the stepping locations as if they were the outermost section to find out if the design is acceptable

is a lot faster. In reality the inside stepped points have slightly lower field density than the outermost part for the same insulation length.

Inspection of the high stress points are given at the Table 3-7

Table 3-7 Inspection of the 1-3-4-4-2 step points

| Position | Insulation Thickness (micron) | Allowed Length | Lenght in 1-3-4-4-2 |
|-----------------|--------------------------------------|-----------------------|----------------------------|
| Outer | 450 | 128.24 | 125 |
| Step1 | 420 | 121.15 | 116.07 |
| Step2 | 360 | 107.69 | 107.14 |
| Step3 | 300 | 93.24 | 89.28 |
| Step4 | 240 | 77.09 | 71.42 |
| Step5 | 180 | 60.79 | 53.57 |
| Step6 | 120 | 43.36 | 35.71 |
| Step7 | 60 | 23.95 | 15.38 |
| Step8 | 30 | 13.04 | 8.92 |

Shortest step length is 8,92 mm and it is greater than the $5 \times 0.45\text{mm}$ which makes modeling valid. None of the steps are longer than the calculated maximum lengths in the table so the design is safe to use. Worst case of allowed winding length vs. the winding length occurs at step 2 and limits this design for maximum application length of 1-3-4-4-2 to 125.65 mm.

Although there is no certain method in creating the irregular design the rule of thumbs can be used as;

- Always adjust the layer boundary one paper thick to get the smallest possible layer height.
- The middle section of the layer is safer so the gain will come from this part by winding longer without making a step.
- Always check if the symmetry is conserved for the repeating layers.

3.8. Chapter Summary

In this chapter a generalized approach to the layer design and modeling the layers of a MV voltage transformer is constructed. It has been found that adding more steps increases the performance but also the manufacturing time. In order to reduce the workload, simulating the smaller section of a layer while keeping it longer than the minimum required length is enough.

Regular layer templates where V/L ratios are constant through the critical point are created. This guaranteed the occurrence of the highest electrical field at the outermost part of the layer and as a result only single critical point for each of these layers is inspected. The maximum allowed lengths for a predetermined electrical field value for the layers with different insulation thickness have been tabulated.

If regular templates that are suggested in this chapter voltage template layers do not satisfy the needs, irregular layer templates can be constructed with the help of the previous simulation data.

Following algorithm can be used to create the layer templates for the designs with different properties:

- 1) Determine the electrical and physical parameters for the coil.
- 2) Simulate the layer for possible simulation lengths with finite element analysis. Construct the available layers by using templates. Check for if the minimum simulation length constraint holds.
- 3) Select the layers suitable to your design layer length, decide on the tradeoffs between the coil volume and the production time
- 4) If no template layer satisfies the design requirements, create trial and error irregular layers via the table that has been constructed.

With the layer template table is made available in this chapter, the next chapter will focus on the determination of the layer lengths. When the length of a layer is known, it will be a design trade off to choose a suitable layer from the table.

CHAPTER 4

LAYER LENGTH DETERMINATION FOR THE HIGH VOLTAGE COIL

The aim of this chapter is to develop a method to determine the layer lengths that will be used in GT30a. The length of the layers will be limited by the window of the core that is being used. The question of how close the wire can be stationed to the core will be determined by simulating the electrical field gradient with FEM. This length also will be dependent on the voltage drop of the respective layer. As the turn number increases, throughout the coil the voltage drop will also increase thus the maximum length of the layer needs to be decreased.

In the previous chapter the cylindrical symmetry of the layers have been used to carry out the analysis in 2D. In this chapter such method cannot be utilized since there is no axis of symmetry due to the rectangular geometry of the core. Using 3D FEM analysis alone with a complex geometry would consume a lot of time compared to the 2D analysis therefore would increase the design cost. Instead first 3D model will be constructed and then a way to represent the 3D model by a 2D simplification model will be discussed.

Simulations of the original and modified designs will be carried out. The results will be discussed. Lastly the final design will be constructed with the help of the finite element analysis.

4.1. 3D Modeling of the Layers

In t chapter 3 it has been made sure that the electric field gradient between the layers do not exceed a certain value. The critical electric field should not be exceeded not only in between the layers but also between the core and the layer edges.

From the point of view of the core the layers will be perceived as copper foils since the wires are closely stacked. Voltage drop from one side to other side of a layer is relatively small when compared to the voltage drop between wires and the core. As a result the wires of the same layer will be assumed to be at the same potential as shown in Figure 4-1.

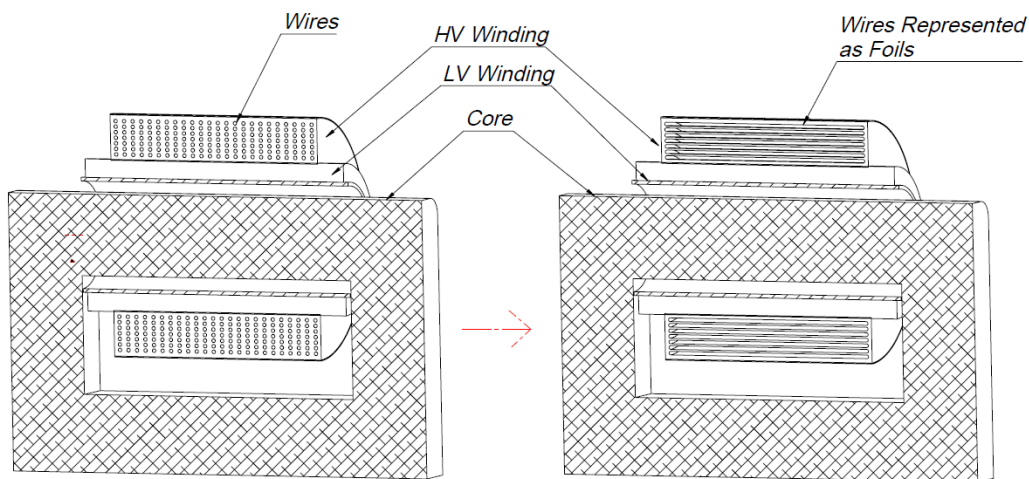


Figure 4-1 Conversion of the wires to the foils for the simulation

In the model of the GT30a every two layers will be modeled as a single copper foil in order to reduce the number of the foils. Ideally every layer should be represented as two foils. The paper insulation in between the layers will be modeled as a single unit similar to Chapter 3.

The core normally has sharp edges due to being constructed from the silicon steel blocks. Sharp edges cause the electric field intensification thus they are unwanted in high voltage designs. To smooth these edges iron core is covered with a carbon paper. In the construction of the model the carbon paper will be counted as the part

of the core since the electrical field is the only concern and that assumption would only effect the magnetic field distribution.

4.1.1 Meshing Strategy

As mentioned in the section 1.4.1 the accuracy of the analysis is dependent on the length of the elements. Thus there is a tradeoff between the simulation time and the accuracy of the results. When we observe the finite element analysis of a single copper layer where the meshes are auto constructed in ANSYS Maxwell 16.03, which is shown in Figure 4-2, it is clear that the field density is maximized at the edges of the copper foil as expected.

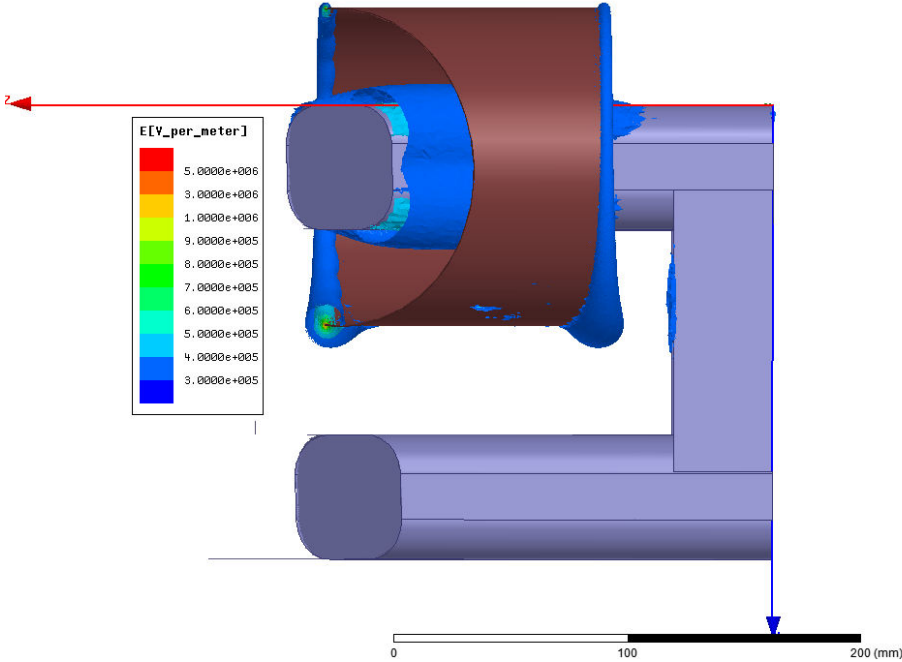


Figure 4-2 3D analysis of a single copper foil with automatic meshing

Highest electrical field values of the analysis shown in Figure 4-2 is about 5.02 kV/mm. Since the mesh density of the solution is low, the result is most probably away from the analytical solution. Instead of increasing the overall mesh density to increase the simulation accuracy, only the area around the edge of the foils where the highest field gradient occur will be reinforced with the dense meshing. The new

mesh for the same geometry produced with this strategy is presented at Figure 4-3. The analysis is renewed under same conditions.

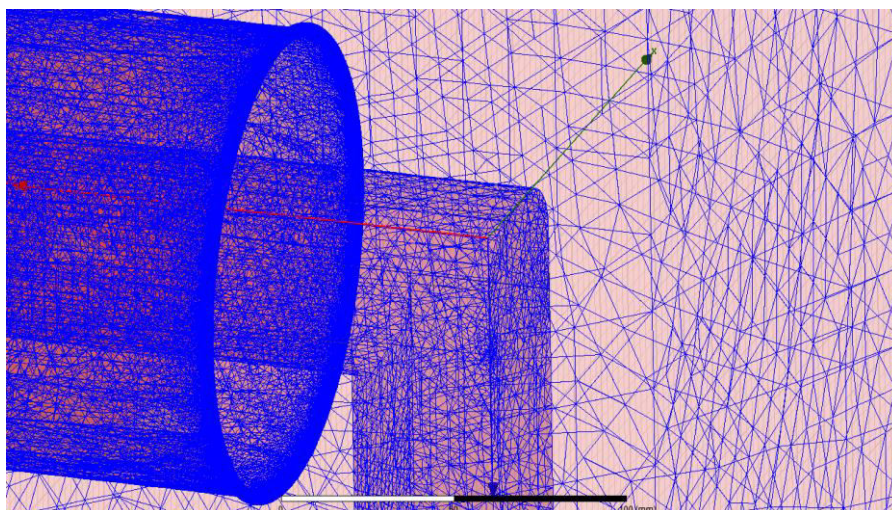


Figure 4-3 Mesh density plot with the density focused on the edge of the copper foil

Only single side of the copper foil is reinforced since the two sides are symmetrical. When the electrical field around the edge inspected in the Figure 4-4 it has been found out that the maximum electric field is 5.298 kV/mm.

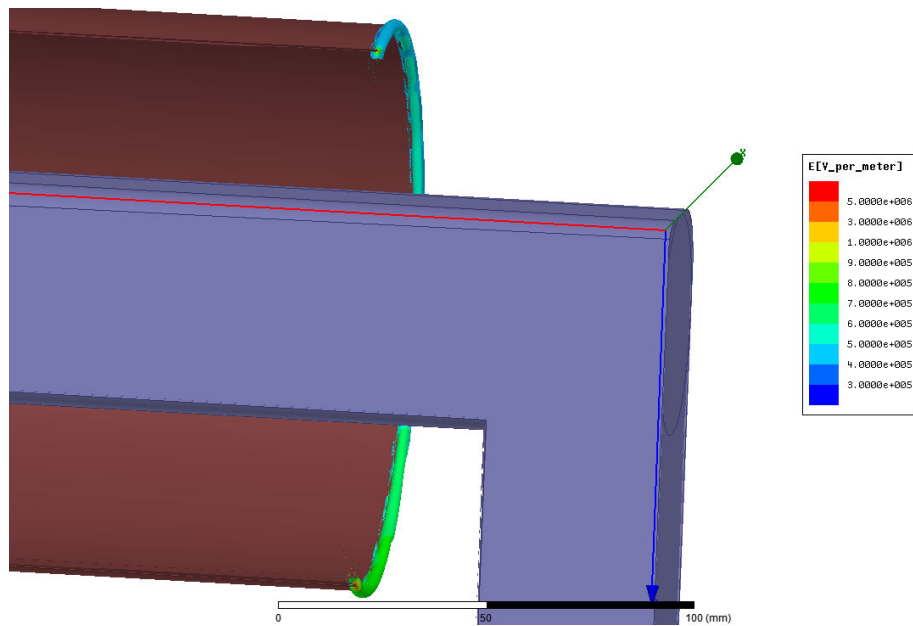


Figure 4-4 Electrical field gradient of the area with focused mesh

The difference in between the auto mesh and the reinforced mesh is around %5,5 percent. Further increasing the meshing density in the region has not provided any recognizable change in the maximum value of the field. All of the remaining 3D analysis in this chapter will be carried out with the same meshing strategy.

4.2. 3D to 2D Mapping

Finite elements model of the GT30a model has over 25 layers. To draw and analyze these layers with 3D analysis with the complex geometry provided by the core and the epoxy resin envelope would consume a lot of time. Moreover, constructing the model itself would take more time compared to the 2D analysis.

With long amount of simulation and modeling time, the possibility of repeating the analysis with small adjustments diminishes due to the sheer amount of time required to apply them. Therefore a method to convert the 3D model to the 2D one will be employed instead of creating the whole 3D model.

When the field distribution in the figure of the single layer is inspected shown in Figure 4-5 it is clear that the highest electrical field intensity occurs at the bottom of

the copper foil where the distance between the foil and the leg of the iron core is smallest.

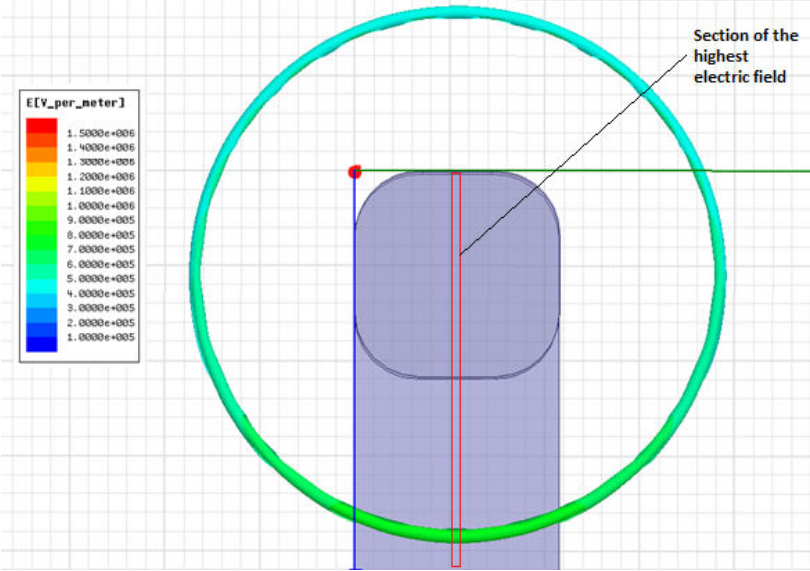


Figure 4-5 Side view of the 3D analysis of the copper foil

Cross section of the bottom part of the coil is represented in the X-Y plane as in Figure 4-6.

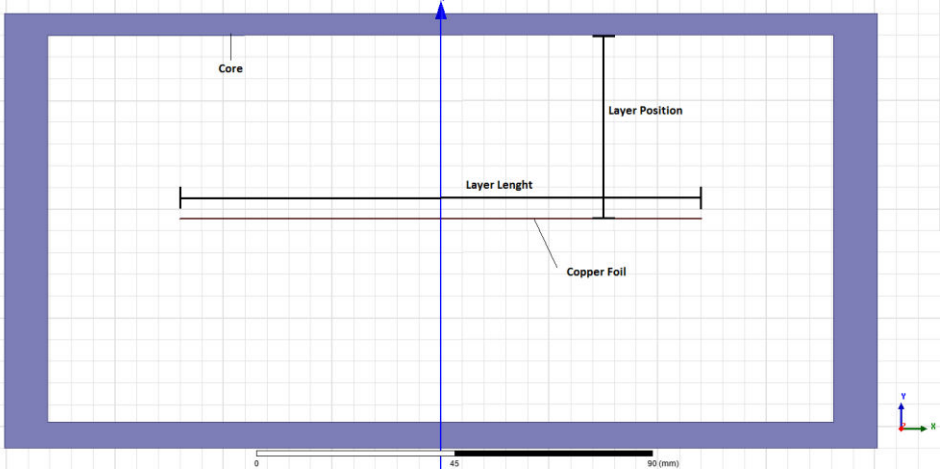


Figure 4-6 Cross section of the highest electrical field area of the 3D analysis represented in X-Y plane

When the analysis done in the X-Y plane, the equivalent 3D model is the infinitely extrusion of the 2D model in the Z plane. While this contradicts with the real 3D model, it could be used for mapping the 2D model back in to the 3D model. For this purpose analysis of a single copper layer with 0.12 mm width will be done in both 3D and 2D for 12 different copper foils. The results of these analysis are given in Table 4-1.

Table 4-1 3D vs 2D analysis result comparison

| Layer Voltage (kV) | Layer Length (mm) | Layer Position (mm) | 3D Emax (kV/mm) | 2D Emax (kV/mm) | 3D/2D (ratio-conversion constant) |
|--------------------|-------------------|---------------------|-----------------|-----------------|-----------------------------------|
| 6 | 120 | 12 | 1.88 | 2.20 | 0.86 |
| 8 | 120 | 27 | 4.26 | 5.39 | 0.79 |
| 10 | 120 | 42 | 5.30 | 8.40 | 0.63 |
| 12 | 120 | 55 | 6.94 | 10.38 | 0.67 |
| 6 | 100 | 12 | 1.71 | 2.16 | 0.79 |
| 8 | 100 | 27 | 3.56 | 5.14 | 0.69 |
| 10 | 100 | 42 | 5.03 | 8.09 | 0.62 |
| 12 | 100 | 55 | 6.32 | 9.93 | 0.63 |
| 6 | 80 | 12 | 1.62 | 2.10 | 0.77 |
| 8 | 80 | 27 | 3.43 | 4.99 | 0.68 |
| 10 | 80 | 42 | 4.78 | 7.82 | 0.61 |
| 12 | 80 | 55 | 5.87 | 9.50 | 0.62 |

From Table 4-1 it is clear that the relation between the 3D and the 2D analysis is dependent on the position and the length of the layer. The convergence of the results increases when the copper foil is near to the core.

The analysis can be done in the 2D and then can be converted to the 3D by simply multiplying with the ratio which is related with the layer position and length. For the positions and the lengths of the foils that are not directly given in the table, the ratio can be calculated assuming the relation between the 3D/2D ratio and size and the position of the foil is linear.

Similar to the Chapter 3 there will be only a few points that will be critical in the design so there is no need to convert the field gradient of the every layer from the 2D analysis.

4.3. 2D Modeling

The initial design and the modified design and the final design will be modeled and simulated with the method proposed in the section 4.2. Since the model in the X-Y plane is symmetrical only one side of the core will be simulated. The electric field between the layers are not going to be inspected since they have already been settled in the chapter 3. Only the last 10 mm of the each layer will be modeled as a foil to reduce the workload.

The 2D X-Y plane electrical field simulations will have following characteristics given in Table 4-2.

Table 4-2 2D simulation parameters

| | | | | | |
|------------------------------|------------|---------|--|-------|-------|
| Wire Diameter | 0.12 | mm | Resin E_r | 4 | E_0 |
| Core window | 89 x 181/2 | mm | Paper E_r | 2,3 | E_0 |
| Coil Voltage | 25 | kV | SF₆ E_r | 1 | E_0 |
| Total Number of Turns | 50461 | turns | Vdrop per mm | 28,24 | V |
| Simulation Error | %0.1 | percent | | | |

4.3.1 2D Model of the Original Design

Initial design of the GT30a has three different layer lengths respectively 106mm, 86mm and 66mm long and their respective positions are 27mm, 42mm and 55.5mm. The insulation paper is 14 mm longer than the layer length for each of them (Figure 4-7).

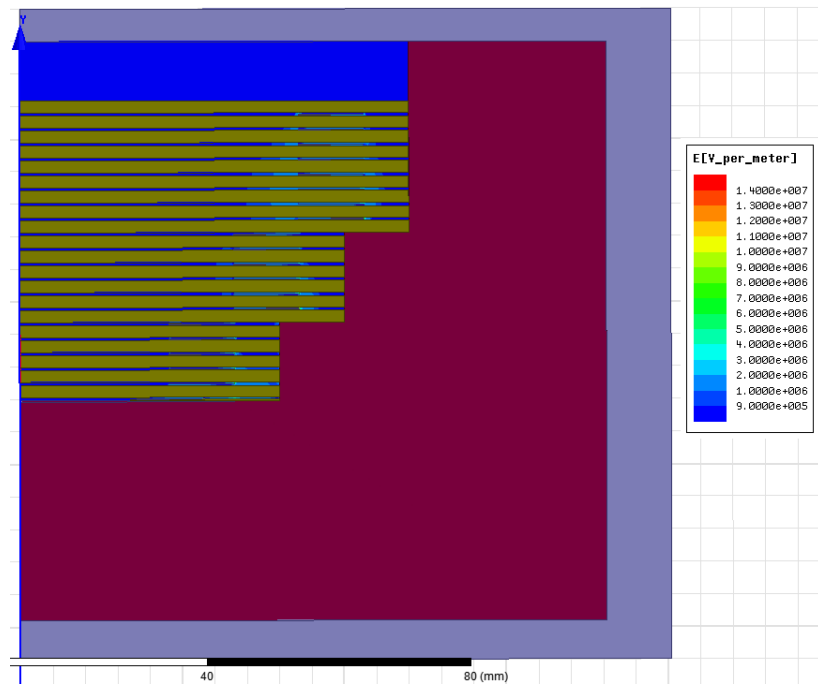


Figure 4-7 2D electrical field analysis of the original GT30a

For the first layer type the maximum electrical field in 2D analysis found out to be 9.66 kV/mm. The layer length is 106 mm and the layer position is 27 mm. Exact conversion constant from 2D to 3D at for this layer is not given at the Table 4-1 but it is known that 2D to 3D conversion constant for 120 mm length and 27mm position is 0.79 and 100mm length 27mm position is 0.69. The layer positions of the first layer and simulated layers in the 2D to 3D conversion are identical. Accuracy difference per mm caused by the difference of the the section length is $(0.79-0.69)/(120-100)= 0.005$. For 106 mm the conversion constant is $6*0.005+0.69 = 0.72$. All of the remaining 2D to 3D conversion constants will be calculated with the same manner. Actual electric field at point m1 is $9.66*0,72 = 6,96$ kV/mm (Figure 4-8).

For the second layer the layer length is 86mm the layer position is 42 mm and the maximum electric field in 2D analysis is 13.6 kV mm. 2D to 3D conversion constant is 0.616. Real maximum value of the field is $13.6*0.616 = 8,37$ kV/mm(Figure 4-9).

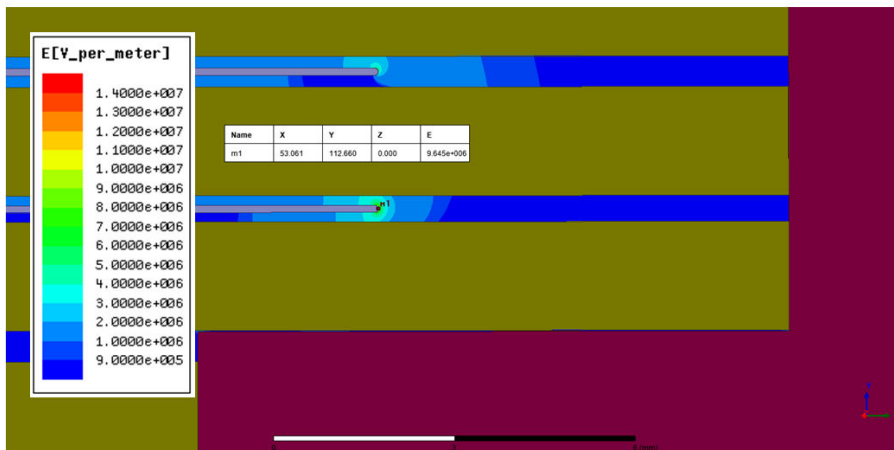


Figure 4-8 Electrical field distribution at the end point of the 106mm layer of the original GT30a

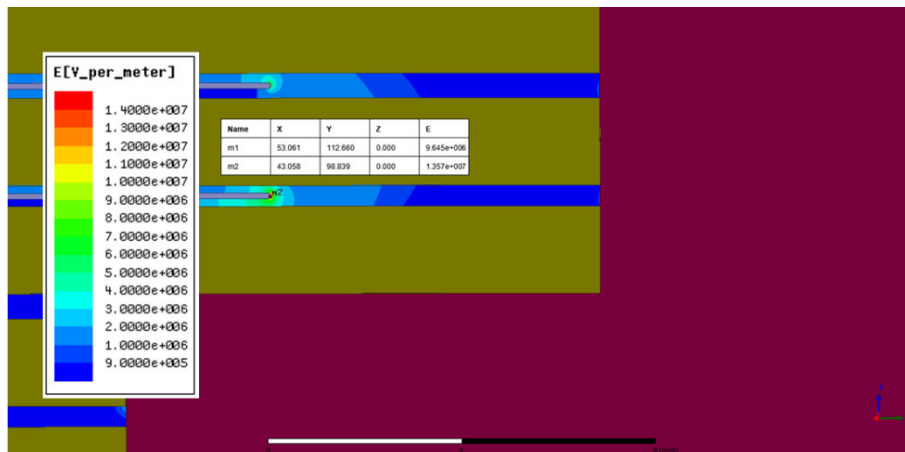


Figure 4-9 Electrical field distribution at the end point of the 86mm layer of the original GT30a

For the last layer the field maximum field intensity in SF₆ is marked with m3 and maximum field strength in the epoxy resin is marked with m4. Layer length is 66 mm and the layer position is 55.5mm. The conversion constant for both of the points are ~0.613. Maximum field stress in the m3 is $7.5 \times 0.613 = 4,6$ kV/mm and in the m4 $12.42 \times 0.613 = 7.61$ kV/mm (Figure 4-10).

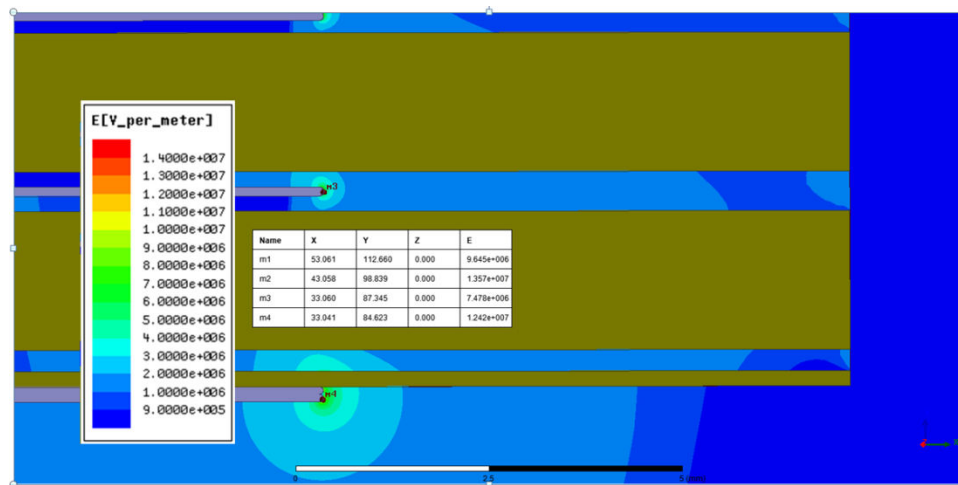


Figure 4-10 Electrical field distribution at the end point of the 66mm layer of the original GT30a

Remarks;

- Electrical field values of the SF₆ gas is below the discharge extinction levels at 5 bar therefore there should be no discharge in the routine test. However at 1 bar of pressure the corona in the SF₆ would not extinct if once incepted.
- The voltage of the simulation is 25 kV/mm. However, the 1 minute power frequency test is carried out at 70 kV/mm. The electric field would be 2,8 times stronger at the test voltage. The stress on the resin at the power frequency test voltage would be 7,61*2,8= 21.3 kV/mm which is dangerously close to the breakdown voltage of the epoxy resin given at the Table 2-3. Since the breakdown characteristics of the solids are unpredictable as discussed in section 2.2.1, this could be the main reasons of the punctures recorded in the Table 1-4.

4.3.2 2D Model of the Modified Design

The modified design constructed in the section 2.4.4 simulated in the same manner as the original. Since the layer layout is the same, the points of interests are identical with the original design with the exception of the screen where the dimensions are changed. Points m1, m2 and m3 are at high stress points of each layer type in SF₆ isolation while m4 is the maximum stress on the epoxy resin.

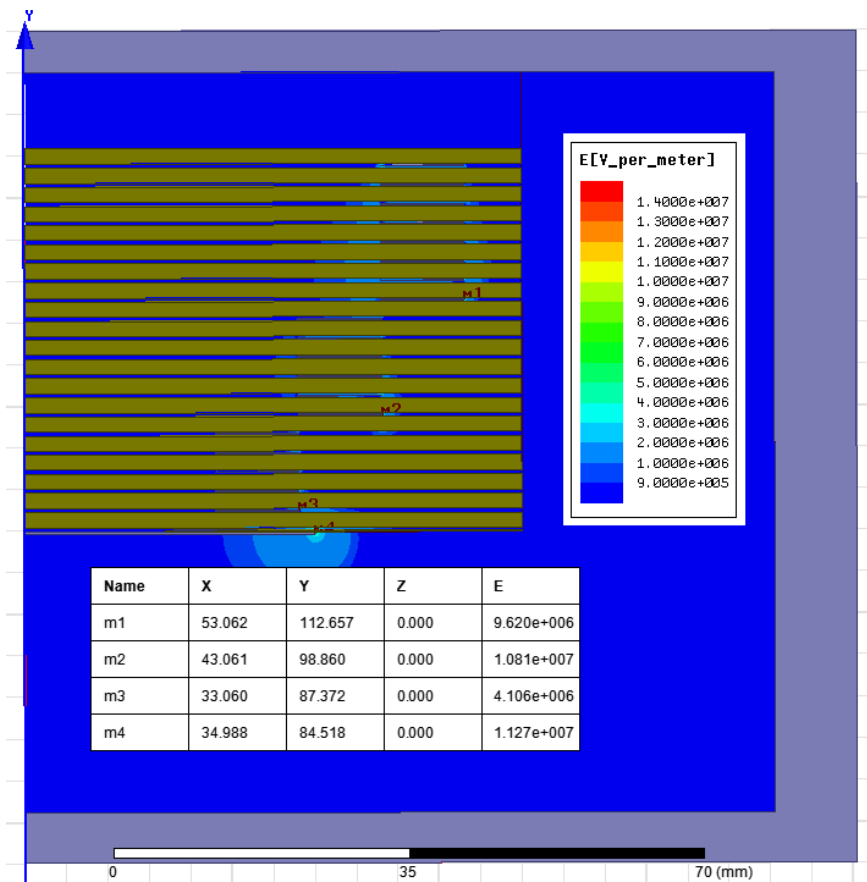


Figure 4-11 Electrical field distribution of the modified design

When the field values are multiplied with the respective conversion constants which are the same as the original:

- $Em1=9.26*0,72 = 6.67 \text{ kV/mm (SF}_6\text{)}$
- $Em2=10.81*0.616 = 6,66 \text{ kV/mm (SF}_6\text{)}$
- $Em3=4.10*0.616 = 2,53 \text{ kV/mm (SF}_6\text{)}$
- $Em4=11.27*0.617 = 6,95 \text{ kV/mm (Epoxy Resin)}$

Remarks;

- Overall electric field values are lower compared to the original design.
- Maximum field value of the epoxy resin at 70 kV pf test would be $6,76*2,8 = 18,93 \text{ kV/mm}$ which is approximately 10 percent lower than the original design.

4.3.3 Construction of the Final Design

In the coil design where the layer lengths are determined the purpose is to minimize the volume, copper loss and leakage inductance while keeping the electrical field intensity within the desired magnitudes. Since GT30a is a protection transformer with allowed accuracy error of %3, the gains in the volume thus the production cost is more important than the accuracy class increase.

In order to accomplish these goal the layer length should be kept as close to the iron core as possible in each layer. For the ideal case each layer would have different lengths as in the case of section 3.2. Likewise the original design, there will be three different layer blocks in the final design to keep the production time and complexity of the final coil similar to the original coil.

In the original design, the insulation paper was 120-100-80 mm long for the respective layer lengths and in the modified design the insulation paper was 120 mm long for all the layers. The core window of the GT30a is 181 mm long which indicates the remaining area is filled with epoxy resin. The dielectric constant of the resin is higher than the dielectric constant of the paper thus it is better to have low volumes of epoxy resin to prevent the electric field amplification as discussed in the section 2.4.2. As a result the paper length in the final design is selected to be 140 mm which leaves the resin 20.5 mm space in each side of the coil. The dimensioning of the epoxy resin mould prevented any further increase in the paper length and reduction in the area of the resin.

The maximum allowed electric field in the SF₆ is selected as 6 kV/mm although it was selected 6.5 kV/mm in section 3.5.2. The reason of this reduction is to increase the safety factor since 2D to 3D conversion utilized in this chapter is not completely precise.

For the electrical stress in the epoxy resin, the purpose is to increase the robustness in the long term and decrease the chance of the partial discharge inception and the puncture in the routine test. Since the behavior of the epoxy resin is not consistent as the insulating gases, it is better to use a larger safety margin Thus the limit

electric stress of the resin is selected as 14,4 kV/mm at 70 kV which is %60 of the epoxy resin electrical breakdown strength given at the Table 2-3. The simulations are carried out at 25 kV where this value would be equal to 5,14 kV/mm.

The safety margin of the resin can be selected up to %80 as proven by the results of the modified design. However selecting a higher value would risk breakdowns. The reason that is selected %60 is to provide extra robustness and operation life. Another factor is since the same mould is going to be used, selecting %80 would result in a too small coil in the final design thus increases the material cost.

The 2D model is constructed with relating the voltage drop of the copper foils with the length of the current and the previous foils. Changing the length of a single foil would change the voltages of the every foil in the model. The total length of the foils thus the number of turns is kept the same. Trial and error is used to determine the lengths of the final designs layers. For each simulation the maximum stress at the critical points converted to the 3D values by using Table 4-1. Then length of the layers consecutively adjusted until the required values are satisfied.

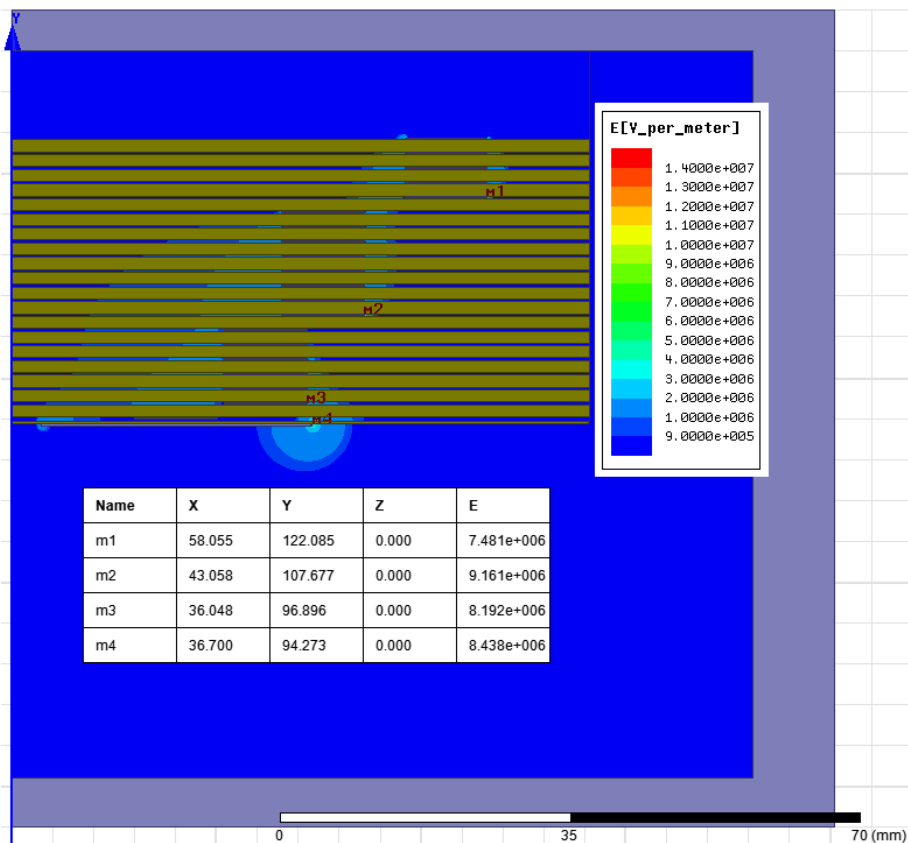


Figure 4-12 Electrical field distribution of the final design

In the design, layer lengths of the first two layer blocks are limited with the stress value of the SF₆ while the last one is limited with the stress value of the epoxy resin. Same screen is used as the modified design which is 0.2mm thick and 4mm longer than the last layer length.

Layer lengths of the final design are 116mm, 86mm and 70mm respectively and their positions are 18mm, 32mm and 45mm. To convert the 2D electric field values to 3D again the multiplication with the respective constants is carried out:

- $Em1=7.48*0,8 = 5,99 \text{ kV/mm (SF}_6\text{)}$
- $Em2=9.16*0.66 = 6,02 \text{ kV/mm (SF}_6\text{)}$
- $Em3=8.192*0.606 = 4,96 \text{ kV/mm (SF}_6\text{)}$
- $Em4=8.438*0.607 = 5,12 \text{ kV/mm (Epoxy Resin)}$

4.3.4 Selection of the Layer Templates

The possible layer templates are constructed in the chapter 3 and presented in Table 3-5. Layer template selection changes the height of the layer thus positioning of the copper foils in the 2D field analysis. Therefore if a layer template is changed the analysis should be repeated. As a result, the design process is iterative between the layer length determination and template selection.

Following layer templates are selected for the design from Table 3-5 and marked with orange color.

- 116mm length 420mm insulation thickness 2-2-2-1 up to turn 15970
- 86mm length 300mm insulation thickness 2-2-1 up to turn 36162
- 70mm length 210mm insulation thickness 2-2-2-1 up to turn 50461

The outermost diameter of the high voltage coil of the final design is 145 mm which is in the limit given at Table 1-3. The last layer is deliberately chosen at the limit of the allowed length to prove the validity of the layer template analysis of the chapter 3.

4.4. Chapter Summary

In this chapter a modeling method for the wires to determine the field at points close to the core is discussed. Since 3D finite element modeling of a coil with 50461 turns would not be feasible first each layer of wires are represented with foils. Then a single foil is analyzed to find the maximum stress point of the model. The 2D slice of the 3D model where the electrical field is maximum constructed. A mapping is done by comparing the results of the 2D analysis to the 3D for 12 points. Remaining points are calculated by assuming linearity. The accuracy of this type of mapping would increase if more points are evaluated however this would also increase the computational time.

2D analysis of the original and modified design carried out and it is found out to be that the field stress at the resin of the original design is dangerously close to the

breakdown strength of the resin. On the other hand, the stress values of the modified design are in the acceptable range. The low failure rate of the modified design given in the Table 2-8 can be attributed to this fact.

By utilizing the 2D to 3D conversion method and the layer template table constructed in the chapter 3 final design has been concluded. The comparison of the final and the original design both having three different layer blocks is presented in Table 4-3. The size difference of the windings can be seen in Figure 4-13. The final design is aimed to satisfy all of the objectives mentioned in the section 1.2. The manufacturing and the evaluation of the design will be carried out in the next chapter to check if the design is valid.

Table 4-3 Comparison of the original and final designs layer parameters

| | | Original | Final |
|----------------------|---------------------------------------|-----------------|--------------|
| Layer Block 1 | Type | 2-2-2-1 | 2-2-2-1 |
| | Winding length (mm) | 106 | 116 |
| | Percentage of the layer type utilized | 87% | 96% |
| | Insulating paper length (mm) | 120 | 140 |
| | Number of turns | 22707 | 15970 |
| Layer Block 2 | Type | 2-2-2-1 | 2-2-1 |
| | Winding length (mm) | 86 | 86 |
| | Percentage of the layer type utilized | 71% | 92% |
| | Insulating paper length(mm) | 100 | 140 |
| | Number of turns | 15139 | 20192 |
| Layer Block 3 | Type | 2-2-2-1 | 2-2-2-1 |
| | Winding length (mm) | 66 | 70 |
| | Percentage of the layer type utilized | 55% | 101% |
| | Insulating paper length(mm) | 80 | 140 |
| | Number of turns | 12615 | 14299 |



Figure 4-13 Original coil (left) and final coil(right)

CHAPTER 5

EXPERIMENTAL RESULTS

The final design has been constructed with the knowledge accumulated in the chapters 2, 3 & 4. Although the simulations indicate that it has better performance than the modified design, which was already successful in the partial discharge test, the final design should be subjected to tests to prove the validity of the design. All of the tests applied will be in accordance with the IEC standards. For different markets additional tests will be required. If the standard of a market is not IEC, slight design modifications may be required.

Ten transformer prototypes are manufactured according to layer design given at section 4.3.4. Nine of those are injected with the SF₆ gas while one of them is injected with Nitrogen (N₂). The reason of the usage of the nitrogen gas is to investigate the possibility to produce the GT30a without using a greenhouse gas. Although N₂ is significantly weaker in terms of insulation than the SF₆ the field stress simulation results of the final design indicates that it can pass the test under 5 bar pressure.

The original, modified and the final designs will be compared in material and production time wise. Since GT30a is a commercial product, it will all come down to the feasibility of the design. The electrical performance of the designs in the tests also will be compared. A design might be costlier but if the performance is high enough it might compensate for its price.

Lastly, at the end of the chapter a conclusion regarding the differences of the original modified and the final design will be presented. The design tradeoffs discussed and it will be decided to which transformer design to use in the mass production.

5.1. Tests Applied to the Final Design

The high voltage coil of the final design is completely different than the original one and that is the only major difference between them. Although the iron core, low voltage winding and the epoxy resin moulds are same for the two designs, the standard lightning impulse, temperature rise and accuracy class type tests will be repeated which will not only prove the validity of the final design to the markets that use IEC standards but also verify the modeling approach applied in chapters 3 & 4.

Type tests will be applied to only to one of the 5 bar SF₆ filled transformers. The routine tests will be applied to the all of the 10 prototypes as the standard dictates. Other than type and the routine tests, the partial discharge test will be repeated with depressurized transformers to prove the fact that the transformers can still be functional even when the insulating gas is leaked which was a design requirement of this thesis.

5.1.1 Standard Lightning Impulse Test

The standard lightning impulse test is a destructive test therefore it is applied to one transformer after all other tests have been completed. The test has been carried out according to the IEC 60060-1 and test setup can be seen in the Figure 5-1.

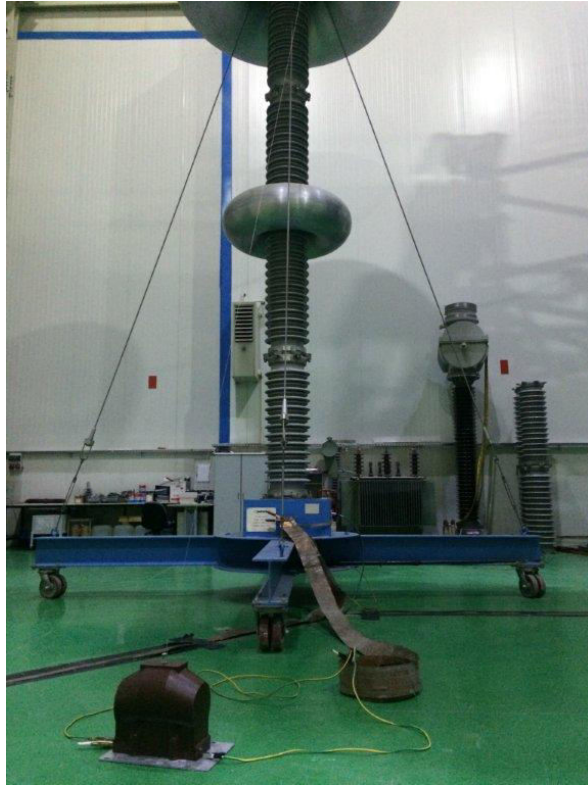


Figure 5-1 Standard lightning impulse test setup

Peak voltage of the impulse applied is 170 kV (Table 1-1). The front time of the applied impulses are $1.1 \pm 0.03 \mu\text{s}$ and the tail time of the impulses are $46 \pm 2 \mu\text{s}$ which are within the allowed limits of IEC 60060-1[34].

15 positive impulses (Figure 5-2) and 15 negative impulses are consecutively applied to the final design transformer with 5 bar SF_6 gas. No puncture occurred and the final design safely passed the test. The transformer, which the test has been applied is discarded.

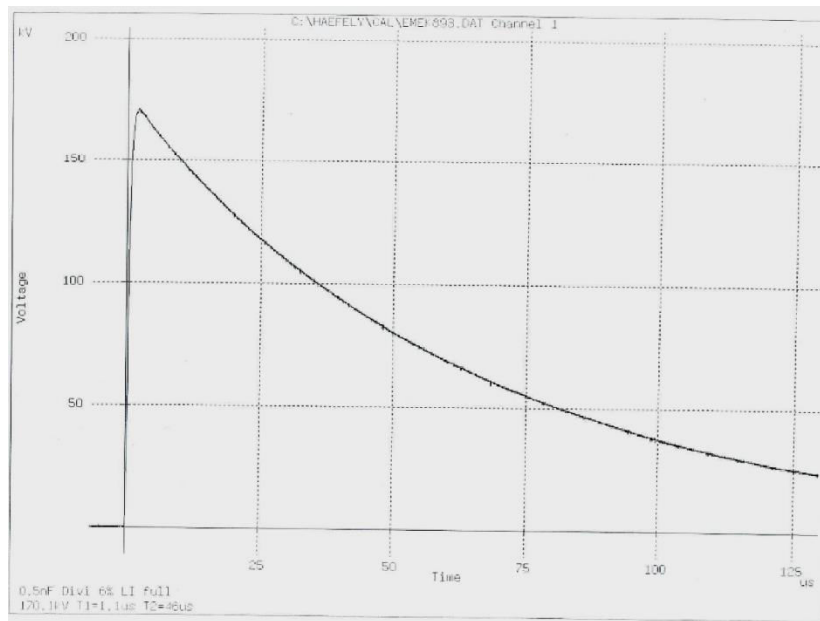


Figure 5-2 Standard Lightning Impulse test positive waveform

5.1.2 Temperature-rise Test

Throughout the thesis the thermal aspect of the design is ignored since the rated power (burden) of the transformer was low. The test is carried out to prove that the new high voltage coil of the final design does not cause overheating.

The initial temperature and the final temperature of the coil are compared when the transformer reaches the steady state. IEC 61869-1 indicates that the transformer is accepted as in the steady state when the temperature increase does not exceed 1 K/h. In Figure 5-3 it can be seen that the transformer reaches steady state after 7 hours.

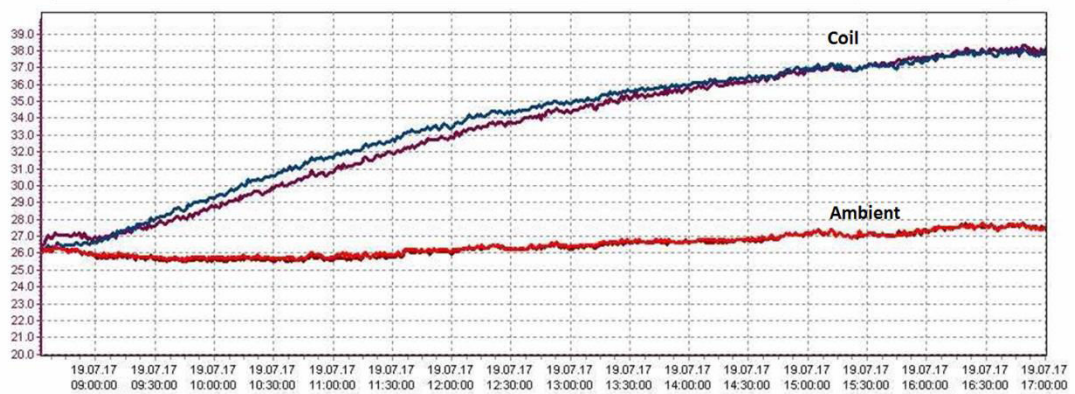


Figure 5-3 Temperature rise test results

The temperature rise limit of the GT30a according to IEC61869-1 clause 6.4.1 is 60 Kelvin. The red color indicates the temperature of the ambient and purple-blue indicates the temperature of the coil which is recorded by two probes. The temperature rise of the final design is found out to be is 38° C -26° C = 12 Kelvin. As expected temperature rise is not a limiting factor in this design.

5.1.3 Test for Accuracy

Likewise to the thermal design, the magnetic design of the transformer is also ignored in the process. To prove that the accuracy of the transformer is in the allowed limits, which is %3 error. The test is carried out according to IEC 61869-1 clause 7.2.6.302. The results are given at Table 5-1.

Table 5-1 Accuracy test result of the final and the original design

| PRIMARY VOLTAGE % Un | %25 BURDEN | | | | %100 BURDEN | | | |
|-------------------------|-----------------|-----------------|-----------------|-----------------|-----------------|-----------------|-----------------|----|
| | RATIO ERROR(%) | | PHASE ERROR(°) | | RATIO ERROR(%) | | PHASE ERROR(°) | |
| | Final /Original | Final /Original | Final /Original | Final /Original | Final /Original | Final /Original | Final /Original | |
| 2 | -0,37 | -0,28 | 19 | 21 | -0,48 | -0,57 | 20 | 21 |
| 5 | -0,37 | -0,28 | 19 | 21 | -0,48 | -0,57 | 20 | 21 |
| 100 | 0,16 | 0,3 | 1 | 3 | 0,03 | -0,16 | 2 | 4 |
| 190 | -0,15 | -0,13 | 12 | 12 | -0,28 | -0,33 | 13 | 13 |

The result of test is satisfactory. To find out how the copper resistance and leakage inductance reacted to the changes done in the high voltage coil, the results of the final design can be compared with the results of the original design also given at Table 5-1.

The accuracy of the transformer at the %100 U_n and %100 burden is checked it has been found out that the error has been shifted from the negative side (%-0.16) to the positive side (%0.03) when the design is changed from the original to the final. This means that the leakage inductance and the copper resistance of the final design is lower than the original design thus the turns are added to compensate for the voltage drop are causing a positive error.

Although the accuracy class is not as critical in the protection voltage transformers as the measurement transformers, it has been proven that carrying out finite element analysis at design of the high coil can lead to reduction the coil size and increase in accuracy.

5.1.4 Power Frequency Withstand and PD Test

The power frequency test and partial discharge test are both type and routine tests. The test setup can be seen in the Figure 5-4. The transformers are first subjected to 1 minute $70 \text{ kV}_{\text{rms}}$ and then the voltage reduced step by step and the necessary discharge measurements are taken. The power frequency test voltage of the GT30a was given in Table 1-1 and the discharge test voltages are taken according to Table 1-5.

Table 5-2 Power frequency and partial discharge test results with 5 bar insulating gas

| Transformer | Insulation | 70 kV 1 min | PD at 43.2 kV(pC) | PD at 24.9 kV(pC) |
|-------------|-----------------|----------------|----------------------|----------------------|
| 171/1520 | SF ₆ | passed | 3 | 3 |
| 171/1521 | SF ₆ | passed | 3 | 3 |
| 171/1522 | SF ₆ | passed | 10 | 3 |
| 171/1523 | SF ₆ | passed | 3 | 3 |
| 171/1524 | SF ₆ | passed | 3 | 3 |
| 171/2133 | SF ₆ | passed | 3 | 3 |
| 171/2134 | SF ₆ | passed | 3 | 3 |
| 171/2135 | SF ₆ | passed | 3 | 3 |
| 171/2136 | N ₂ | passed | 3 | 3 |
| 171/2137 | SF ₆ | passed | 3 | 3 |

Allowed limit of the standard is 5 pC at 24.9 kV and 10 pC at 43.2 kV. The test results are given in the Table 5-2 and the test setup is given at the Figure 5-4. Since the noise level of the system is at 3 pC it could not be noticed if the actual transformer discharge is lower than that value. All of the transformers including the nitrogen insulated one passed the test safely.



Figure 5-4 Partial discharge test setup

Remarks;

- Transformer number 171/1522 has partial discharge at the limit of the standard. This discharge most likely to be caused from the epoxy resin due to a production error. Since the epoxy resin field value of the final design have a large safety factor this error is tolerated. If this transformer was a modified or a original design it could have been resulted in puncture or excessive discharge.
- When desired the final design of the GT30a can be produced with the N₂ gas instead of the SF₆ which is cheaper and environmentally friendly.

5.1.5 Power Frequency Withstand and PD test with the Leaked Gas

One of the design requirements given at section 1.2 is the robustness against the possible gas leakages. The voltage of the GT30a is ~20 kV under normal operation conditions. In the previous section it has been checked that transformers do not have any partial discharge therefore it has been proven that the epoxy resin is discharge free.

The same procedure is applied with the only difference being the gas insulation of the transformer is leaked to the atmospheric pressure. If the partial discharges are not observed at the 24.9 kV it means that the discharge due to the ionization of the insulating gas extinguish before the 24.9 kV.

Since the partial discharges in gases do not increase their magnitude by time like the solid insulation they would not contribute the aging process with the condition that there is no discharge already in present at operating conditions. The test voltage is 24.9 kV while the operating voltage is 20 kV, which gives %20 percent margin of safety.

Table 5-3 Power frequency and partial discharge test results with leaked insulating gas

| Transformer | Insulation | 70 kV 1 min | PD at 43.2 kV(pC) | PD at 24.9 kV(pC) |
|-------------|-----------------|----------------|----------------------|----------------------|
| 171/1520 | SF ₆ | passed | 3 | 3 |
| 171/1521 | SF ₆ | passed | 10 | 3 |
| 171/1522 | SF ₆ | passed | 100 | 3 |
| 171/1523 | SF ₆ | passed | 3 | 3 |
| 171/1524 | SF ₆ | passed | 100 | 3 |
| 171/2133 | SF ₆ | passed | 100 | 3 |
| 171/2134 | SF ₆ | passed | 50 | 3 |
| 171/2135 | SF ₆ | passed | 150 | 3 |
| 171/2136 | N ₂ | passed | 200 | 10 |
| 171/2137 | SF ₆ | passed | 30 | 3 |

Remarks;

- The partial discharges of the SF₆ filled transformers extinguishes before the 24.9 kV completing the goal of the leakage robust design. However the discharge of the nitrogen filled transformer does not extinguish, which is expected since the electrical strength of the nitrogen is less than half of the SF₆ (Figure 2-4).
- The performance at 43.2 kV is varying for each transformer which means that the coils produced are not identical either due to the production error or due to the material tolerances.

5.2. Comparison of the Initial, Modified and the Final Design

In this thesis so far three different designs with the same design properties but different designs have been introduced namely the original, modified and the final design. Final design also have two subtypes depending on the insulation gas utilized. GT30a is a commercial product therefore its price should be remain competitive while it performance should be adequate regarding the standards.

To compare and evaluate the designs economically material costs and the production times will be inspected. In order to compare the performances the test

data of each design and the maximum electric field intensities found out by the simulations will be used.

5.2.1 Material and Production Time Comparison

All of the designs are manufactured from identical cores. The coil of the final design has smaller outer diameter and larger length compared to the modified and the original designs. In the original design, the paper insulation length changes depending on the layer type while in the modified and the final design the paper kept constant. These differences along with the change of the layer type and lengths in the final design cause the differences in the materials used in the production and the manufacturing time of the coil given. These differences are presented in Table 5-4.

Table 5-4 Material and production time comparison of the coils

| Design | Epoxy Resin Mixture (kg) | Insulating Paper(kg) | Magnet Wire (kg) | Material Cost | Coil Manufacturing Time |
|----------|--------------------------|----------------------|------------------|---------------|-------------------------|
| Original | 15.8 | 0.69 | 2.26 kg | 53.46 € | 216 min |
| Modified | 14.5 | 0.74 | 2.26 kg | 52.03 € | 224 min |
| Final | 14.9 | 0.84 | 1.91 kg | 50.995 € | 196 min |

The cost unit cost of the epoxy resin is around 1.6€, insulating paper is around 13€ and magnet wire is around 8.5€ per kilogram. When the material cost of the total resin, wire and paper is calculated, the original design is 53.46 €, modified design is 52.03€ and final design is 50.995€.

The final design is slightly cheaper in terms of material and moreover it has the lowest manufacturing time. Although the cost of the designs are very close to each other, in a mass production even the minor difference can add up to provide a major economic boost.

5.2.2 Performance Comparison

Along with the ability to pass the type test, one of the most important factor when evaluating a design is the success rate in the routine tests. Even when a design is

less expensive if the failure rate is high in the routine test, the overall cost would be higher than an expensive design.

The electrical performance comparison of the initial, modified and the final designs are given in the Table 5-5.

Table 5-5 Electrical field performance comparison of the designs

| Design | Total Production Number | Fail rate due to PD and puncture | Max Efield in resin at 25 kV (kV/mm) | Max Efield in gas at 25 kV (kV/mm) |
|---------------|--------------------------------|---|---|---|
| Original | 4206 | %14.3 | 7.61 | 8,37 |
| Modified | 240 | %1.25 | 6.95 | 6.67 |
| Final | 10 | %0 | 5,12 | 6,02 |

Original design is unusable due to the high failure rate in the partial discharge and power frequency type test. On one hand modified design is viable since the rate of failure is acceptable. On the other hand the final design have lower electrical stress which would absorb manufacturing mistakes. Number of the transformer manufactured is not enough to show an accurate representation of failures due to partial discharges but it is expected to be lower than the modified design due to the fact that only ten prototypes of the final design are produced. However if the mass production continues with the final design it is expected to have lower failure rates than the modified design thanks to reduced maximum electric field in the design.

5.3. Design Trade Offs

The modified design, the final design with SF₆ and the final design with N₂ are all suitable for manufacturing regarding their performance. To choose which one to utilize is depending on the expectation from the transformer. The trade offs are robustness, cost and the environmentally friendliness.

If the modified design continued to be produced it will be neither environmentally friendly nor resistant to gas leakage. Furthermore, it would have %36 more electric field stress at the resin that would affect the aging and %10 percent more electric

field stress in the SF₆ compared to the final design. Only advantage of the modified design is it has been produced over 200 without a problem therefore the current manufacturing system is already arranged for its production. In order to create the least expensive design, a new design based of the analysis carried out in the chapters 3 and 4 can be created with changing the limiting stress values to the modified designs current values. This would require a new epoxy resin mould and a new iron core but it would also reduce the overall production cost.

If the final design with SF₆ is used in the serial production, it would have low electrical field values which increases the reliability and the life expectancy of the product. Its cost is similar to the modified design. This design also does not cause partial discharges under operating conditions even when the SF₆ is leaked. However it has two drawbacks: Firstly, it utilizes the SF₆ greenhouse gas and secondly a less expensive design which would fulfill the same requirements of the IEC can be adopted.

The final design filled with N₂ has the advantage of being environmentally friendly, which means it can be exported to the markets that are regulating the usage of the SF₆ like the European Union. N₂ is also a cheaper gas than SF₆ but the amount used in the GT30a would not make a significant difference to the cost. The design with N₂ has the same field stresses in the epoxy resin with the final design with SF₆ which means that the expected life would be identical. It is not resistant to gas leakages since N₂ gas is weaker in terms of insulation when compared to the SF₆. A leakage resistant design with N₂ can be manufactured but it would be larger and would require a new mould and core. To compensate the size the magnetic design of the GT30a can be revised by changing the material of the core that allows operation with higher flux density.

5.4. Chapter Summary

In this chapter the tests to the final design have been carried out. It has been found out that the final design is suitable for production according to IEC standards. Tests

also applied to the depressurized coils to measure the robustness of the final design. Results indicated that final design fulfills all the objectives given at the section 1.2.

In terms of performance, the designs other than the original are suitable for the mass production. In terms of cost all of the designs have similar values except the original design, which has increased cost due to the failed items.

N₂ has been used in the one of the coils instead of the SF₆ to check the potency of the gas as an insulating medium. Since only one coil produced a detailed data could not be collected but it is safe to say that this gas can be adapted to GT30a after manufacturing more samples and repeating the type tests.

The modified design will remain mass the serial production for now because of the convenience in manufacturing. It is expected to change from the modified design to the final design with a new mould that reduces the material cost in the upcoming months.

CHAPTER 6

CONCLUSIONS & FUTURE WORK

6.1. Conclusions

Traditional gas insulated inductive MV voltage transformers are expected to be widely used at least a couple of decades. There are a few ways to improve the performance of these transformers. The first thing can be done is to utilize materials that have better electrical characteristics. The second thing can be done is to use advanced tools for using the materials that are available to their operational limits. This thesis focused on to the second way by using the finite elements method as a tool to improve the electrical field distribution inside the high voltage coil.

To develop a finite modeling method, a problematic transformer named GT30a has been used as an example throughout the thesis. GT30a had the partial discharge and puncture problem in the routine tests that are applied according to the IEC standards. Both of these problems can be tracked down to field strength intensity thus can be solved with proper redistribution of the field via finite elements simulations.

Partial discharges in the solid and gas mediums are discussed. The limits of the materials used in the GT30a are inspected to be able to determine the critical field stresses that are going to be used as limits in the simulation. Small adjustments have been made to develop the modified design as a temporary solution. Modified design has slightly better electric field stresses compared to the original design.

The coils are consisted of layers which are repeated until the desired turn value is reached. In an ideal case, each turn would have different position in space to have the minimum electric field inside the layer. Since this is not practical due to the requirement of extremely thin paper, possible layer templates are determined by utilizing 30 micron insulation paper which is readily available.

Layer length determination required 3D analysis since there was no axis of symmetry. Instead of carrying out 3D analysis, an approximate mapping is done between the 3D and 2D which enabled faster simulation. With the layer lengths and templates are determined final design has been concluded. The final design subjected to the tests and satisfied all of the design objectives given in section 1.2. A coil with N_2 has also been tested to inspect the possibility of environmentally friendly production. The result was satisfactory. In comparison to the standard inductive voltage transformers, this approach results in a smaller volume consumption due to the more precise calculations.

The final design developed in this thesis is superior to the original design in every aspect. It has reduced electric field values which relieves the insulation thus decreasing the losses due to the partial discharges and punctures. It has slightly lower material cost and also has lower manufacturing time. Last but not least, the high voltage coil of the final design is smaller in volume which allows the usage of a smaller mould if desired.

With the modeling method developed in this thesis proven to be effective, the rest is to set the objective of the design. There are tradeoffs between the total production cost, robustness and the environmentally friendliness.

Overall design algorithm can be summarized as the following :

- 1) Obtain the design parameters of the transformer
- 2) Obtain the magnetic design properties of the transformer
- 4) Set the objectives for the design
- 3) Determine the insulating materials that will be utilized and their properties

- 4) Determine the allowed field strengths for the insulating materials by taking the objectives in regard.
- 5) Construct the layer template table
- 6) Construct the mapping from 2D to 3D
- 7) Determine the layer lengths
- 8) Finalize and test the design according to the regarding standards

The approximate time to create a design with this method would take around 3 weeks. The manufacturing and testing process would take up to 2-3 weeks. These values can change depending on the facilities that are available.

6.2. Future Work

Although this thesis has covered the finite elements modeling of the transformer and solved the partial discharge problem there is still room for improvement.

First of all the prototypes are designed with the materials that have already been in use of the GT30a production. Further improvement and experimenting can be executed by changing the type of the insulating paper and the epoxy resin. As for the insulating gas the different mixtures of SF₆ and N₂ can be implemented and their performances can be compared.

Another aspect of the design that can be added to the process is the optimization. After the objectives of the design have been chosen, the length and template determination can be done with an optimization algorithm. The objective could either be the total cost minimizing or maximum electric field minimizing depending on the requirements. Genetic algorithm would be suitable for such attempt since it is expected to have many independent variables. Also such optimization problem would suffer from local minimums and vast requirement of the computational burden. To speed up the process, the initial starting point of the algorithm can be selected with manual iteration as have been done in this thesis.

REFERENCES

- [1] W. M. Flanagan, "Handbook of Transformer Design & Applications," p. 237, 1993.
- [2] S. Teszszky, "History of Transformers," *IEEE Power Eng. Rev.*, vol. 16, no. 12, p. 9, 1996.
- [3] M. Sanaye-Pasand, A. Rezaei-Zare, H. Mohseni, S. Farhangi, and R. Iravani, "Comparison of performance of various ferroresonance suppressing methods in inductive and capacitive voltage transformers," *2006 IEEE Power India Conf.*, vol. 2005, pp. 909–916, 2005.
- [4] T. Sawa, K. Kurosawa, T. Kaminishi, and T. Yokota, "Development of optical instrument transformers," *IEEE Trans. Power Deliv.*, vol. 5, no. 2, pp. 884–891, 1990.
- [5] M. Kanoi, G. Takahashi, T. Sato, and M. Higaki, "Optical Voltage," no. January, 1986.
- [6] M. Saitoh *et al.*, "Electronic Instrument Transformers for Integrated Substation Systems," *Transm. Distrib. Conf. Exhib. 2002 Asia Pacific. IEEE/PES . IEEE.*, pp. 459–464, 2002.
- [7] International Electrotechnical Commission (IEC), "IEC 60038 IEC standard voltages," 2002.
- [8] International Electrotechnical Commission (IEC), "IEC 61869-3 Additional requirements for inductive voltage transformers," 2011.
- [9] M. Ieda, "Dielectric Breakdown Process of Polymers," *IEEE Trans. Electr. Insul.*, vol. EI-15, no. 3, pp. 206–224, 1980.
- [10] International Electrotechnical Commission (IEC), "IEC 61869-1 Instrument transformers," 2007.
- [11] E. Barkanov, "Introduction to the finite element method," *Introd. To Finite*

Elem. Method, pp. 1–70, 2001.

- [12] O. C. Zienkiewicz and R. L. Taylor, “The Finite Element Method Volume 1 : The Basis,” *Methods*, vol. 1, p. 708, 2000.
- [13] L. Niemeyer, “The ALESSANDRO VOLTA Lecture A Generalized Approach to Partial Discharge Modeling,” vol. 2, no. 4, pp. 510–528, 1995.
- [14] International Electrotechnical Commission (IEC), “IEC 60270 High-voltage test techniques - Partial discharge measurements,” 2000.
- [15] S. A. Boggs and U. Systems, “Partial Discharge: Overview and Signal Generation 8,” vol. 6, no. 4, 1990.
- [16] C. Laurent and C. Mayoux, “Partial Discharge - Part XI: Limitations to PD as a Diagnostic for Deterioration and Remaining Life,” *IEEE Electr. Insul. Mag.*, vol. 8, no. 2, pp. 14–17, 1992.
- [17] S. Boggs, “Fundamentals of Partial,” vol. 16, no. 5, 2000.
- [18] P. H. F. Morshuis, “Degradation of solid dielectrics due to internal partial discharge: Some thoughts on progress made and where to go now,” *IEEE Trans. Dielectr. Electr. Insul.*, vol. 12, no. 5, pp. 905–913, 2005.
- [19] M. Goldman, a Goldman, and R. S. Sigmond, “The corona discharge, its properties and specific uses,” *Pure Appl. Chem.*, vol. 57, no. 9, pp. 1353–1362, 1985.
- [20] H. Search, C. Journals, A. Contact, M. Iopscience, and I. P. Address, “Stochastic modelling of electrical treeing: fractal and statistical characteristics,” vol. 1536.
- [21] M. Leijon, M. Dahlgren, L. Ming, and A. Jaksts, “A Recent Development in the Electrical Insulation Systems of,” pp. 10–15.
- [22] W. Larson and A. Yezer, “The energy implications of city size and density,” *J. Urban Econ.*, vol. 90, pp. 35–49, 2015.

- [23] S. Okabe, N. Hayakawa, H. Murase, H. Hama, and H. Okubo, "Common insulating properties in insulating materials," *IEEE Trans. Dielectr. Electr. Insul.*, vol. 13, no. 2, pp. 327–335, 2006.
- [24] G. C. Stevens and A. M. Emsley, "Review of chemical indicators of degradation of cellulosic electrical paper insulation in oil-filled transformers," *IEE Proc. - Sci. Meas. Technol.*, vol. 141, no. 5, pp. 324–334, 1994.
- [25] L. G. Christophorou, J. K. Olthoff, and R. J. Van Brunt, "Sulfur hexafluoride and the electric power industry," *IEEE Electr. Insul. Mag.*, vol. 13, no. 5, pp. 20–24, 1997.
- [26] L. G. Christophorou, *Gases for Electrical Insulation and Arc Interruption: Possible Present and Future Alternatives to Pure SF6*. 1997.
- [27] G. Camilli, "Gas-insulated Power Transformers," *IEE Proc. - Electr. Power Appl.*, vol. 107 A, pp. 375–382, 1960.
- [28] E. Onal and G. Komurgoz, "Calculation of Corona Inception Voltages in N₂ + SF₆ Mixtures via Genetic Algorithm," no. 34469.
- [29] H. Jo, G. Wang, S. Kim, and G. Kil, "Comparison of Partial Discharge Characteristics in SF₆ Gas Under AC and DC," vol. 16, no. 6, pp. 323–327, 2015.
- [30] Y. Qiu and M. C. Siddagangappa, "Prediction of breakdown voltages of binary gas mixtures in uniform electric fields," *IEEE Trans. Electr. Insul.*, vol. EI-20, no. 3, pp. 651–653, 1985.
- [31] M. Bagheri, B. T. Phung, and M. S. Naderi, "Impulse Voltage Distribution and Frequency Response of Intershield Windings," pp. 32–40, 2016.
- [32] P. Apparatus, H. T. Windings, and R. Van Nuys, "Sept/Oct 1978 INTERLEAVED," no. 5, pp. 1946–1954, 1978.
- [33] "Michalewicz Z. Genetic Algorithms + Data Structures = Evolution

Programs (3ed).PDF.” .

- [34] International Electrotechnical Commission (IEC), “IEC 60060-1, High-voltage test techniques - Part 1: General definitions and test requirements,” 2010.

GT30a Original Design Winding Diagram

| TEMEL TASARIM BİLGİLERİ | | | | | | |
|---|---------------------|---|-------------------------|---|---|----------------|
| SİSTEM ANMA GERİLİMİ (kV) | | 34,5 $\sqrt{3}$ | İZOLASYON SEVİYESİ (kV) | | 36 / 70 / 170 | |
| GERİLİM FAKTÖRÜ | | 1,2 x Un sürekli / 1,9 x Un 30 sn. | FREKANS | 50 | STANDARTLAR TS 718 EN 60044-2/IEC 60044-2 | |
| PRİMER TERMINAL ÖLÇÜLERİ (mm) | | | | YH4004/26 , M10x20 TERMINAL DUYU PİRİNÇ | | |
| İZOLATÖR ÖLÇÜLERİ (İÇ ÇAPxYÜKSEKLİK) (mm) | | | KREPAJ MESAFESİ (mm) | | | |
| SARGI NO | PRİMER GERİLİM (kV) | SEKONDER GERİLİM (V) | TERMINALLER | YÜK (VA) | SINIF | |
| 1 | 34,5 $\sqrt{3}$ | 100 $\sqrt{3}$ | 1a-1n | 10 | 3P | |
| SARGI DİYAGRAMI | | | | | | |
| | | | | | | |
| SEKONDER SARM SEKİL DİYAGRAMI | | | | | | |
| Primer başlangıç çapı : Ø77.00 | | Sekonder Başlangıç Çapı : Ø59.00 | | | | |
| 1.kademe | 2 kat 30 μ | 0,5 mm Presbant (3 tur) : DK1001/05 Gen.(mm) : 180 | | | | |
| | | Kraft Kağıdı : DK0103/10 (12/100x1020 KRAFT KAĞIDI), 170 mm | | | | |
| | | Sekonder Bitiş Çapı : Ø69.92 | | | | |
| | | SEKONDER - PRİMER ARASI İZOLASYON | | | | |
| | | 1.kademe : 160 mm 12/100x1020 KRAFT KAĞIDI, Ø77'ye kadar | | | | |
| 2.kademe | 2 kat 30 μ | | | | | |
| 3.kademe | 2 kat 30 μ | | | | | |
| MAX Primer bitiş çapı : Ø164.91 +1 | | | | | | |
| TASARIM BİLGİLERİ | | | | | | |
| SEKONDER SARGI | | | | | | |
| SARGI NO | TAP NO | TUR | TEL ADET VE ÇAP | KAT | TUR / KAT | |
| 1 | 1a-1n | 147 | 1 adet Ø1.5 | 2 | 74+73 | |
| PRİMER SARGI | | | | | | |
| TUR | TEL ÇAP | GALET ADEDİ | KADEME | KAGIT GENİŞLİĞİ (mm) | SARM GENİŞLİĞİ (mm) | TUR SAYISI |
| 50461 | Ø0.12 | 1 | 1 | 120 | 106 | 22707'ye kadar |
| | | | 2 | 100 | 86 | 37846'ya kadar |
| | | | 3 | 80 | 66 | 50461'e kadar |

GT30a Final Design Winding Diagram

| TEMEL TASARIM BİLGİLERİ | | | | | | |
|---|------------------------------------|-------------------------|---|--|-------------------------------|----------------|
| SİSTEM ANMA GERİLİMİ (kV) | 34.5/3 | İZOLASYON SEVİYESİ (kV) | 36 / 70 / 170 | | | |
| GERİLİM FAKTÖRÜ | 1.2 x Un sürekli / 1.9 x Un 30 sn. | FREKANS | 50 | STANDARTLAR | TS 718 EN 60044-2/IEC 60044-2 | |
| PRİMER TERMINAL ÖLÇÜLERİ (mm) | KREPAJ MESAFESİ (mm) | | YH4004/26 , M10x20 TERMINAL DUYU PİRİNÇ | | | |
| İZOLATÖR ÖLÇÜLERİ (İÇ ÇAPxYÜKSEKLİK) (mm) | | | | | | |
| SARGI NO | PRİMER GERİLİM (kV) | SEKONDER GERİLİM (V) | TERMINALLER | YÜK (VA) | SINIF | |
| 1 | 34.5/3 | 100/3 | 1a-1n | 10 | 3P | |
| SARGI DİYAGRAMI | | | | | | |
| | | | | | | |
| SEKONDER SARIM ŞEKLİ DİYAGRAMI | | | | | | |
| Primer başlangıç çapı : Ø77.00 | | | | | | |
| 1.kademe | | | 2 kat 30 µ | Sekonder Başlangıç Çapı : Ø59.00 0.5 mm Presbant (3 tur) : DK1001/05 Gen.(mm) : 180 Kraft Kağıdı : DK0103/10 (12/100x1020 KRAFT KAĞIDI), 170 mm Sekonder Bitiş Çapı : Ø69.92 SEKONDER - PRİMER ARASI İZOLASYON 1.kademe : 160 mm 12/100x1020 KRAFT KAĞIDI, Ø76'ya kadar | | |
| 2.kademe | | | 2 kat 30 µ | | | |
| 3.kademe | | | 1 kat 30 µ | | | |
| MAX Primer bitiş çapı : Ø145.1+1 | | | | | | |
| TASARIM BİLGİLERİ | | | | | | |
| SEKONDER SARGI | | | | | | |
| SARGI NO | TAP NO | TUR | TEL ADET VEÇAPI | KAT | TUR / KAT | |
| 1 | 1a-1n | 147 | 1 adet Ø1.5 | 2 | 74+73 | |
| PRİMER SARGI | | | | | | |
| TUR | TEL ÇAPI | GALET ADEDİ | KADEME | KAĞIT GENİŞLİĞİ (mm) | SARIM GENİŞLİĞİ (mm) | TUR SAYISI |
| 50461 | Ø0.12 | 1 | 1 | 140 | 116 | 15970'e kadar |
| | | | 2 | 140 | 86 | 36162'ye kadar |
| | | | 3 | 140 | 70 | 50461'e kadar |